Investigation on Cytoophidium Function and Filament-Forming Proteins



QINGJI SHEN

Wolfson College

MRC Functional Genomics Unit

Department of Physiology, Anatomy and Genetics

University of Oxford

Submission in fulfilment of the requirements for the degree of

Doctor of Philosophy (DPhil)

Hilary Term 2017

Investigation on Cytoophidium function and filament-forming proteins

A thesis submitted for the degree of DPhil in Physiology, Anatomy and Genetics

Abstract

In 2010, three independent groups reported that cytidine-5'-triphosphate synthase could form a filamentous structure. The term "cytoophidium" was coined in recognition of its observed serpent-like structure in *Drosophila* cells. In the last seven years of study on cytoophidia, lots of models and hypotheses related to cytoophidia have been put forward. In 2014, three independent studies pointed out that the CTP synthase-based cytoophidium is a functionally inactive structure. These studies built models for the inhibition of the enzyme by filamentation; research on cytoophidia had transited from descriptions to mechanisms. In this thesis, I study the function of the cytoophidium from two major aspects. Firstly, I describe the effects of dimerization and tetramerization interphases of CTP synthase mutants on filament assembly in *Drosophila melanogaster*, suggesting that the cytoophidium is an enzymatically inactive structure. Secondly, through a genome-wide screening of filament-forming proteins in *Saccharomyces cerevisiae*, I identify nine novel filament-forming proteins and select one candidate, asparagine synthetase, for further study of the stress regulation of cytoophidia. Results show that heat shock, cold shock, osmotic stress and oxidative stress induce filament formation of asparagine synthetase. These results provide new insights into the function of cytoophidia, the components of cytoophidia and filamentation regulation, indicating new possibilities in cell biology and enzymology.

Qingji Shen

Wolfson College

Hilary Term 2017

Statement of Authorship

I confirm that all the work presented in this thesis was performed in the MRC Functional Genomics Unit, Department of Physiology, Anatomy and Genetics, University of oxford from 2012 to 2017. Except where acknowledged, all work presented was conducted by the author of this thesis Qingji Shen. No part of this thesis has been submitted for any other degree in this University or elsewhere.

Qingji Shen

Acknowledgments

Firstly, I would like to thank Professor Ji-long Liu for giving me this great opportunity to study in his lab in the MRC Functional Genomics Unit and undertake the researches presented in this thesis. I would like to thank Professor Ji-long Liu for his dedicated guidance and endless support throughout the four-year DPhil study. Thanks to his every precious advice during my study, I have grown up from a student with limited knowledge and experience to a DPhil candidate who can conduct independent research and make contributions to my field. His determination and enthusiasm to science are infectious and also keep me confident and motivated during researches. Things I learn from him will always be beneficial to my future career and life.

I also own my sincere thanks to Dr Andrew Bassett, Dr Stuart Grice, Dr Omur Tastan, Dr Lydia Hulme, Dr Sanjay Ghosh and Dr Gerson Keppeke for their generosity with their time and knowledge to support my research and life in Oxford. Furthermore, I would like to thank all the past and present members of Liu lab, the MRC Functional Genomics Unit and the Department of Physiology, Anatomy and Genetics for contributing scientific discussion and positive, friendly and cooperative atmosphere in which to work. My special thanks go to: Dr Gabriel Aughey, Dr Jing Zhang, Muhammad Mohd Kassim, Dr Yong Huang, Dr Chia-Chun Chang, Aphrodite Zhao and Dr Yixing Wu for their frequent favours and advices on my research.

Meanwhile, I would like to grant my sincere thanks to the China Scholarship Council (CSC) and University of Oxford for their sponsorship “China Scholarship Council-University of Oxford Scholarships”, which fully supported me during my DPhil period.

Finally, I would like to thank my family and friends for supporting and encouraging me when I was in hard times.

Contents

Abstract **1**

Statement of Authorship **2**

Acknowledgments **3**

Contents **4**

List of Figures **8**

List of Tables **10**

List of Abbreviations **11**

Chapter 1 Introduction

1.1 CTP synthase cellular compartmentation and the discovery of cytoophidia **13**

1.2 CTP synthase catalytic activity and regulation **16**

1.3 Cytoophidium components and assembly **19**

1.4 Cytoophidium regulation and function **23**

1.5 Difference and interaction of self-assembling structures: IMPDH based- cytoophidia as an example **26**

1.6 Filament-forming proteins and their relevance to human diseases **27**

1.7 Model organisms: The *Drosophila* cell line and the budding yeast *S. cerevisiae* **28**

1.8 Project aims and thesis structure **30**

Chapter 2 Materials and Methods

2.1 S2R+ cell culture **32**

2.2 Transfection of S2R+ cells **32**

2.3 S2R+ cells stable lines selection **32**

2.4 S2R+ cell immunofluorescence and microscopy **33**

2.5 Generation of CTP synthase point mutation expression vectors **33**

2.6 Yeast strains, medium and culture **33**

2.7 Screening of filament-forming proteins **34**

2.8 Quantification of filament-forming proteins **34**

2.9 Protein-protein interaction analysis **35**

2.10 The budding yeast stress assays **36**

Chapter 3 Characterisation of the basic filament formation unit of cytoophidia

3.1 Introduction

3.1.1 CTP synthase functions as a tetrameric enzyme **37**

3.1.2 Oligomerization is a common way to regulate metabolic enzymes activity **42**

3.1.3 Several oligomeric metabolic enzymes self-assemble into electron microscope scale fibres **43**

3.1.4 Aims of this chapter **46**

3.2 Results

3.2.1 Transfection of S2R+ cells with CTPsyn-YFP induces cytoophidium formation. **47**

3.2.2 Mutation at the CTP synthase oligomer interface disrupts cytoophidium assembly **49**

3.2.3 Cytoophidium assembly occurs in response to nutrient stress in S2R+ cells **55**

3.3 Discussion

3.3.1 Models for cytoophidium assembly **57**

3.3.2 Cytoophidium assembly occurs in response to nutrient stress suggests cytoophidium is an inactive structure **59**

3.3.3 Model of molecular redistribution as a response to intrinsic and extrinsic signal. **60**

3.3.4 Other literature supporting the “inactive hypothesis” **63**

3.3.5 Comparison of function between IMPDH- and CTP synthase-based cytoophidia **67**

Chapter 4 Filamentation of metabolic enzymes in *Saccharomyces cerevisiae*

4.1 Introduction

4.1.1 Protein localization in the budding yeast **69**

4.1.2 Membraneless organelles in the budding yeast *Saccharomyces cerevisiae* **71**

4.1.3 Filament-forming proteins in *Saccharomyces cerevisiae* **72**

4.1.4 Growth phase regulation of the Yeast Saccharomyces cerevisiae **74**

4.1.5 Aims of this chapter **76**

4.2 Results

4.2.1 Foci-forming proteins in the budding yeast **77**

4.2.2 Filament-forming proteins in the budding yeast **82**

4.2.3 Heterogeneities of cytoophidia in *Saccharomyces cerevisiae* **88**

4.2.4 Nutrient deprivation induces filament formation in most cases **91**

4.2.5 Prolonged culturing cannot make foci-forming proteins form filaments **93**

4.2.6 Filamentation in the nucleus **94**

4.2.7 Clusters of filament-forming proteins **96**

4.2.8 Clusters of foci-forming proteins **97**

4.3 Discussion

4.3.1 Comparison of protein localization data with previous screening **102**

4.3.2 Limitations of this screening **102**

4.3.3 Summary **103**

Chapter 5 Growth and stress regulation of yeast ASNS filaments

5.1 Introduction

5.1.1 Asparagine synthetase catalytic activity and regulation **105**

5.1.2 Asparagine synthetase is relevant to human disease **108**

5.1.3 Stress pathways in the budding yeast *S. cerevisiae* **110**

5.1.4 Aims of this chapter **114**

5.2 Results

5.2.1 Filament formation of Asn1p, Asn2p and Ura7p keeps changing along the budding yeast growth curve **115**

5.2.2 Glucose deprivation induces filament formation **118**

5.2.3 Heat shock induces filament formation **120**

5.2.4 Cold shock induces filament formation **122**

5.2.5 Osmotic stress induces filament formation **124**

5.2.6 Oxidant hydrogen peroxide affects filament formation of ASN1 and ASN2 .. **126**

5.2.7 Summary of the stress-dependent Asn1p, Asn2p and Ura7p filaments **128**

5.3 Discussion

5.3.1 Is the budding yeast filament formation under stress regulated by transcriptional control? **132**

5.3.2 Comparison of Ura7p filaments stress reaction between the budding yeast *Saccharomyces cerevisiae* and the fission yeast *Schizosaccharomyces pombe* **135**

5.3.3 Conclusion **138**

Chapter 6 Overall Discussion

6.1 Chronological and systematic summary of current research on cytoophidia **139**

6.2 Oligomeric state and cytoophidium function **144**

6.3 Further study and challenges concerning the components of cytoophidia **147**

6.4 Is cytoophidium an enzyme stabilizer against protein degradation? A hypothetical model and future direction for analysing cytoophidium function **148**

6.5 The study on filament-forming proteins: the implications for diseases **151**

6.6 Concluding remarks **153**

References **154**

List of publication **166**

List of Figures

Figure 1.1 Cytoophidia found in several organisms 15

Figure 1.2 De novo synthesis of CTP catalysed by CTPS 16

Figure 1.3 IMPDH catalyses the synthesis of XMP as a rate-limiting step of de novo synthesis of guanine nucleotides 20

Figure 1.4 Process of cytoophidium assembly in a mammalian cell line 22

Figure 3.1 Diagram of CTP synthase molecular tetramerization 39

Figure 3.2 Point mutations on CTP synthase 40

Figure 3.3 Molecular structure of mutation sites at the CTP synthase oligomer interface 41

Figure 3.4 Samples of metabolic enzymes that self-assemble into fibres 45

Figure 3.5 Transfection of CTPsyn-YFP into S2R+ cells 48

Figure 3.6 Percentage of cells containing cytoophidia in untreated S2R+ and cells after transient transfection 48

Figure 3.7 Mutations at the CTP synthase oligomer interfaces disrupt cytoophidium assembly 52

Figure 3.8 Quantification of cytoophidium length in each mutant 53

Figure 3.9 Western blot data showing relative CTP synthase abundance in cells transfected with mutant CTP synthase expression constructs 54

Figure 3.10 Cytoophidium assembly occurs in response to nutrient stress 56

Figure 3.11 Model A: CTP synthase dimer is the basic unit of cytoophidium 58

Figure 3.12 Model B: CTP synthase tetramer is the basic unit of cytoophidium 58

Figure 3.13 One proposed model of cytoophidium assembly in response to nutrient or development conditions 62

Figure 3.14 The levels of glutamine in three groups of cells 68

Figure 3.15 The levels of nucleotide during DAU treatment in HEK 293T cells 68

Figure 4.1 Filament-forming proteins identified by Noree et al 73

Figure 4.2 Confirmation of filament-forming proteins in *S. cerevisiae* 83

Figure 4.3 Novel filament-forming proteins identified in *S. cerevisiae* 84

Figure 4.4 Filaments forming in the cytoplasm and nucleus 95

Figure 4.5 Protein-protein analysis of filament-forming proteins in the budding yeast 98

Figure 4.6 Protein-protein analysis of foci-forming (filament-forming proteins included) proteins in the budding yeast 100

Figure 5.1 Asparagine synthetase ribbon structure of *E.coli* 106

Figure 5.2 Continuing culturing of Asn1p, Asn2p and Ura7p GFP-tagged yeast. 117

Figure 5.3 Filament formation regulated by carbon nutrient starvation 119

Figure 5.4 Filament formation regulated by heat shock 121

Figure 5.5 Filament formation regulated by cold shock 123

Figure 5.6 Filament formation regulated by osmotic stress 125

Figure 5.7 Filament formation regulated by peroxide oxidative stress 127

Figure 5.8 Possible model for Asn1p/Asn2p and Ura7p filaments formation under stress 131

Figure 5.9 Transcript level data of Asn1/2p and Ura7p along growth curve and under stresses 134

Figure 6.1 A systematic view of subjects related to cytoophidia 141

Figure 6.2 A hypothetical model for cytoophidium function as an enzyme stabilizer 149

List of Tables

Table 3.1 Summary of CTP synthase-based cytoophidium formation conditions 61

Table 3.2 Mutants and their influence to filament formation from three individual studies ... 66

Table 4.1 Subcellular localization categories 70

Table 4.2 Foci-forming proteins in *S. cerevisiae* 78

Table 4.3 Filament-forming proteins in *S. cerevisiae* 85

Table 4.4 Comparison of percentage of cells containing cytoophidia between the exponential phase and the diauxic shift 90

Table 4.5 Comparison of the percentage of cells containing cytoophidia in nutrient-deprived cells and after the diauxic shift 92

Table 4.6 Table of filament-forming proteins related to glutamine/glutamate metabolism 97

Table 4.7 KEGG pathways analysis of filament-forming proteins in STRING 10 99

Table 4.8 Pathway analysis of foci-forming proteins 101

Table 4.9 Comparison of protein localization data with previous screening 104

Table 5.1 Summary of the stress responses of Asn1p, Asn2p and Ura7p filaments 129

Table 5.2 Summary of the stress responses of CTP synthase-based filaments in *S. cerevisiae* and *S. pombe* 136

Table 6.1 Chronological summary of key research related to cytoophidia 142

Table 6.2 Oligomeric state of filament-forming metabolic enzymes 146

List of Abbreviations

ACC	acetyl-CoA carboxylase
ALL	acute lymphoblastic leukaemia
ANLL	acute non-lymphoid leukaemia
ASN	asparagine
ASNase	asparaginase
ASNS	asparagine synthetase
ATP	adenosine triphosphate
cAMP	cyclic adenosine monophosphate
C-cytoophidium	cytoplasmic cytoophidium
CONV	5-chloro-4-oxo-L-norvaline
CPEC	cyclopentenyl cytosine
CRPC	castration-resistant stage of prostate cancer
CTP	cytidine triphosphate
CTPS	cytidine-5'-triphosphate synthase
CWI	cell wall integrity pathway
DAU	3'-deazauridin
DNA	deoxyribonucleic acid
DON	6-diazo-5-oxo-L-norleucine
DONV	5-diazo-4-oxo-L-norvaline
EM	electron microscope
FBS	fetal bovine serum
GEO	gene expression omnibus
GFP	green fluorescent protein
H_2O_2	hydrogen peroxide
HbS	sickle haemoglobin
HCC	hepatocellular carcinoma
HEp-2	human epithelial type 2
HSE	heat shock elements
HSP	heat shock protein
HSR	heat shock response
IMPDH	inosine monophosphate dehydrogenase

KEGG	Kyoto Encyclopedia of Genes and Genomes
MPA	mycophenolic acid
mRFP	monomeric red fluorescent protein
mRNA	messenger ribonucleic acid
NaCl	Sodium chloride
NAD+	oxidized nicotinamide adenine dinucleotide
NADH	reduced nicotinamide adenine dinucleotide
N-cytoophidium	nuclear cytoophidium
ORF	open reading frame
OSR	oxidative stress response
P-bodies	processing bodies
PBS	phosphate-buffered saline
PCR	polymerase chain reaction
PERK	protein kinase RNA-like endoplasmic reticulum kinase
PKA	protein kinase A
RNA	ribonucleic acid
ROS	reactive oxygen species
RR	rods and rings
rRNA	ribosomal ribonucleic acid
SGD	Saccharomyces Genome Database
STRE	stress responsive elements
TOR	target of rapamycin
XMP	xanthosine-5'-phosphate
YFP	yellow fluorescent protein

Chapter 1 Introduction

1.1 CTP synthase cellular compartmentation and the discovery of cytoophidia

Each cell is a complex factory in which thousands of biochemical reactions take place. Compartmentation, which means to spatially separate individual systems, improves cellular efficiency by facilitating the effective collision of certain biomolecules within a region and preventing the interference of other molecules. This is critical for the proper and effective functioning of any highly ordered living organisms.

Compartmentation is facilitated by the formation of membranous organelles. Mitochondria, the heart of the cell factory, provide a unique microenvironment by maintaining the optimal pH and ion conditions for ATP synthase to synthesize ATP as a cellular energy resource. The nucleus, the control centre, stores DNA sequences that are critical for replication and transmission of genetic information. In addition to these vital organelles, which have been comprehensively studied for several decades, many cellular-scale self-assembling structures made up of which are constituted by metabolic enzymes have been discovered in recent years. These intracellular bodies vary in shape from simple foci to complex filaments, and are equally diverse in enzymatic function, ranging from involvement in carbon or nitrogen metabolism to nucleotide biosynthesis. However, the roles of these newly discovered systems in cell remain unclear.

In 2010, three independent groups reported that cytidine-5'-triphosphate synthase (CTPS) could form a filamentous structure (Figure 1.1). The term "cytoophidia" was coined by one of these groups in recognition of its observed serpent-like structure in *Drosophila* cells. Cytoophidia were first identified in nurse cells and oocytes in *Drosophila melanogaster* [1]. Later on, cytoophidia were also identified by antibody staining in tissues including lymph glands, salivary glands, testes, accessory glands, the brain, the trachea and the gut [2]. At

approximately the same time, a similar structure was identified in bacteria *Caulobacter crescentus*. This structure was found to regulate the curvature of *C. crescents* cells independently of their catalytic function [3]. In the budding yeast *Saccharomyces cerevisiae*, two yeast CTP synthase proteins, Ura7p and Ura8p, were also found to form filamentous structures. This structure could transform from foci to filaments depending on the environment [4]. Shortly after this, in 2011, this structure was identified in mammalian cultured cells HeLa P4. Meanwhile, CTP synthase inhibitor DON was found to promote the formation of cytoophidia [5]. Another group identified that human epithelial type 2 (HEp-2) cells and mouse embryonic stem cells also contain cytoophidia. They referred to these filamentous structures as rods and rings (RR), based on their unique filamentous morphology in mammalian cells [6]. After this, cytoophidia were also identified in another kind of commonly used yeast, *Schizosaccharomyces pombe*. Detailed study on cytoophidium dynamics showed the asymmetric inheritance of cytoophidia in *S. pombe* [7].

With the discovery of more and more similar filament-forming proteins, in order to simplify the terminology, we refer to all these metabolic enzyme-containing serpent-shaped structures as cytoophidia in the following passages.

From prokaryotic single-cell model bacteria to eukaryotic single-cell model yeast and multiple-cell model fruit fly, mouse, or human tissue, CTP synthase-based cytoophidium exists across the whole kingdom of living organisms with a similar morphology, which suggests that it is a highly conserved structure during evolution. This high conservation not only indicates the relevance and popularity of cytoophidia, but also provides us with an opportunity to compare and borrow different studies from various organisms. These similarities and differences provide us with a better view on the evolution and diversity of cytoophidia. However, the emerging information about cytoophidia indicates that they might

behave quite differently in different organisms, reminding us to be careful when taking data and conclusions about cytoophidia from one organism and applying them to another.

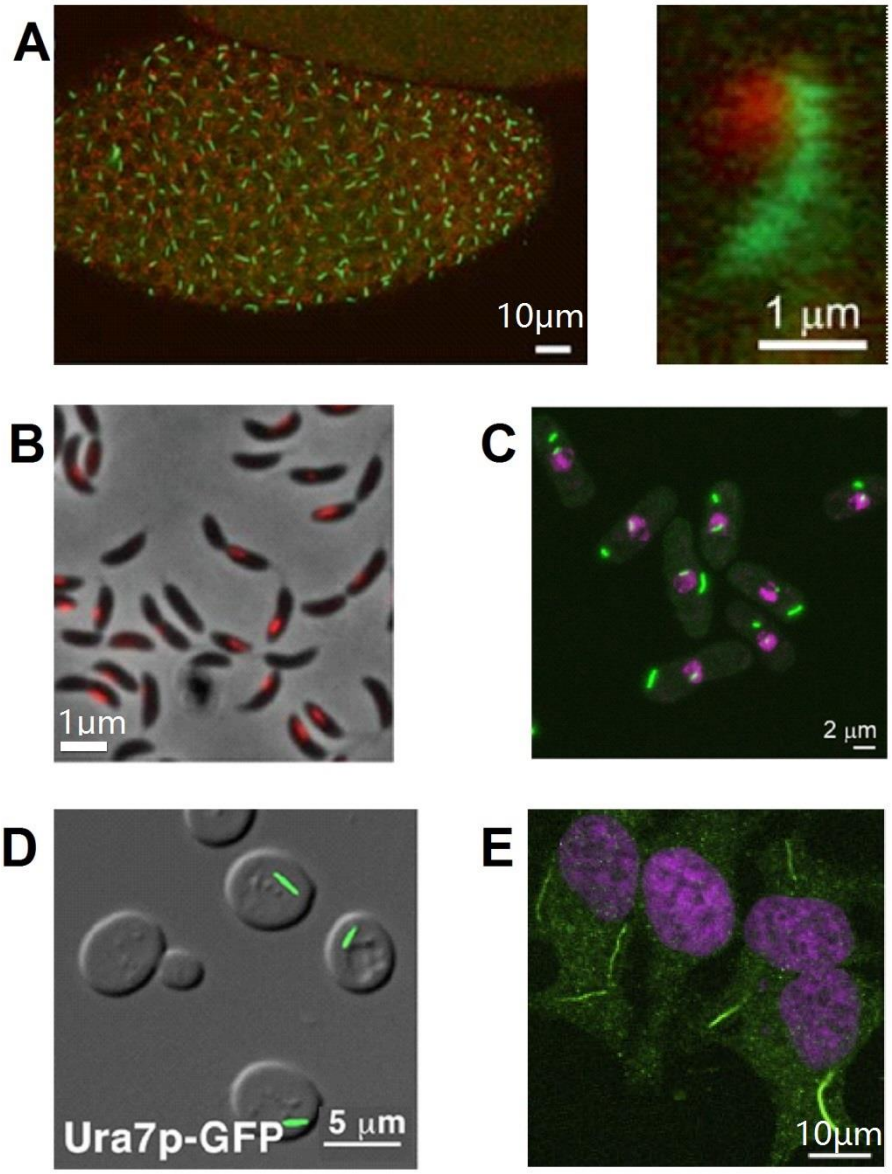


Figure 1.1 Cytoophidia found in several organisms

(A) CTP synthase assembles into cytoophidia in *D. melanogaster* egg chamber follicle cells [2]; **(B)** CTP synthase in *C. crescentus* as filamentous structures [3]; **(C)** CTP synthase expressed under the endogenous promoter in *S. pombe* as filamentous structures [7]; **(D)** CTP synthase in *S. cerevisiae* as filamentous structures [4]; (E) CTP synthase in human HeLa P4 cells as filamentous structures [5]

1.2 CTP synthase catalytic activity and regulation

The biochemical properties of CTP and CTP synthase provide first-hand information for understanding why and how CTP synthase assembles into filaments. CTP is a substrate for RNA synthesis, and is a coenzyme involved in the metabolism of glycerophospholipids and the glycosylation of proteins. It can be synthesized through either the salvage pathway or the de novo pathway. CTP synthase catalyses the rate-limiting step of the de novo CTP biosynthesis[8]. Without CTP synthase, the cell is unable to generate sufficient cytidine for CMP/CDP/CTP synthesis. CTP synthase catalyses the ATP-dependent phosphorylation on the 4-oxygen atom of UTP, resulting in the 4-carbon electrophilic and a vulnerability to reaction with ammonia[9] (Figure 1.2). Glutamine (Gln) is the amino group source in this reaction. This reaction also produces the by-product glutamate (Glu). Due to the high demand of nucleotides in cells, this enzyme also plays an important role in maintaining a glutamine-glutamate balance. However, in bacteria, CTP synthase can also utilize NH_3 as nitrogen source [10].

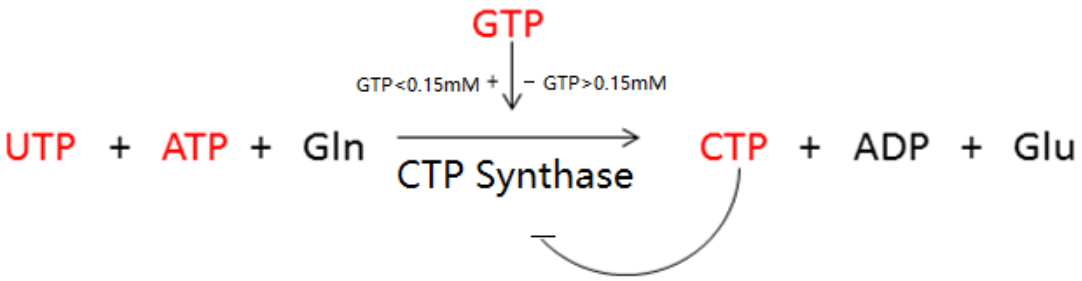


Figure 1.2 De novo synthesis of CTP catalysed by CTPS

All four nucleotides are involved in the CTP synthase catalysis mechanism. GTP acts as positive allosteric regulator at concentrations lower than 0.15mM and negative allosteric regulator at concentrations higher than 0.15mM. CTP acts as a negative allosteric regulator.

CTP synthase is tightly regulated by all kinds of nucleoside triphosphate. As substrates, the intracellular concentrations of UTP and ATP positively regulate the enzyme activity. As a product, CTP is a feedback inhibitor of CTP synthase, the binding site of which overlaps with that of UTP [11]. GTP functions as both a positive and negative allosteric regulator of CTP synthase. GTP activates Gln-dependent CTP synthase by promoting the hydrolysis of glutamine in normal concentrations. However, GTP inhibits Gln-dependent CTP formation at concentrations higher than 0.15mM, and inhibits NH3-dependent CTP formation at all concentrations [12]. In human cells, CTP synthase has been proven to be activated to its highest level at the physiological ATP, GTP and glutamine concentration [13].

CTP synthase inhibitors have been studied intensively over the previous decades as a promising target for cancer treatments. 6-Diazo-5-oxo-L-norleucine (DON) is one of the most studied inhibitors of CTP synthase. DON is a glutamine antagonist and a non-standard amino acid. It is used as an inhibitor for several glutamine-utilizing enzymes, including CTP synthase, Carbamoyl phosphate synthase, FGAR amidotransferase, Guanosine monophosphate synthetase, PRPP amidotransferase, Mitochondrial glutaminase, NAD synthase and Asparagine synthetase. Due to its similarity to glutamine, DON can enter the catalytic centre of these glutamine-utilizing enzymes and inhibit them by irreversible alkylation [14]. Acivicin and thiourea dioxide are also analogues of glutamine, and inhibit the enzyme activity of CTP synthase in a similar way to DON and other kinds of glutamine utilizing enzymes [15].

Another group of CTP synthase inhibitors are xanthine and its derivatives. The inhibition effect of purine ring to CTP synthase has been verified in xanthine, uric acids, caffeine, and other analogues. The inhibition effect of xanthine derivatives is believed to arise due to an effect of xanthine heterocycle on the quaternary structure of CTP synthase. Even though the inhibitor binding site is not known yet, it is suggested that unlike the glutamine antagonist

inhibitors, the xanthine based inhibitors do not appear to disrupt the ATP/UTP-dependent formation of CTP synthase tetramers and this inhibition effect is reversible [16].

CTP synthase is highly conserved across species. In the budding yeast *S. cerevisiae*, two genes, *URA7* and *URA8*, encode two isoforms of CTP synthase. However, in the fission yeast *S. pombe*, only one gene Cts1 encodes this enzyme. The CTP synthase genes between these two major yeasts share 62% identity. In humans, CTP synthase is encoded by two genes, *CTPS1* and *CTPS2*, which share 74.6% identity with each other. Human CTP synthase shares around 50% identity with the CTP synthase from yeast *S. cerevisiae*. In *D. melanogaster*, CTP synthase is encoded by a single gene, *CG6854*. This gene produces two transcript variants CTPsyn isoform A and CTPsyn isoform B. The sequence of CTPsyn isoform B is 91% identical with that of isoform A, yet only the isoform A forms cytoophidia. This is believed to be a consequence of the presence of a 56-aa region in the N-terminus of isoform A, not in isoform B [17].

In both *S. cerevisiae* and humans, both genes are redundant. The single copy of CTP synthase gene in *D. melanogaster* and *S. pombe* makes it easier to study without the redundant effect.

1.3 Cytoophidium components and assembly

Seven years have passed from the first discovery of cytoophidia. In these years, cytoophidia and similar filamentous structures were identified in more and more organisms. During this period of ground-breaking research, several key questions were discussed. What molecules are assembled on the cytoophidia? How do cytoophidium assemble from single molecules into filaments? What is the regulative system behind cytoophidium assembly, and what is its physiological function?

Components on cytoophidia

There is no doubt that the first member identified as cytoophidia is CTP synthase-based cytoophidia. In *Drosophila*, there are two transcript isoforms of CTP synthase: CTPsyn A (also named CTPsyn C in previous literature) and CTPsyn B. Only CTPsyn A protein forms cytoophidia [17]. Meanwhile, overexpression of CTPsyn A induced larger cytoophidia in *Drosophila* egg-chamber and culture cells [17-19].

Another component identified on cytoophidia is inosine monophosphate dehydrogenase (IMPDH). IMPDH is a metabolic enzyme which catalyses a rate-limiting step in de novo nucleotide biosynthesis. IMPDH catalyses the transition of inosine-5'-monophosphate (IMP) into xanthosine-5'-phosphate (XMP) and generates NADH from NAD+ at the same time (Figure 1.3). In the next steps, XMP is converted into GMP. IMPDH controls the balance of AMP and GMP. It is a fundamental enzyme in almost all organisms, related to DNA/RNA synthesis metabolism.

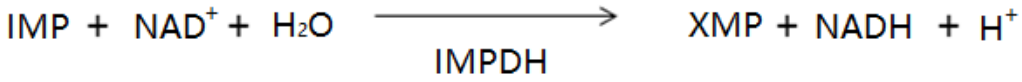


Figure 1.3 IMPDH catalyses the synthesis of XMP as a rate-limiting step of de novo synthesis of guanine nucleotides

IMPDH was first believed to be always co-localized with CTP synthase on cytoophidia, therefore CTP synthase-based cytoophidium and IMPDH based-cytoophidium were believed to be identical [6]. However, a more precise study on IMPDH-based cytoophidia indicated that CTPS and IMPDH were localized in two independent and different cytoophidia. Sometimes they co-localized in the same filamentous structures for some unknown reasons. However, in most situations, these two kinds of cytoophidia were completely separate [20].

In the budding yeast *S. cerevisiae*, two genes encode CTP synthase, i.e. *URA7* and *URA8*. Ura7p and Ura8p were found to be exactly co-localized. There is a partial co-localization among Psa1p (GDP-mannose pyrophosphorylase), Glt1p (Glutamate synthase) and Ura7p [4].

Assembly of cytoophidia

The assembly of CTP synthase into cytoophidia in NIH/3T3 cells was studied by Gou et al. in 2014 [19]. In this study, live imaging video of GFP-fused CTP synthase showed the whole process of cytoophidium formation. First, disperse CTP synthase formed small dots in cytoplasm, which gradually grew into small filamentous structures, shorter and thinner than that of the mature cytoophidia. Later, small filaments fused into large cytoophidia in cytoplasm. Two small cytoophidia were able to fuse, either end to end to form a longer

cytoophidium, or side to side for a thicker cytoophidium. Repeated fusion of small cytoophidia finally resulted in mature linear cytoophidia. Sometimes these linear cytoophidia fused its own ends and became a circle [19]. One review paper divided this process into five phases: nucleation, elongation, fusion, bundling and circularization [20] (Figure 1.4).

Nuclear localized cytoophidia

When it was first discovered, cytoophidium was believed to assemble in cytoplasm. This seemed reasonable, since CTP synthase is an enzyme which catalyses a reaction in cytoplasm. However, nucleus localized cytoophidia were identified in mammalian cell lines and *S. pombe* in 2014 in two independent studies [7, 19]. In Chapter 4 of this thesis, I also described the nuclear localization of CTP synthase-based cytoophidia and asparagine synthetase-based cytoophidia in the budding yeast. Morphologically speaking, nuclear cytoophidia are much thinner and shorter than their cytoplasm equivalents. The molecular and functional differences between nuclear and cytoplasmic cytoophidia are still unknown.

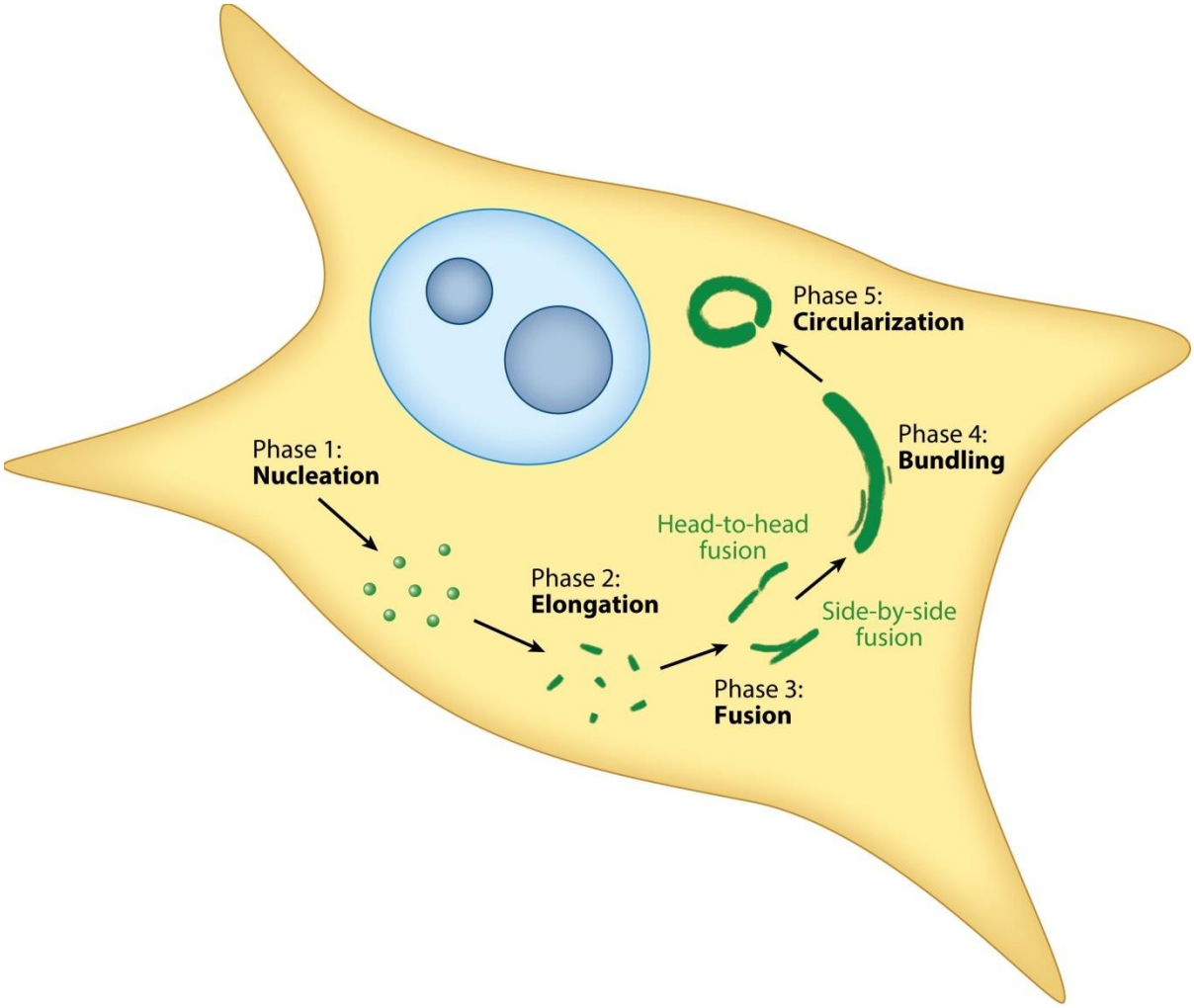


Figure 1.4 Process of cytoophidium assembly in a mammalian cell line

The process of cytoophidium assembly in mammalian cell line is divided into five phases: nucleation, elongation, fusion, bundling and circularization. Picture adapted from [21]

1.4 Cytoophidium regulation and function

Regulation of cytoophidia

The cytoophidium is a dynamic organelle like structure, and its assembly and disassembly of cytoophidium happen at the same time as a chemical equilibrium. The assembly and disassembly are tightly regulated by metabolic pathways and environmental conditions.

As the basic component of cytoophidia, it is no surprise to find that the CTP synthase level has an impact on cytoophidium assembly. In follicle cells of the *Drosophila* ovary, RNAi of CTP synthase gene caused the disassembly of cytoophidia [5], and overexpression of CTP synthase increased either the length or the thickness of cytoophidia [17]. In *C. crescents*, overexpression of CTP synthase not only increased the length and thickness of cytoophidia, but also changed the shape of the cell [3].

The proto-oncogene Myc was also found to regulate cytoophidium assembly in *Drosophila*. In the normal development process of a fly egg chamber, the cytoophidia in the follicle cells disassemble significantly during the transition from stage 10A to stage 10B, which coincides with the drop of Myc expression. Experiments proved that the knock-down of Myc resulted in the disassembly of cytoophidia before stage 10A, and the overexpression of Myc resulted in cytoophidium assembly after stage 10B. Myc is necessary for cytoophidium assembly [22]. Quantitative PCR results showed that CTP synthase mRNA level decreased when Myc was knocked down, and overexpression of Myc increased the CTP synthase mRNA level, indicating that Myc may affect cytoophidium assembly by regulating the protein level of CTP synthase.

Another study suggested that proto-oncogene Cbl (an E3 ubiquitin ligase) controls the filament assembly of CTP synthase in *Drosophila* without changing the protein level of CTP

synthase. Proteasome inhibitor MG132 resulted in the disassembly of cytoophidia, and deubiquitinase inhibitor Pr619 protected cytoophidia from the disassembly effect of MG132 treatment. It is still unclear whether Cbl controls CTP synthase filamentation through direct ubiquitination, but the importance of Cbl in cytoophidium regulation has been verified [23].

CTP synthase inhibitor DON has been shown to regulate the filament assembly of cytoophidia. DON treatment promotes the assembly of cytoophidia in *Drosophila* and mammalian cell lines [5], but it disassembles cytoophidia in *C. crescents* [3]. The reasons underlying the difference in DON regulation between these systems still remains unexplained.

Environmental conditions also regulate cytoophidium assembly. In the budding yeast *S. cerevisiae*, nutrient stress such as glutamine deprivation and carbon deprivation induces the formation of CTP synthase-based cytoophidia [4]. The study of environmental regulation of cytoophidia is one of the major topics of this thesis. More examples of cytoophidia regulated by environmental stress in *Drosophila* and the budding yeast will be presented and discussed in Chapters 3 and 5.

The function of cytoophidia

In prokaryotic systems, cytoophidia, which cover almost the whole length of bacteria cell, have been shown to function as a cytoskeleton and play an important role in maintaining cell shape [3]. However, in other systems, this effect is weak and not yet reported.

Cytoophidia have also been found to play an important role in development. Cytoophidia in *Drosophila* egg chamber follicle cells disassembled during the transition from stage 10A to 10B. In *Drosophila* larvae, cytoophidia disassembled during the reactivation of developmentally arrested neuroblasts [18]. However, the concrete reason for cytoophidia disassembly and assembly during those developmental processes remains elusive.

Three studies in 2014 pointed to the assembly of cytoophidia as a way of enzyme activity regulation. Even though three totally different organisms were used in these three studies, similar conclusions were put forward on cytoophidium function. The studies suggested that cytoophidia contained inactive CTP synthase. The assembly into filament covered the active site of CTP synthase and inhibited the enzyme activity of CTP synthase [18, 24, 25]. Chapter 3 of this thesis is also published as a part of Aughey et al. 2014[18]. Details on the storage function and enzyme activity sequestering will be presented in Chapter 3.

Apart from the function above, some function was predicted from the presently known properties of cytoophidia. As the formation of filament effectively protects most proteins from degradation, combined with the theory of inactivation of enzyme on CTP synthase-based cytoophidia, it is believed that the assembly of metabolic enzymes can prolong protein half-life, prevent unnecessary protein degradation, and sequester unnecessary enzyme activity. When cells re-enter proper growing conditions, cells are able to react to the new environment as quick as possible thanks to these storage bodies [21].

1.5 Difference and interaction of self-assembling structures: IMPDH based-cytoophidia as an example

IMPDH was first found to assemble into filamentous structures in cells under the treatment of an IMPDH inhibitor, mycophenolic acid (MPA), in 2006. EM-scale fibres were also observed under MPA treatment [26]. After the discovery of CTP synthase-based cytoophidia, IMPDH and CTP synthase were found to co-localize on the filament or ring-like structures under the treatment of CTP synthase inhibitor DON and Acivicin, and IMPDH inhibitor Ribavirin in mammalian cell line HEp-2 [6]. In this study, IMPDH and CTP synthase appeared to co-localize on the same structure all the time. However, in a more detailed later study, IMPDH-based cytoophidia and CTP synthase-based cytoophidia were proven to be two totally independent filamentous structures in both HeLa cells and COS-7 cells [20]. These two filaments reacted differently in response to different treatment. IMPDH-based cytoophidia were induced under DON, MPA and ribavirin, while CTP synthase-based cytoophidia were only sensitive to DON treatment. A partial (31%) co-localization of these two cytoophidia was only found under DON treatment [20]. Another study showed that IMPDH-based cytoophidia were detected in 293T cells, while CTP synthase-based cytoophidia were hardly detectable. The treatment of MPA induced the assembly of independent IMPDH-based cytoophidia and CTP synthase-based cytoophidia.

The treatment of another kind of CTP synthase inhibitor 3'-deazauridin (DAU) induced IMPDH-based cytoophidia and CTP synthase-based cytoophidia at the same time. However, the co-localization and abundance of these two kinds of cytoophidia kept changing after treatment. More hybrid cytoophidia and IMPDH-based cytoophidia were found in the first two hours after treatment than during the following hours [27]. These results show that these two kinds of cytoophidia are independent but interact with each other under certain conditions, and that both cytoophidia are in very strict and precise regulation.

1.6 Filament-forming proteins and their relevance to human diseases

CTP synthase and IMPDH are indispensable for DNA replication and cell proliferation, as the enzymes that are essential for de novo synthesis of purine and pyrimidine nucleotides. Since the fast-growing cells are much more sensitive to the functional fluctuation of metabolic enzymes than other cells, both CTP synthase and IMPDH are hot targets for cancer treatment. In a rat hepatoma model, CTP synthase activity was found to increase fourfold in medium-growth tumours and tenfold in fast-growing tumours [28]. A kind of CTP synthase inhibitor cyclopentenyl cytosine (CPEC), showed promising activity in some malignancy models, especially acute non-lymphoid leukaemia (ANLL). A Phase I trial of this drug has been undertaken in patients with solid tumours, but an unexplained cardiotoxicity occurred in some patients [29]. Recently, it was also reported that the loss-of function of *CTPS1* in humans impaired the response to antigen receptor-mediated activation of activated T and B cells, thus causing a kind of novel immunodeficiency. This study also suggested *CTPS1* as a possible therapeutic target for immunosuppressive drugs [30].

Regarding the relations of filamentation and cancer pathways, proto-oncogene Myc and Cbl in *Drosophila* were found to regulate the filament assembly of CTP synthase. This suggests the regulation of proto-oncogenes to cytoophidia. Cytoophidia can be an indicator for cancer or other abnormal cells through a detailed study.

The rods and rings (namely cytoophidia) structures were also found to be prevalent in HEp-2 cells of hepatitis C patients after interferon and ribavirin treatment through the immunostaining of human autoantibodies [31].

Even though there has been much study of CTP synthase inhibitors over the past decades, no CTP synthase inhibitors are currently being used as clinic drugs due to its toxicity. The study

on cytoophidia and its regulation on CTP synthase may open a new door for drug design by suggesting a potential mild regulation of cytoophidia to CTP synthase enzyme activity.

1.7 Model organisms: The *Drosophila* cell line and the budding yeast *S. cerevisiae*

In this thesis, the *Drosophila* cell line S2R+ and the budding yeast *S. cerevisiae* are chosen to be the major model organisms.

Drosophila was first used as a model organism in Thomas Hunt Morgan's putative genetic experiments in 1908. After that, *Drosophila*, with its irreplaceable advantages, became a popular organism in genetics, cell biology, and developmental biology. *Drosophila* is a very small and easy-culturing organism, with a short generation time and large number of descendants, saving lots of time and cost during research. Meanwhile, there are lots of genetic tools for *Drosophila* model, such as balancer chromosomes, transposon-mediated mutagenesis, RNAi gene interference, the UAS-GAL4 expression system, and CRISPR gene editing. The prosperity of *Drosophila* research has also led to a boom in serious *Drosophila* resources such as stock centres, specific antibodies, expression vectors, and cell lines. The *Drosophila* model is also a very good simulation for human diseases. Around 60% of *Drosophila* genes are conserved in human genome, and 77% of genes in human diseases, have orthologues in *Drosophila* [32, 33]. The single copy of CTP synthase gene in *Drosophila* also simplifies gene manipulation processes during research, compared with organisms with redundant CTP synthase genes (such as mammalian and yeast systems).

There are several reasons to choose the *Drosophila* cell line S2R+ as the model organism in the study of Chapter 3 on dimerization and tetramerization mutants of CTP synthase. Firstly, the endogenous CTP synthase level in the S2R+ cells is low, and cytoophidia do not assemble in the normal conditions. This provides a clear background for the overexpression study of mutant CTP synthase. Secondly, the mutants in S2R+ can easily be introduced into

Drosophila in vivo systems for follow-up study from the perspective of development. Finally, to prove the inactive model of cytoophidia, we also introduced results on filament assembly in *Drosophila* tissue development and tissue starvation reactions. Using S2R+ cells line kept up the consistency of organism in the whole research.

The budding yeast *S. cerevisiae* genome was the first eukaryotic genome to be sequenced in 1996 [34]. Since it shares a similar regulation network with humans as a eukaryotic model, the yeast system is mostly used for the study of gene regulation mechanisms and cellular processes. As a model organism, the budding yeast *S. cerevisiae* is small, tough, quick-growing and easy-culturing. With a total number of around 6,000 genes, it is commonly used for high-throughput screening studies. There are also lots of genetic tools in the budding yeast, such as gene expression plasmids, gene replacement, and yeast two-hybrid systems.

The budding yeast system is used in Chapters 4 and 5 on the screening of filament-forming proteins and the study of filament assembly under stresses for the following reasons. First, there is a commercialized endogenous GFP-tagged library for the budding yeast, which enables the high-throughput screening of filament and foci-forming proteins in Chapter 4. The current data in yeast protein networks also enables an effective analysis of protein-protein interaction among those filament-forming proteins. Moreover, the previous studies in protein regulation and stress reaction in the budding yeast *S. cerevisiae* may provide explanation for the assembly of asparagine synthetase-based cytoophidia under stresses in Chapter 5.

1.8 Project aims and thesis structure

The studies on cytoophidia began in 2010. Research conducted over the last seven years has provided us with a brief view on the components, regulation, and function of cytoophidia. However, the study of cytoophidia is still in its infant stage. Every new discovery may provide us with totally new concepts and views on cell biology and developmental biology. The newly developed methods in molecular biology, bioinformatics and other related subjects also make the process of studying cytoophidia different from other organelles and organelle-like structures. In this thesis, I sought to answer questions from several perspectives for a deeper and wider understanding on cytoophidia.

In Chapter 3, from the perspectives of cytoophidium structure and function, I examined a group of mutants for effects on the dimerization and tetramerization interphases of *Drosophila* CTP synthase in S2R+ cells. Through the identification of those mutants, I unveiled the relationship between oligomerization of CTP synthase molecules and cytoophidium assembly. I concluded that cytoophidia are composed of dimer-form inactive CTP synthases and function as a storing pool for inactive CTP synthase.

In Chapter 4, in order to discover new filament-forming proteins, I conducted a screening with two colleagues (Hakimi Kassim and Yong Huang) of the whole set of yeast GFP clone collection (4,159 strains) for filament-forming proteins after one day of culturing. The results showed all filament-forming or foci-forming proteins found after one day of culturing. I also researched the function and relationships of those filament-forming proteins, especially metabolic enzymes. This part of the research drew a whole map of filament-forming proteins and thus provided us with a good opportunity to link metabolic pathways and cell compartmentalization.

In Chapter 5, from the perspective of regulation and stress reaction pathways, I focused on the filament-forming proteins Asn1p and Asn2p (which share some common attributes with CTP synthase) and conducted experiments on the influence of the growth stages and the stresses on the assembly of filament or foci structures of asparagine synthetase and CTP synthase in the budding yeast *S. cerevisiae*. This part of the research project provides us an overall view on the interplay between cytoophidium formation and stress pathways, and casts light on the discovery of potential filament regulators or regulation pathways.

In Chapter 6, I discuss these findings in the context of the current understanding of cytoophidia, and make recommendations for the following steps of cytoophidia and cellular compartmentation studies.

Chapter 2 Materials and Methods

2.1 S2R+ cell culture

S2R+ cell lines were obtained from the *Drosophila* Genome Resource Centre (DGRC). The complete medium for S2R+ cells is Schneiders Invitrogen (Catalogue no. 11720-034) *Drosophila* Medium, containing 10% heat-inactivated fetal bovine serum (FBS). Heat-inactivated FBS is added to a final concentration of 10% before use. Cells are cultured at 30°C without CO_2 requirement. For general maintenance of cells, pass S2R+ cells when cell density is between 0.6 to 2×10^7cells/ml and split at a 1:2 to 1:5 dilutions.

2.2 Transfection of S2R+ cells

S2R+ cells were diluted to 1×10^6cells/ml and left to settle on coverslips in a 24-well plate overnight. 1µg of DNA and 3µL of Fugene-HD were added to 50µL of water and left at room temperature for 20 minutes. The DNA-Fugene solution was dropped evenly onto the S2R+ cells and left for transfection for 24 hours. A final concentration of 0.7mM $CuSO_4$ was added to induce protein expression for 10 hours before harvesting after the use of metallothionein promoter in expression vectors.

2.3 S2R+ cells stable lines selection

To generate stable cell lines, expression constructs were co-transfected with pCo-Puro, a puromycin resistance plasmid, in a ratio of 9:1, and grown in Schneiders medium containing 7µg/ml puromycin for 2 weeks. Transfected cells were collected every 4-5 days by centrifugation, and cell pellets were re-suspended in fresh medium containing 7 µg/ml puromycin. Standard growth and maintenance techniques established for S2R+ cells were applied. In particular, the cells were never allowed to be at a density below 2×10^6 cells/ml.

Protein expression was induced with 0.5mM $CuSO_4$ when the cell density reached 7.5×10^6 cells/ml.

2.4 S2R+ cell immunofluorescence and microscopy

All cells were fixed in 4% paraformaldehyde in PBS for 10 minutes and washed with PBT (1X PBS + 0.5% horse serum + 0.3% Triton X-100). Tissues were incubated in primary antibodies overnight, washed with PBT then incubated overnight in secondary antibodies. Hoescht 33342 (1µg/ml) was used to label DNA. Samples were imaged by confocal microscopy. ImageJ software was used for image processing and cytoophidium length measuring.

2.5 Generation of CTP synthase point mutation expression vectors

Destination vectors were constructed with Gateway method. pENTR/D-TOPO CTPS-C was constructed by Azzam G. Single base pair substitutions were made on entry vector by the Quickchange mutagenesis method. PCR primers were designed to include the nucleotide of interest. PCR was performed on the entry vector using Phusion high fidelity polymerase (NEB). After amplification, template DNA was digested by Dpn1. Mutated plasmid was purified with MinElute low volume PCR purification kit (Qiagen) and transformed into *E. coli* DH5α cells.

pMT-W, pMT-WV, pMT-VW were used as a recombination backbone of destination vector for S2R+ cell expression. pMT-W, pMT-WV, pMT-VW are modified from pAW, pAWV, pAVW by Aughey G. with the substitution of metallothionein promoter.

2.6 Yeast strains, medium and culture

The *S. cerevisiae* strains used in this study were derived from the yeast GFP clone collection comprising 4159 GFP-tagged ORFs [35]. All yeast strains originate from a parent strain with

the genotype MATα his3Δ1 leuΔ0 met15Δ0 ura3Δ0 (S288c). During the screening, all yeast strains were replicated into 96-well plates consisting of 150 μL of YPD medium using a pin tool and sealed with MicroAmp™ adhesive film to reduce well-to-well contaminations. All strains were grown at 32°C for 24 hours for the screening of filament-forming proteins.

YPD medium used in the experiment are YPD broth (Y1375 Sigma) with the components as Bacteriological peptone, 20 g/L, Yeast extract, 10 g/L, Glucose, 20 g/L; YPD agar (Y1500 Sigma-Aldrich) with the components as Bacteriological peptone, 20 g/L, Yeast extract, 10 g/L, Glucose, 20 g/L, Agar, 15 g/L.

2.7 Screening of filament-forming proteins

Cells were fixed in 4% paraformaldehyde for ten minutes. The fixed cells were washed by PBS, then cells were visualised under 40 times objective on an inverted microscope (Nikon Eclipse Ti, Japan). Cells showing filaments were picked out for confocal imaging. Hoechst 33342 was added for nucleus visualisation. Imaging of fixed samples was acquired under 63 times objective on a laser-scanning confocal microscope (Leica TCS SP5 II confocal microscope, Germany).

2.8 Quantification of filament-forming proteins

All yeast strains were grown overnight and diluted to an OD_{600} of ~0.05 in 3 mL of YPD at 32°C in the incubator (300 r/min) and kept for a certain time according to experimental purposes. For stress assays, cells were exposed to stresses for a certain time before fixation.

Cells were transferred into 1 mL micro centrifuge tubes and spun down for 1 min at 4000 r/min. The medium was decanted and 100 μL of 4% paraformaldehyde was added to each tube to fix the cells for 10 min, and then the cells were washed twice with PBS.

Before visualization, a few microliters of cell suspension were transferred onto the slides, followed by hot agarose gel (60°C) to avoid movement of the cells during imaging. The samples were covered with coverslips and inverted, and some pressure was applied to remove excess liquid. The coverslips were further sealed with nail polish to avoid drying out the samples. Once the nail polish had dried, the samples were ready for microscopic analysis.

The percentage of cells containing filaments was quantified by capturing images in at least four different areas containing a minimum of 100 cells each, using a laser-scanning Leica TCS SP5 II confocal microscope with a 63 times oil objective lens. The average length of filaments was calculated by at least 100 randomly chosen filamentous structures from captured images. All images were taken at multiple focal planes and then compressed into a single image.

Image processing was carried out using ImageJ software. The experiments were repeated three times independently, and data were presented as a 95% confidence interval in most situations in the bar graph. The data were analysed by One-Way Anova (multiple comparisons) to reveal differences.

2.9 Protein-protein interaction analysis

Protein-protein interaction analysis was carried out by using the “Search Tool for the Retrieval of Interacting Genes/Proteins” (STRING) database version 10 (http://string-db.org/) [36]. In the networks from STRING, nodes are proteins and edges are the predicted functional associations between proteins based on primary databases containing KEGG and GO and primary literature. Various active prediction methods can be chosen for STRING analysis, such as neighbourhood, gene fusion, co-occurrence, co-expression, experiments, databases, homology and text mining. In the current study, all of the prediction methods were used with medium confidence score 0.400.

2.10 The budding yeast stress assays

In the glucose deprivation assay, the exponential phase cells (12 hours culturing) were centrifuged and added into standard medium, YP medium (1% yeast extract, 2% peptone), distilled water, and 2% glucose solution. After one hour at culturing 32°C, cells were fixed and pictures were taken by confocal microscopy. In the glucose recovery assay, 2% glucose was added into the culturing system. After one hour at culturing 32°C, cells were fixed and pictures were taken by confocal microscopy.

In the heat shock assay, cells were cultured to the desired phase and treated with 37°C heat shock for one hour, 42°C heat shock for five minutes, or 32°C for one hour control. After heat shock, cells were fixed and pictures were taken by confocal microscopy.

In the cold shock assay, cells were cultured to the desired phase and treated with 0°C cold shock for one hour or 32°C for one hour control. After the cold shock, cells were fixed and pictures were taken by confocal microscopy.

In the osmotic stress assay, cells were cultured to the desired phase and treated with NaCl at the final concentration of 0.5M or 1M at 32°C for one hour. After treatments, cells were fixed and pictures were taken by confocal microscopy.

In the oxidative stress assay, cells were cultured to the desired phase and treated with H_2O_2 at the final concentration of 0.2mM or 2mM at 32°C for one hour. After treatments, cells were fixed and pictures were taken by confocal microscopy.

Chapter 3 Characterisation of the basic filament formation unit of cytoophidia

3.1 Introduction

3.1.1 CTP synthase functions as a tetrameric enzyme

CTP synthase consists of two domains, a synthase domain (also named as ALase domain) and an aminotransferase domain (also named as GATase domain). Previous studies have shown that neither monomer nor dimer units have enzyme activity. CTP synthase is only functional in its tetrameric form [37-39]. CTP synthase assumes this tetrameric structure in the presence of its substrates, ATP and UTP. At low concentrations of ATP and UTP, the active CTP synthase tetramer dissociates first into dimeric and then to monomeric units [40]. When the subunit concentration increases, polymerization occurs [37]. Removal of Mg^{2+} or UTP will reduce the tetramer forming under a detectable level. Removal of ATP or CTP can partially reduce the tetramer forming of enzyme. Even though tetramerization is necessary for enzyme activity, enzyme activity is not a necessity for tetramerization. The inhibition effect of CTP to CTP synthase does not disturb CTP synthase tetramerization [39]. Meanwhile, the presence of CTP synthase inhibitors thiourea dioxide and DON prevents the formation of tetramer from dimer [40]. The aminotransferase domain has been found to locate away from the interface that is involved in tetramer formation, so that the former is not altered or obstructed during oligomer formation. A diagram of CTP synthase tetramerization is shown in the following figure (Figure 3.1).

A detailed study on CTP synthase tetramer structure of *S. solfataricus* provided us with a list of monomer-monomer interfaces and dimer-dimer interfaces of CTP synthase (Figure 3.2). In the following research, I choose 5 sites from this list and verify their counterparts in

Drosophila CTP synthase. The reconstruction of *Drosophila* CTP synthase tetramer structure proved that the sites V114, M156, and E160 were on the monomer-monomer interphase and the sites G151 and R163 were on the dimer-dimer interphase of CTP synthase (Figure 3.3).

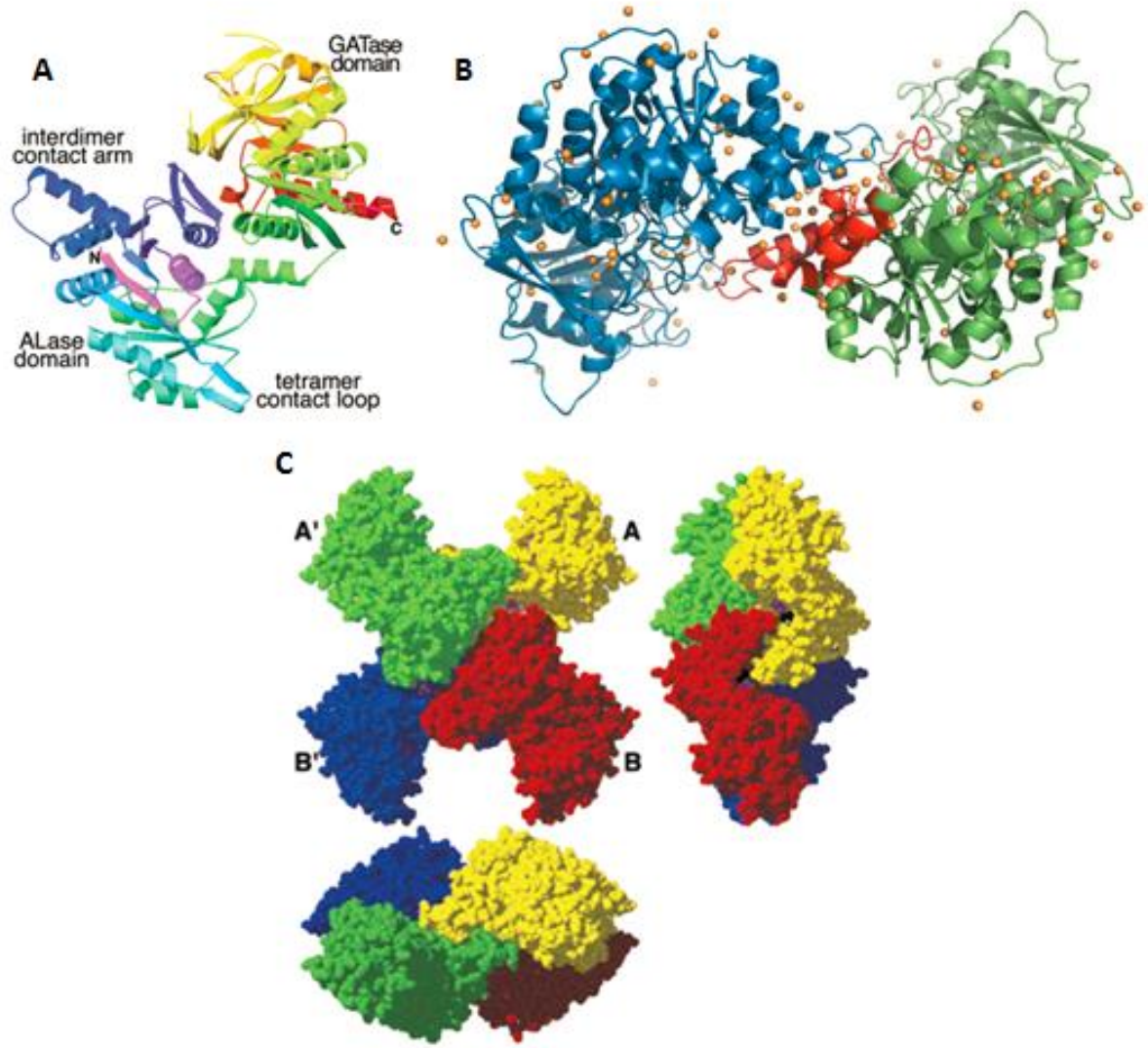


Figure 3.1 Diagram of CTP synthase molecular tetramerization

(A) Ribbon diagram of the *E. coli* CTP synthase monomer (picture adapted from [41]); **(B)** Dimeric structure of *S. solfataricus* CTP synthase. Molecule A is displayed in green and molecule B in blue. The dimeric interface of the A molecule is shown in red. Water molecules are shown in orange (picture adapted from [42]); **(C)** Three views of the *E.coli* CTP synthase tetramer, along the crystallographic b axis (left), a axis (right), and c axis (bottom). The unique molecules in the asymmetric unit, A and B, are related to their A' and B' symmetry mates by the crystallographic 2-fold axis along c. The tight soluble dimers, A-A' and B-B', tetramerize via the A-B and A'-B' interfaces in response to ATP and UTP binding [41].

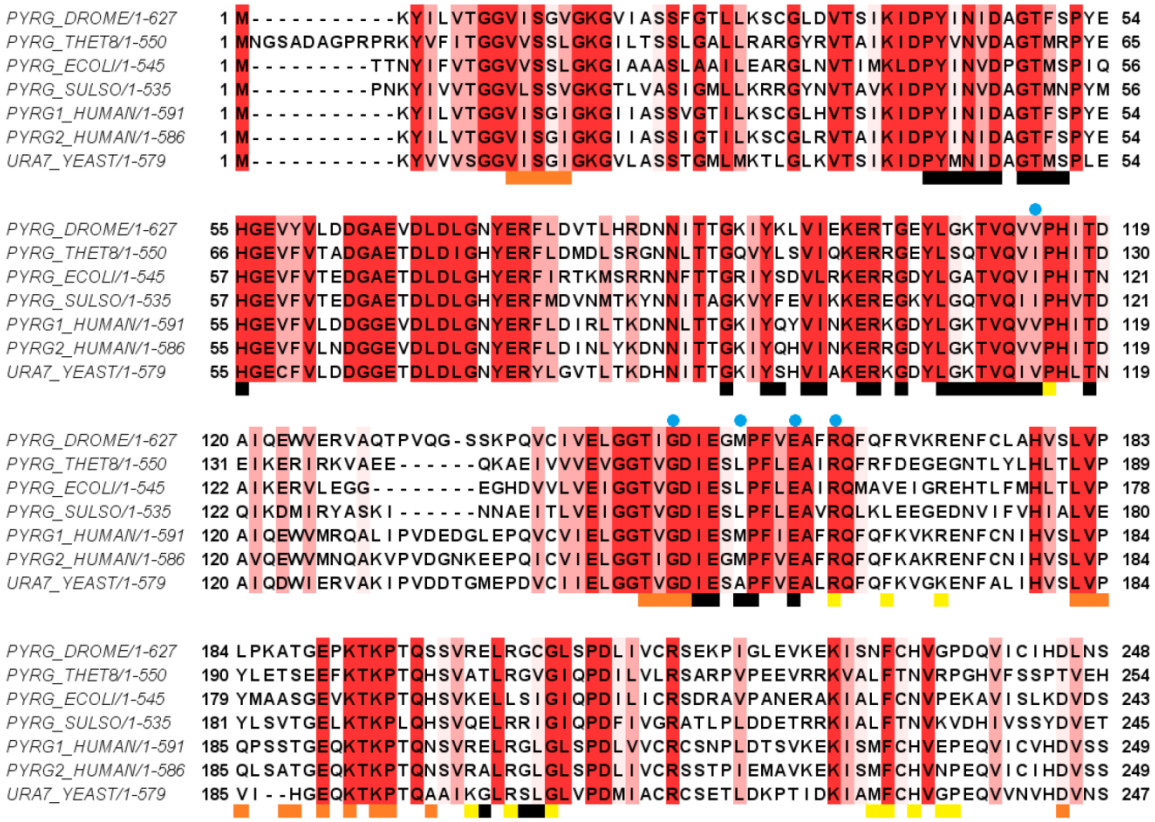


Figure 3.2 Point mutations on CTP synthase

Sequence alignments of CTP synthase orthologues include *Drosophila* (cytoophidium-forming isoform), *T. thermophilus*, *E. coli*, *S. solfataricus*, human *CTPS1*, human *CTPS2* and *S. cerevisiae*. Black bars indicate predicted monomer-monomer interfaces, orange bars indicate predicted dimer-dimer (tetramer) interfaces, and yellow bars indicate other tetramer interfaces. The interface site data are from *S. solfataricus* CTP synthase structure [42]. Identical residues in the alignment are marked by red boxes; similar residues are shown in lighter red. Mutants described in this study are marked with blue circles on top.

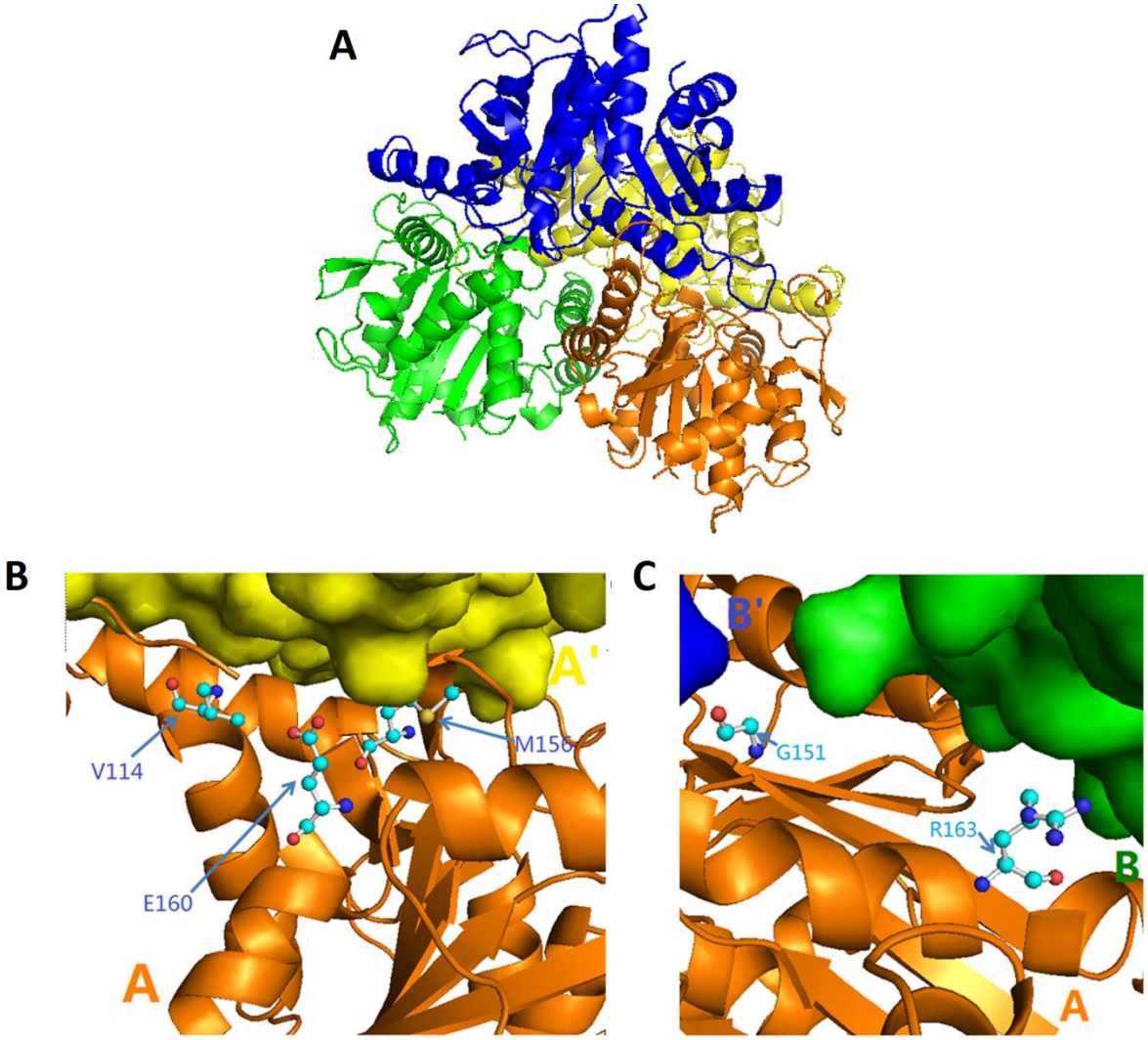


Figure 3.3 Molecular structure of mutation sites at the CTP synthase oligomer interface

(A) The CTP synthase tetramer consists of a pair of dimers, shown in yellow/orange and green/blue; **(B)** Mutagenesis sites on dimer interface of A (orange)-A' (yellow) (CTPsyn^{V114F}, CTPsyn^{M156I} and CTPsyn^{E160K}). A' is shown as surface view, and mutated residues are shown with individual atoms. Red: oxygen, dark blue: nitrogen, light blue: carbon, yellow: sulphur; **(C)** Mutagenesis sites on tetramer interface of A (orange)-B (green) (CTPsyn^{R163H}), A-B'(blue) (CTPsyn^{G151E}). B and B' are shown as surface view, and mutated residues are shown with individual atoms. Red: oxygen, dark blue: nitrogen, light blue: carbon (pictures were generated with pyMOL)

3.1.2 Oligomerization is a common way to regulate metabolic enzymes activity

Oligomeric proteins, which have the ability of forming a larger polymer or oligomer by two or more subunits, are believed to constitute 35% of the total protein sets [43]. Metabolic enzymes constitute a large subunit of these proteins. About 70% to 80% metabolic enzymes have the ability to form oligomer under physiological conditions [44, 45]. The average oligomeric state is tetrameric [46]. Oligomeric proteins with a higher number of subunits are less prevalent, and even-numbered oligomeric proteins are much more than odd-numbered ones [44, 45]. Most oligomeric proteins are symmetrical [23].

Several evolutionary advantages are believed to have led to the prevalence of oligomeric proteins. The most significant advantage of oligomerization is that oligomerization is the foundation for cooperativity and allosteric regulation, introducing an additional regulation approach for enzyme activity [47]. Oligomerization also provides additional active sites for proteins. Roughly one-sixth of oligomeric enzymes have active sites at subunit interfaces. Moreover, from the aspect of transcription and translation, the likelihood of error increases greatly along with the size of protein. A larger size of functioning oligomer can be produced with less error through oligomerization than by direct synthesizing. The formation of larger oligomers is also believed to combat protein degradation and denaturation. From the aspect of evolution, oligomeric proteins are subjected to amplified selective pressure, which leads to earlier selection for both beneficial and deleterious mutants [48]. The major disadvantages of oligomerization and all high-order aggregates might be the slow diffusion rate, which limits the rates of effective collision with substrate and thus reaction efficiency [49].

3.1.3 Several oligomeric metabolic enzymes self-assemble into electron microscope scale fibres

In recent years, many key metabolic enzymes have been identified to form electron microscope (EM) scale fibres in vitro (Figure 3.4). It is important to tell the EM-scale fibres apart from what I introduced as cytoophidia in the previous part of this study. The major differences between these two concepts are scale and detection methods. EM-scale fibres are detected by EM in vitro, mostly from purified enzymes, indicating a molecular scale of study. This can be compared with cytoophidia, which are detected by confocal microscope though antibody staining or GFP reporter, indicating the in vivo compartmentation of protein on a larger cellular scale. EM-scale fibres do not have to aggregate into cytoophidium scale filaments in vivo, but cytoophidia are highly likely to be constituted from a complex of the same or different groups of EM-scale fibres.

The most studied self-assembling fibre is acetyl-CoA carboxylase (ACC), a key enzyme in carbon utilization. Acetyl-CoA carboxylase is able to form homo-hexamers and then stack into longer fibres [50]. The formation of fibres greatly elevates the activity of acetyl-CoA carboxylase. The high concentration, dephosphorylation of acetyl-CoA carboxylase, and allosteric binding of citrate to acetyl-CoA carboxylase promote the formation of fibres [51].

β-glucosidase from oats was also found to form EM-scale fibres in vitro. Like acetyl-CoA carboxylase, β-glucosidase is a homo-hexameric enzyme. One research study on β-glucosidase fibres proved that longer fibres were more active and more resistant to inhibitors than shorter ones [52].

In nitrogen metabolism, glutamine synthase in *E. coli*, which drives the ATP-dependent addition of ammonia to glutamate to form glutamine, was also found to aggregate into fibres [53]. This enzyme is dodecameric in *E. coli* and decameric in yeast [54]. In the eyes of

mammals, a specific glutamine synthetase forms crystallins, a kind a filamentous structure, for eye protection [55].

Glutamate dehydrogenase, which degrades glutamate into α-ketoglutarate and ammonia, was found to aggregate into highly ordered fibre bundles [56].This enzyme forms homo-hexamers in cells.

In the nucleotide biosynthesis metabolism, IMPDH catalyses the NAD-dependent oxidation of inosine monophosphate (IMP) and turns it into xanthosine monophosphate for the follow-up synthesis of guanosine nucleotides. Purified IMPDH forms homo-tetramers similar with CTP synthase and then assembles into larger fibres [26].

Another well-known example for fibre formation is pathological human sickle haemoglobin (HbS). Human haemoglobin exists as a homo-tetramer for the transportation of oxygen. Haemoglobin does not form fibres in normal conditions, but a single mutant on haemoglobin causes its transition into HbS. HbS aggregates into fibres, leading to cell dysfunction and causing sickle-cell disease.

All the examples above suggest that some oligomeric proteins tend to form larger scale fibres in certain conditions. The attributes of fibres relating to activity, regulation and so on differ widely from case to case, but it is believed to be an additional method of regulating the metabolic process in cells [57].

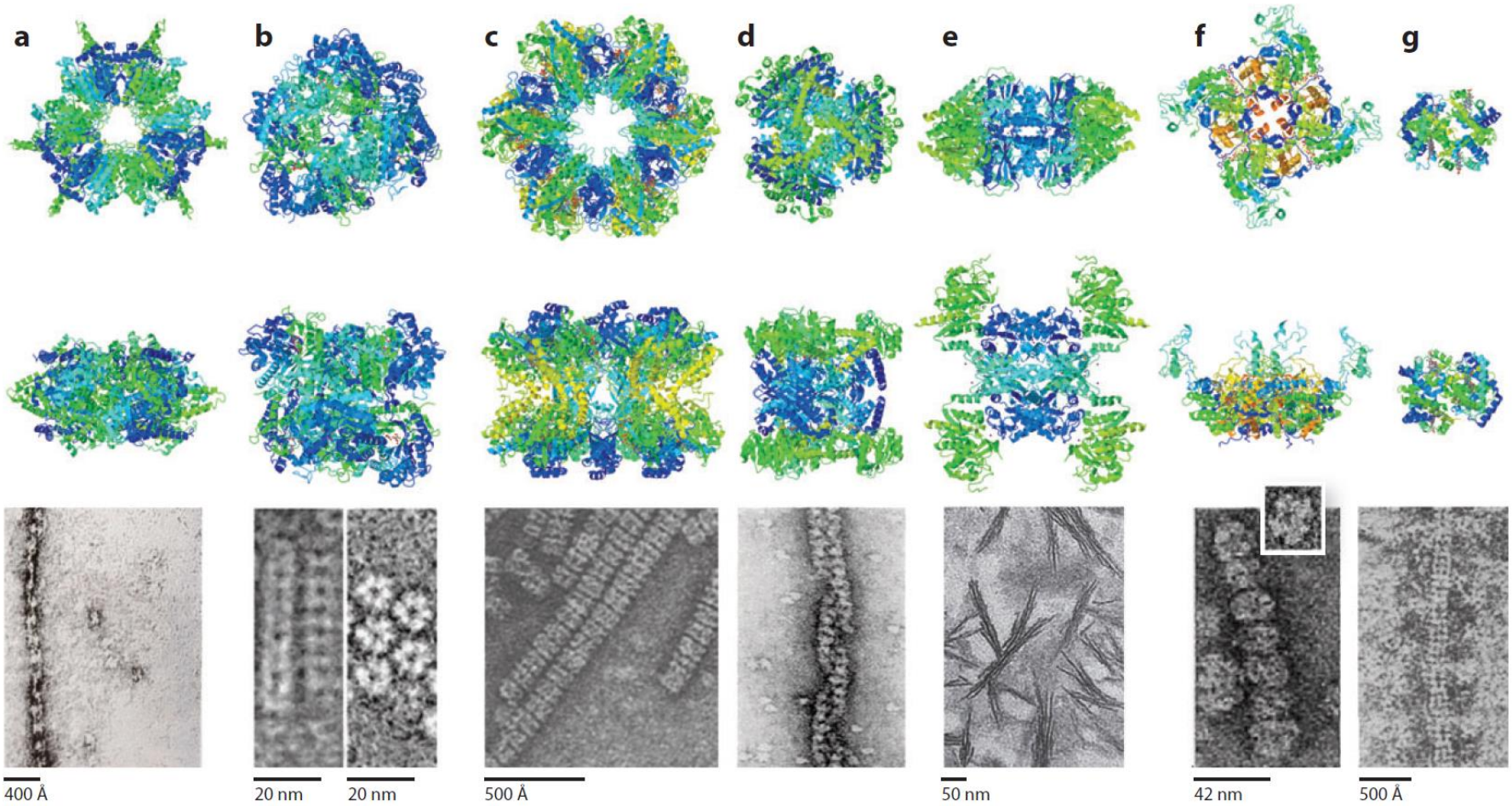


Figure 3.4 Samples of metabolic enzymes that self-assemble into fibres

(A) Acetyl-CoA carboxylase; **(B)** β-glucosidase; **(C)** Glutamine synthetase; **(D)** Glutamate dehydrogenase. Scale not provided; **(E)** CTP synthase; **(F)** Inosine monophosphate dehydrogenase; **(G)** Human sickle-cell mutant haemoglobin. All crystal structure images created with Jmol (adapted from [57])

3.1.4 Aims of this chapter

It has been suggested that many metabolic enzymes tend to form oligomers when catalysing reactions in cells. Meanwhile, due to the intrinsic symmetric structures of oligomeric enzymes, they have a relatively higher possibility of forming EM-scale fibres, which are probably basic subunits of cytoophidia (the cellular scale filaments). The following experiments were designed based on the fact that CTP synthase forms cytoophidia in cells and is a tetrameric enzyme. I set up a group of mutants on the dimerization and tetramerization interphases of *Drosophila* CTP synthase in S2R+ cells to study the relationship between oligomerization of CTP synthase molecules and cytoophidium formation. In this way, I predicted the basic molecular unit of CTP synthase-based cytoophidia. Meanwhile, combined results on filament assembly in *Drosophila* tissue development and tissue starvation responses, I am attempting to identify the function of cytoophidia and answer the question of whether CTP synthase in cytoophidia is active or inactive.

3.2 Results

3.2.1 Transfection of S2R+ cells with CTPsyn-YFP induces cytoophidium formation

Since CTP synthase is only expressed in a basal level in S2R+ cells, cytoophidia can hardly be detected by immunostaining in a cultured (Schneider's medium, 10%FBS, 30°C) S2R+ cell. Transient transfection of CTPsyn-YFP reveals an overexpression profile of CTP synthase in S2R+ cells, where diffused cytoplasmic CTPsyn-YFP and filamentous CTPsyn-YFP signals could be detected (Figure 3.5). Due to the relatively low transfection efficiency, around 30% of cells displayed visible fluorescent signals. Filament length varied from 1μm to 10μm. The percentage of cells containing filament was 35.9±2.1% (data generated form three independent slides counting) (Figure 3.6).

Most filaments were short and straight, while few of them were curved. Most cells showed a pattern of a single relatively short and thin filament, while a few cells showed a pattern of a bundle of filaments (Figure 3.5 C). The amount of cytoophidia might vary depending on the expression level resulting from the different copy number and expression level in different cells.

Antibody staining for CTP synthase in the transfected cells has been done to confirm the filaments were not artificial effects.

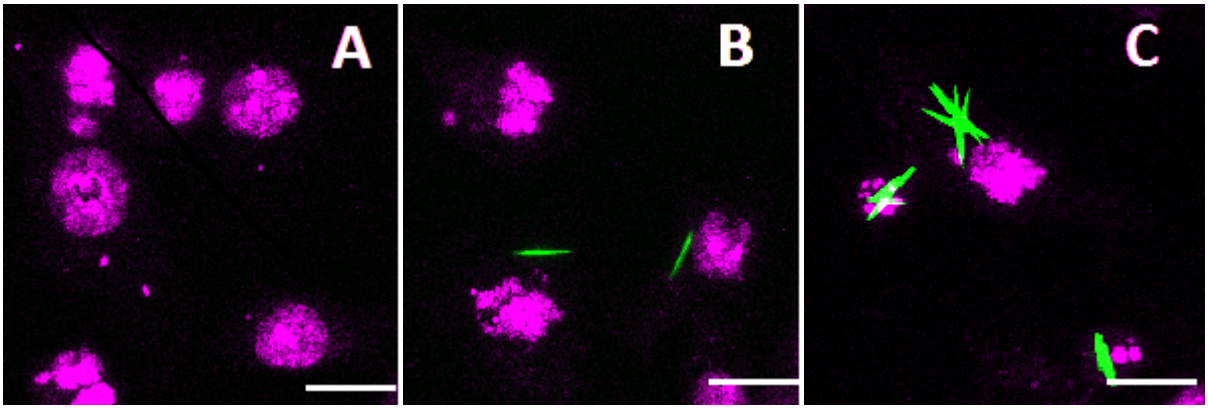


Figure 3.5 Transfection of CTPsyn-YFP into S2R+ cells

(A) Untransfected S2R+ cells; **(B)** Transfected cells with a single filament. Most filaments were short and straight, while a few of them were curved; **(C)** Transfected cell with a large number of cytoophidia. A few cells showed a pattern of a bundle of filaments. Scale bar, 10um, anti-CTP synthase shown in green, nuclear marker shown in magenta

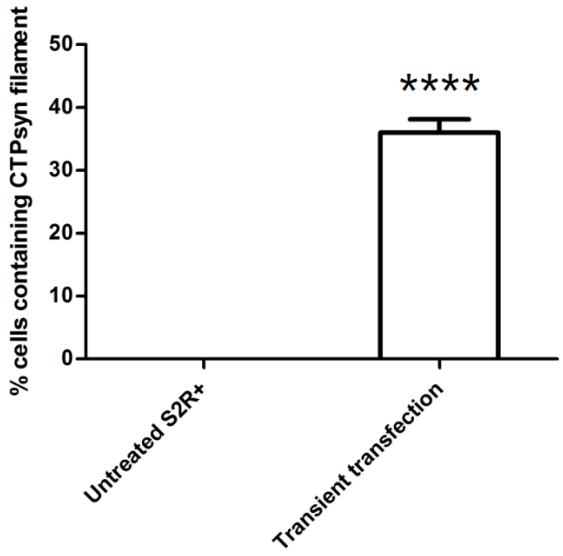


Figure 3.6 Percentage of cells containing cytoophidia in untreated S2R+ and cells after transient transfection

Around 35% of cells contains CTP synthase filament after transient transfection. Data generated from counting three independent slides. Error bar shows SEM.

3.2.2 Mutation at the CTP synthase oligomer interface disrupts cytoophidium assembly

Previous studies have shown that the end product inhibition of CTP synthase by CTP is critical for the regulation of the enzyme activity itself [41, 58, 59]. In the budding yeast *S. cerevisiae*, a mutation at the CTP binding site of CTP synthase disrupts the end product inhibition by CTP [60].

Site-directed mutagenesis was used to construct a point mutation at the equivalent conserved CTP synthase residue ($CTPsyn^{E160K}$) in a CTPsyn-YFP expression vector. When $CTPsyn^{E160K}$ was transfected into *Drosophila* S2R+ cells, cytoophidium formation was completely disrupted, although diffuse cytoplasmic YFP signals could be detected, along with numerous punctate structures (Figure 3.7 D). Similar results have previously been reported in *S. cerevisiae*, indicating that the regulation of cytoophidium formation by end-product inhibition is an evolutionary conserved phenomenon [4].

Allosteric binding of CTP has previously been shown to induce CTP synthase tetramer formation [59]. It has also been demonstrated that treatment with the CTP synthase inhibitor, 6-Diazo-5-oxo-L-norleucine (DON), reduces the amount of CTP synthase tetramerization in *E.coli* ,which suggests that the tetramer form of CTP synthase may be excluded from cytoophidia [40]. From these data, it is unclear whether monomers, dimers, or tetramers are incorporated into cytoophidia. I therefore decided to investigate the effect of mutations influencing residues at the tetramer or dimer interfaces of CTP synthase on cytoophidium assembly. Five mutated CTP synthase were constructed and transfected into S2R+ cells. Cytoophidium length was then measured and compared (Figure 3.8).

Tetramer interface mutations induced cytoophidium assembly in S2R+ cells

I constructed point mutations in CTPsyn-YFP at the tetramer interfaces (CTPsyn^{G151E} and CTPsyn^{R163H}) and assayed for filament formation in S2R+ cells. Both CTPsyn^{G151E} and CTPsyn^{R163H} resulted in significantly longer cytoophidia when expression was induced in S2R+ cells compared to wild-type protein controls. Unlike the wild-type, in which filaments were mostly straight and sharp, filaments in these two mutants tended to be extremely curved and serpent-like (Figure 3.7 B, E). These data indicate that tetramer formation is not necessary for CTP synthase to form cytoophidium.

Dimer interface mutations disturbed cytoophidium assembly in S2R+ cells

To determine whether CTP synthase dimer formation is necessary for cytoophidium formation, I constructed point mutations at the monomer-monomer interface, predicted to disrupt dimer formation (CTPsyn^{V114F} and CTPsyn^{M156I}). Both CTPsyn^{V114F} and CTPsyn^{M156I} resulted in significantly shorter cytoophidia when expressed in S2R+ cells. Short and broken filaments were found in these mutants (Figure 3.7 C, F). Cytoophidium formation was partly disturbed in these two mutants rather than completely disrupted, as in CTPsyn^{E160K} (Figure 3.7 D).

Protein abundance is not a significant confounding factor in mutants

It is unclear whether the difference of cytoophidium length is due to incomplete disruption of dimer formation in CTPsyn^{V114F} and CTPsyn^{M156I} or due to CTP synthase level differences in each mutation. To determine whether changes in cytoophidium formation were due to changes in CTP synthase abundance, western blots were performed to detect the relative amounts of expressed proteins for each mutant (Figure 3.9). Comparison of relative CTP synthase abundance indicates that CTPsyn^{V114F} and CTPsyn^{G151E} appear to have similar

amount of protein level compared with wild-type. However, CTPsyn^{R163H}, CTPsyn^{M156I}, and CTPsyn^{E160K} displayed significantly less protein abundance. CTPsyn^{R163H} displayed longer cytoophidia than wild-type, despite lower protein abundance, whereas CTPsyn^{M156I} and CTPsyn^{E160K} displayed significantly less cytoophidia and had clear morphological differences. This result indicated that reduce of length in CTPsyn^{V114F} and the increase of length in CTPsyn^{R163H} were independent with protein level.

In the western blot, I also found a small band migration for CTPsyn^{R163H}, CTPsyn^{M156I}, and CTPsyn^{E160K}. This could be explained as a structural change caused by these mutations which slightly increased the protein migration rate. Meanwhile the wild-type control showed a double band around the size of CTP synthase. This only happened in the wild-type situation. The cause of the doublet is as yet unknown.

From the results of the western blot, I concluded that CTP synthase increase was not a significant confounding factor in the interpretation of these phenotypes. Together with these results, I concluded that CTP synthase dimers may be the oligomer subunits of cytoophidia, while tetramers may not be necessary for cytoophidium assembly.

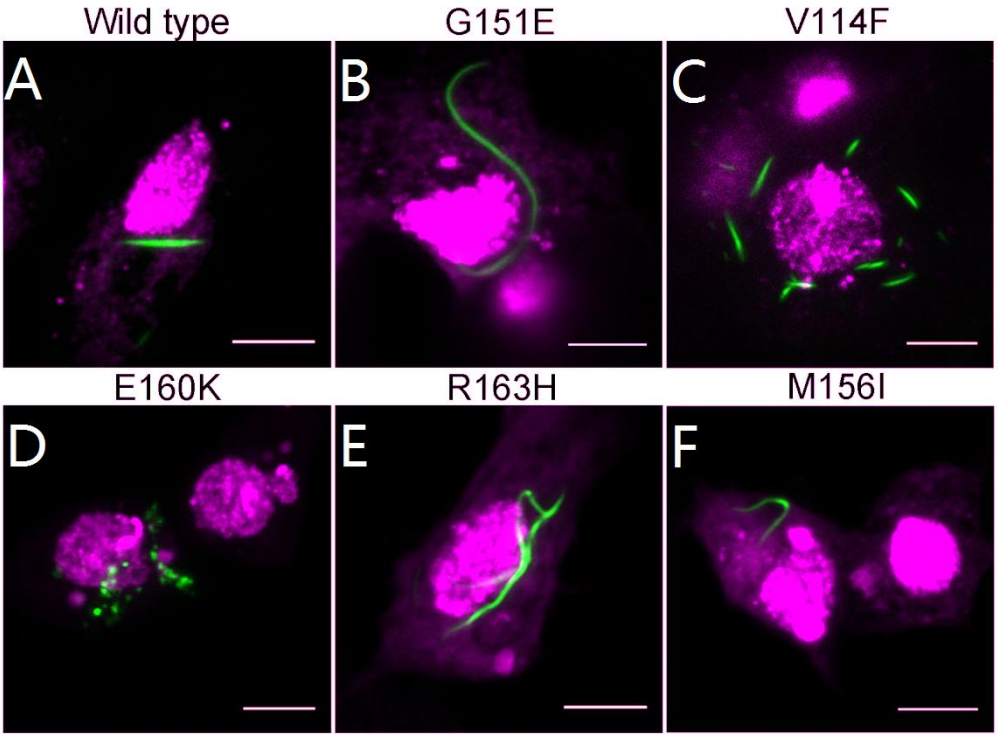


Figure 3.7 Mutations at the CTP synthase oligomer interfaces disrupt cytoophidium assembly

CTPsyn^{E160K} substitution completely disrupts cytoophidium formation when ectopically overexpressed in S2R+ cells, although punctate CTP synthase structures are still visible in the cytoplasm. Mutation modifying residues at the dimer-dimer interface: CTPsyn^{G151E} and CTPsyn^{R163H} (predicted to disrupt CTP synthase tetramer formation) resulted in significantly longer cytoophidia compared to wild-type CTP synthase. Mutations modifying residues at the monomer-monomer interface: CTPsyn^{V114F} and CTPsyn^{M156I} (predicted to disrupt CTP synthase dimer formation) resulted in significantly shorter cytoophidia compared to wild-type. Scale bars: 20μm. Images are representative

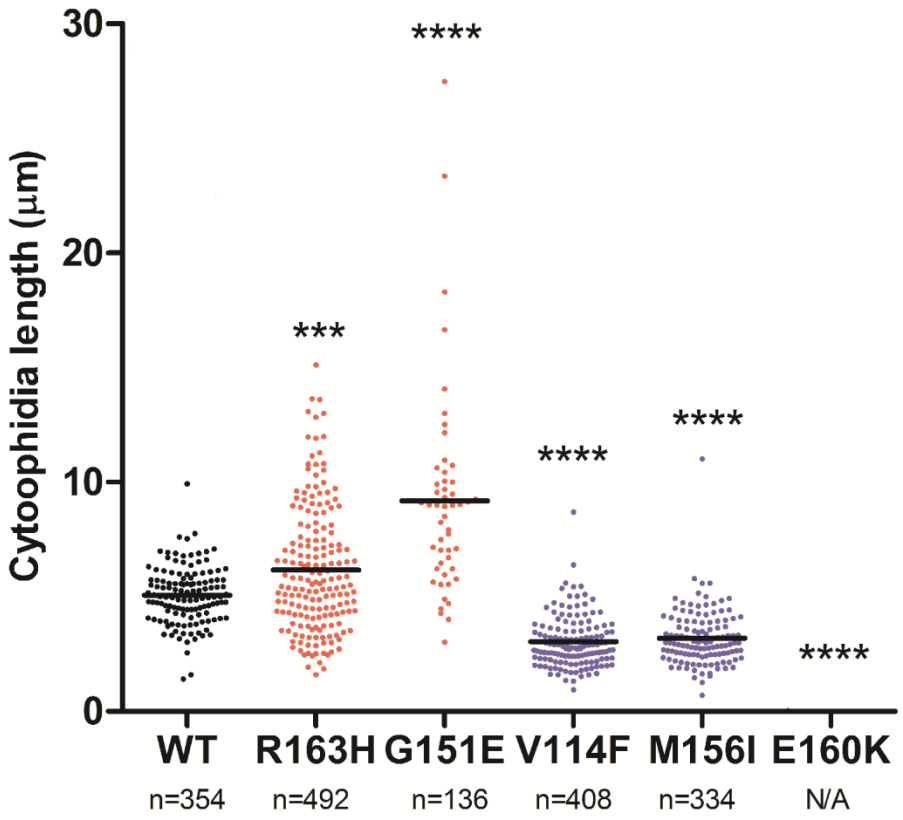


Figure 3.8 Quantification of cytoophidium length in each mutant

CTPsyn^{G151E} and CTPsyn^{R163H} resulted in significantly longer cytoophidia compared to wild-type CTP synthase. CTPsyn^{V114F} and CTPsyn^{M156I} results in significantly shorter cytoophidia compared to wild-type. At least 50 cells were counted per well. One way ANOVA ****P<0.0001, ***P<0.001

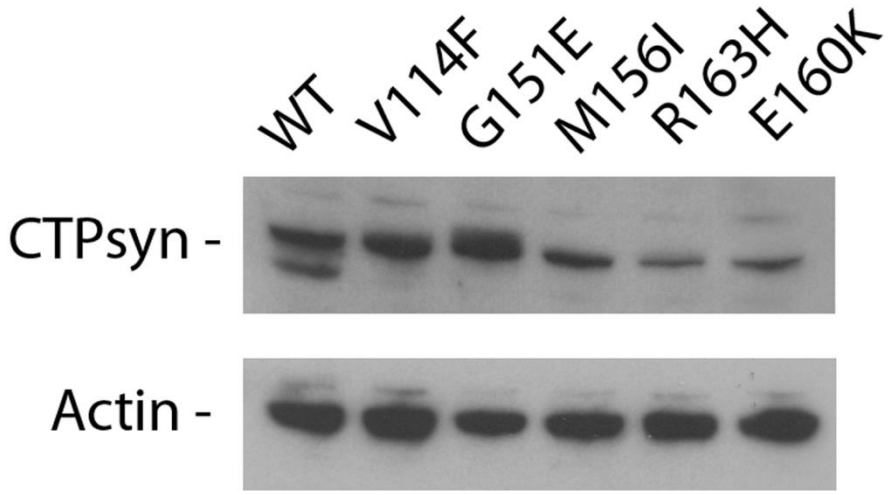


Figure 3.9 Western blot data showing relative CTP synthase abundance in cells transfected with mutant CTP synthase expression constructs

A CTP synthase antibody were used to detect target protein by western blot. CTPsyn^{R163H}, CTPsyn^{M156I}, and CTPsyn^{E160K} appear to have significantly decreased protein levels compared with wild-type, while CTPsyn^{V114F} and CTPsyn^{G151E} appear to have similar protein levels compared with wild-type.

3.2.3 Cytoophidium assembly occurs in response to nutrient stress in S2R+ cells

It has previously been shown that *S. cerevisiae* cells grown in medium lacking glucose exhibited greater numbers of CTP synthase-based filaments [4]. This effect could be reversed by the addition of glucose. To see if the response to nutrient stress is evolutionarily conserved for un-transfected wild-type *Drosophila* S2R+ cells, the cell culture medium was removed from S2R+ cells in logarithmic growth and incubated with PBS. Cells were examined by immunofluorescence at various time points to determine the effect of nutrient stress on cytoophidium assembly. A significant increase in the number of cytoophidia was seen after one hour, the shortest interval measured. Percentages of cells with visible cytoophidium formation reached a maximum of around 20% after four hours in PBS. The observed response of cytoophidia to nutrient stress could be reversed by the re-addition of whole medium (Figure 3.10). It remains unclear whether the increased cytoophidium formation displayed by nutrient restricted cells is a consequence of cell cycle arrest. To answer this question, Edu staining was performed to label S-phase cells in nutrient restricted cells to give an indication of the number of cells exiting the cell cycle. No significant change in Edu staining was seen following five hours of nutrient restriction, indicating that cell cycle arrest is not necessary for cytoophidium formation in cells undergoing nutrient restriction (Figure 3.10).

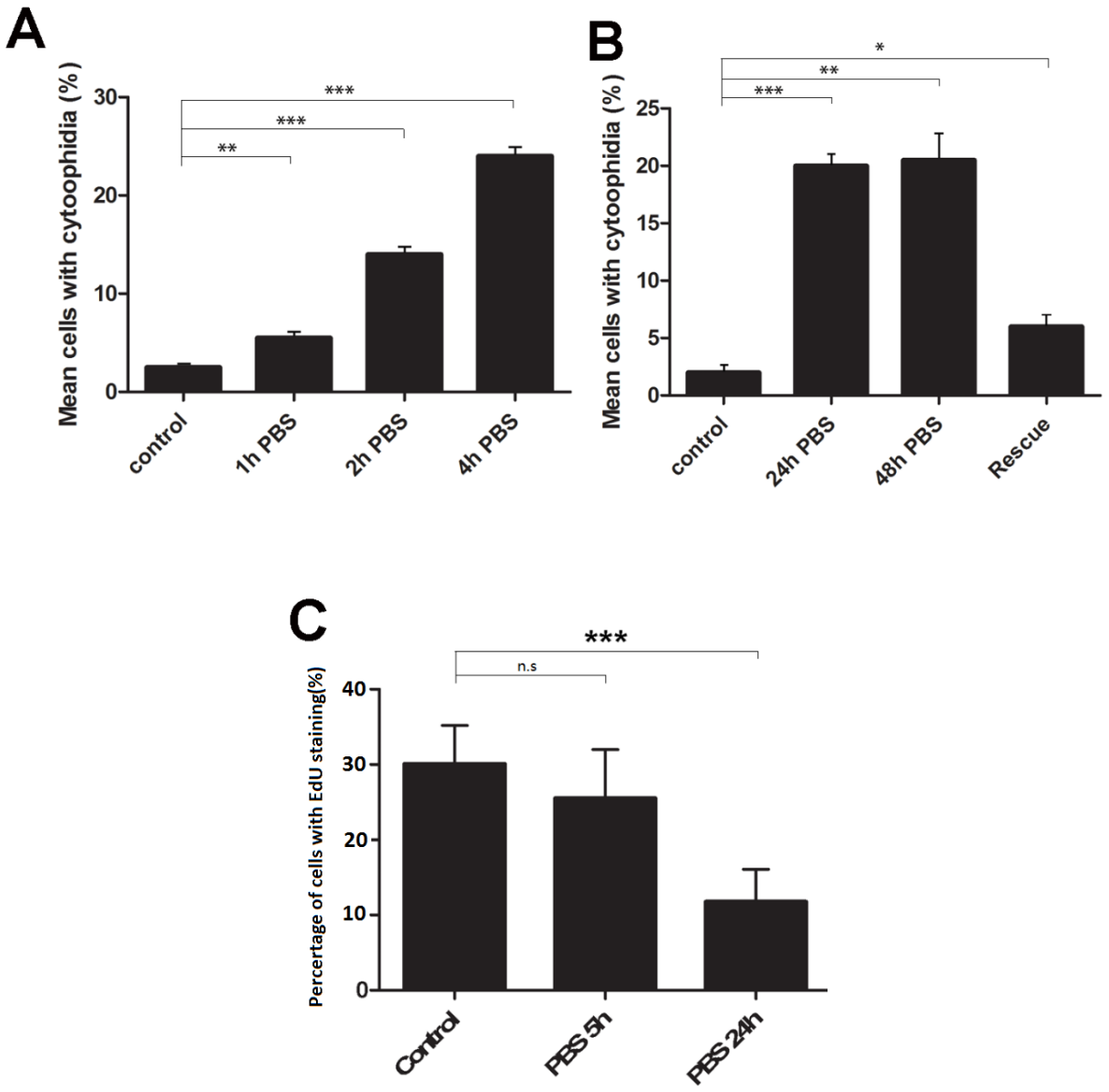


Figure 3.10 Cytoophidium assembly occurs in response to nutrient stress

(A) Mean number of cells containing visible cytoophidia increases significantly after one hour nutrient-restricted treatment. The percentage keeps growing after two hours and four hours treatment. Control cells are maintained in complete *Drosophila* Schneider's medium. At least 100 cells were counted from ten sites per well from at least three independent replicates**; (B)** Cells with increased numbers of cytoophidia following nutrient restriction (24 hours) can be rescued by the addition of whole medium. Cells were examined two hours after re-introduction of whole medium; **(C)** No significant change in the percentage of EdU-marked cells is observed before five hours PBS treatment, indicating that cell cycle arrest is not necessary for cytoophidium formation in S2 cells. ***P<0.001, **P<0.01, *P<0.05

3.3 Discussion

3.3.1 Models for cytoophidium assembly

The data from Figure 3.7 indicates that, in S2R+ cells, mutation on the CTP synthase tetramer interface induced filament assembly, while mutation at the CTP synthase dimer interface inhibited overall filament assembly.

Several interpretations are possible for this result. If mutations in both the dimer and tetramer interface indeed disturb dimerization or tetramerization, this could indicate that dimerization is essential for cytoophidium formation, whereas tetramer formation is dispensable for cytoophidium assembly. This conclusion suggests a model in which dimer CTP synthase is the basic building block of cytoophidia and the polymerization of CTP synthase dimers contributes to cytoophidium formation (Figure 3.11). In this model, dimer mutations are partly incapable of forming filament, which leads to the shorter average length. Meanwhile, tetramer mutations are partly incapable of forming cytoophidium tetramers. According to chemical equilibrium, more dimer would accumulate, which leads to a higher number and length of filaments. The results fit this model nicely.

An alternative model would be that CTP synthase tetramer is the fundamental unit of cytoophidia. It is possible that mutations at the dimer interface prevent both dimerization and tetramerization, and subsequently inhibit cytoophidium assembly (Figure 3.12). In this scenario, longer filaments may be observed, with mutations at the tetramer interface if the mutations generated in this study act as gain of function mutants (thus facilitating tetramer formation). The latter phenomenon then leads to an enhancement in the formation of cytoophidia.

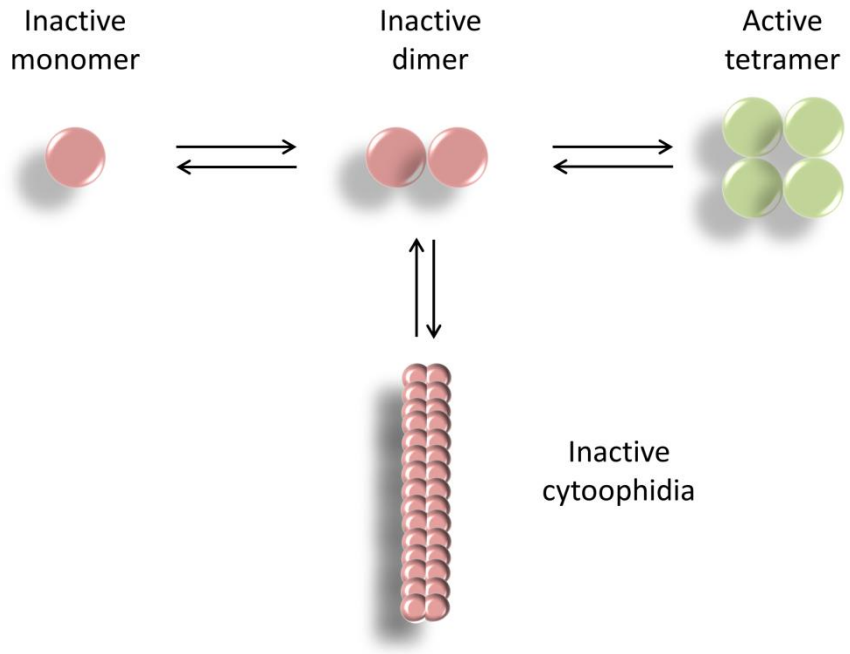


Figure 3.11 Model A: CTP synthase dimer is the basic unit of cytoophidium

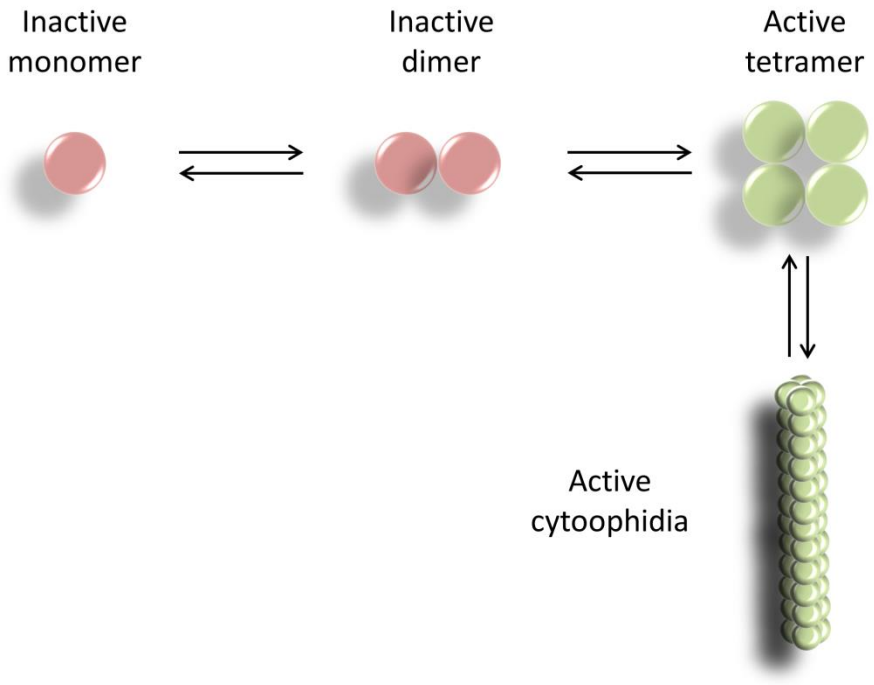


Figure 3.12 Model B: CTP synthase tetramer is the basic unit of cytoophidium

These two models may lead to two distinctly different interpretations of the activity of cytoophidia. In model A, since the enzymatically inactive CTP synthase dimer is the basic unit of cytoophidium, cytoophidium (which is composed of inactive CTP synthase dimer) should be inactive. In model B, since the enzymatically active CTP synthase tetramer is the basic unit of cytoophidium, cytoophidium (which is composed of active CTP synthase tetramer) can be either active or inactive, depending on the conformation change of tetramers after assembly into cytoophidia.

It is also worth mentioning that the mutants study in this chapter are based on overexpression analysis of mutated CTP synthase. However, the overexpression study itself may have several drawbacks. The most common concern of is that the protein level of overexpression is much higher than the physiological protein level, which may lead to artefacts. Another concern is that overexpression study skips gene regulation, transcript editing and translation regulation, so that it cannot explain the complicated dynamic and regulation of natural assembled cytoophidia.

3.3.2 Cytoophidium assembly occurs in response to nutrient stress suggests cytoophidium is an inactive structure

The data from Figure 3.10 suggests that nutrient deprivation of S2R+ cells for four hours can significantly induce cytoophidium assembly, while cell cycle is not apparently affected. More experiments have also been done to show this regulation is conserved in animal tissues in vivo [18]. In imaginal discs of *Drosophila* L3 larvae, cells showed a diffused CTP synthase signal when fed a normal diet. However, in larvae raised on a nutrient restricted diet, the imaginal discs are smaller and cytoophidia are highly prevalent.

Another model is the redistribution process during *Drosophila* neurogenesis. In a normal diet situation, the majority of neuroblasts remain quiescent during the early 1st instar larval stage.

Neuroblasts exit quiescence and re-enter the cell cycle during the late 1st and early 2nd stages. For those cells in the early 1st instar stage, cytoophidia were observed. As neuroblasts exited quiescence (late 2nd stage), cytoophidia CTP synthase became diffuse. When food was removed for 24 hours during late 2nd stage, cytoophidia became prevalent again. Re-feeding starved larvae promoted cytoophidium disassembly [18].

In summary, CTP synthase localization in cell changes as part of adaptive metabolic response to inactivate cytoplasmic CTP synthase during nutritional stress both in vitro and in vivo. The in vivo data of CTP synthase redistribution process in *Drosophila* neurogenesis also become supportive data for Model A (Figure 3.11) in the previous discussion, i.e. the inactive dimer as the basic unit of cytoophidia.

3.3.3 Model of molecular redistribution as a response to intrinsic and extrinsic signal

One major challenge in research on cytoophidia is that cytoophidia can only be observed in limited tissues or under limited conditions. The behaviour of filaments in different species, cell types, treatments and conditions is totally different. Here I provide one possible model (Figure 3.13) to summarize the reported cases of cytoophidium assembly (Table 3.1).

In most of cells with low CTP synthase concentration (S2R+ cells, HeLa cells, L3 larvae imaginal discs), CTP synthase is diffused in the cell and few filaments can be detected. Filaments assemble in response to nutrient stress or developmental conditions. The assembly of filaments can sequester CTP synthase enzyme activity as a consequence of a slowing down of the overall metabolic responses. When CTP synthase is overexpressed in cells, the concentration of CTP synthase is high enough to form filament. Different patterns of cytoophidia in different tissues may be caused by different CTP synthase concentrations, as well as filament-regulating processes such as nutrient restriction or DON treatment.

Table 3.1 Summary of CTP synthase-based cytoophidium formation conditions

Species	Cell type	Condition	Treatment	Phenotype	Reference
Drosophila	S2R+	cultured cell	normal	No filaments	[18]
Drosophila	S2R+	cultured cell	DON treatment 4ug/ml 24h	60% cells with filament	[18]
Drosophila	S2R+	cultured cell	Overexpression	35% cells with filament	[18]
Drosophila	S2R+	cultured cell	PBS treatment 4h	25% cells with filament	[18]
Drosophila	Imaginal discs	L3 larvae	normal	No filaments	[18]
Drosophila	Imaginal discs	L3 larvae	food removed for 24h	Abundant filaments	[18]
Drosophila	Neuroblasts	Early L2 larvae	normal	Abundant filaments	[18]
Drosophila	Neuroblasts	Late L2 larvae	normal	No filaments	[18]
Drosophila	Neuroblasts	Late L2 larvae	food removed for 24h	Abundant filaments	[18]
Homo sapiens	Hela	cultured cell	normal	5% cells with filament	[5]
Homo sapiens	Hela	cultured cell	DON treatment 4ug/ml 24h	40% cells with filament	[5]
S. cerevisiae	-	-	Starvation	26% cells with filament	[4]
C. crescentus	-	-	Overexpression	Abundant filaments	[3]
C. crescentus	-	-	Overexpression+1μM DON	No filaments	[3]
Drosophila	Follicle cells	Stage 10a	normal	Abundant filaments	[22]
Drosophila	Follicle cells	Stage 10b	normal	Very few filaments	[22]

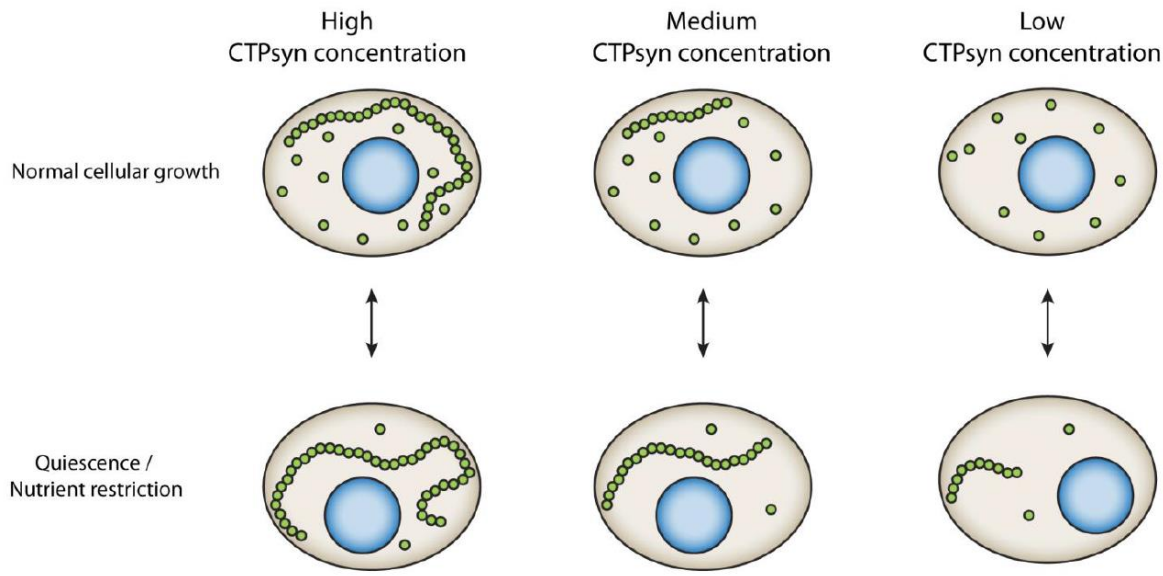


Figure 3.13 One proposed model of cytoophidium assembly in response to nutrient or development conditions

In most of cells with low CTP synthase concentration (S2R+ cells, HeLa cells, L3 larvae imaginal discs), CTP synthase is diffused in the cell and few filaments can be detected. Filaments assemble in response to nutrient stress or developmental conditions. Overexpression of CTP synthase may lead to filament formation due to high CTP synthase concentration.

3.3.4 Other literature supporting the "inactive hypothesis"

The CTP synthase filament assembling process and filament function have been much studied in recent years. The results of Chapter 3 contributed to the 2014 article "Nucleotide synthesis is regulated by cytoophidium formation during neurodevelopment and adaptive metabolism" [18]. In the same year, two other articles on similar topics were published, with the titles of "Common regulatory control of CTP synthase enzyme and filament formation" [24] and "Large-scale filament formation inhibits the activity of CTP synthetase" [25]. These three independent research papers were published in the same year and focused on the similar topics in three distinctive organisms: human cells, insect cells, the budding yeast and bacteria.

The first article (Aughey, G.N., et al., 2014 [18]) showed that cytoophidium formation in *Drosophila* occurs during nutrient deprivation in both cultured cells and starved neuroblasts of the *Drosophila* larval central nervous system. At the same time, we concluded that CTP synthase dimers may be the oligomer subunits of cytoophidia, while tetramers may not necessarily be required for cytoophidium assembly through overexpression of mutated CTP synthase in *Drosophila* cultured cells. We showed global metabolic profiling demonstrated that CTP synthase overexpression does not significantly alter CTP synthase-related enzyme activity, suggesting cytoophidium formation facilitates metabolic stabilization. In addition, the CTP pool in CTP synthase overexpression human stable cell lines only increased moderately. All these facts supported the idea that inactive CTP synthase is incorporated into cytoophidia, the cytoophidium is formed from inactive CTP synthase dimer, and the formation of cytoophidium is a regulation of active CTP synthase level and the CTP pool.

The second article (Noree, C., et al., 2014 [24]) showed the same results in the budding yeast *S. cerevisiae* with different mutants, i.e. the blocking of tetramerization increased the frequency of CTP synthase formation (G148A). Meanwhile, they showed mutation in the

ATP-binding site of CTP synthase increase filament formation (D70A and E146A), which supports the role of tetramerization in filament formation frequency with the fact that ATP binding can modulate tetramer formation. In addition, they showed that filaments were significantly induced by the mutations on the GTP binding sites (R381M or R381P, which inhibit GTP binding and activation of CTP synthase). All these facts supported the argument that blocking of CTP synthase tetramerization or activation results in longer filaments, and therefore supported that CTP synthase polymerizes in the way of inactive dimers interacting with each other and forms cytoophidia, which is exactly same with what (Aughey, G.N., et al., 2014 [18]) has claimed.

The third article (Barry, R.M., et al., 2014 [25]) conducted research on *E. coli* and in vitro, which showed that polymerization inhibited activity of CTP synthase in vitro with light scattering measurement. Meanwhile they showed polymerization is induced by its product CTP and repressed by its substrate ATP, which is consistent with the "inactive model of filament". They also showed cryo-electron microscopy of in vitro CTP synthase filaments. From the EM study, they showed CTP synthase tetramers stacked on top of one another with the arms of the adjacent Xs interdigitated. There was a minor rearrangement of tetramerization interface in the filament relative to the crystal structure. Even though all of those enzyme active sites are solvent accessible, which means UTP, ATP and glutamine can freely diffuse into filaments, the transfer route of ammonia between the synthase domain and the aminotransferase domain seems be blocked by this rearrangement, which is the possible reason for enzyme inhibiting [25].

In summary, the three articles above supported the argument that the filament is inactive. With the concrete data from four different species, we can safely come to the conclusion of the "inactive filament model". The mutants in these three articles are summarized in Table 3.2.

However, according to the basic unit of filament, these three arguments have different views in the basic unit of filament. With the EM results, (Barry, R.M., et al., 2014 [25]) put forward a different model from (Aughey, G.N., et al., 2014 [18]) and (Noree, C., et al., 2014 [24]) in which polymer was based on a tetramer rather than a dimer. There are therefore two different models for the polymerization of enzymes into small fibers: a tetramer model and a dimer model. The tetramer model claims that small fibers are composed of interdigitated Xs of inactive CTP synthase tetramer, whereas the dimer model claims that small fibers are composed of enzymatically inactive dimers. This difference may be caused by the difference between in vivo filament and in vitro filament. The in vitro filaments which were generated in (Barry, R.M., et al., 2014 [25]) did not necessarily have the same structure as the in vivo ones studied in the first two articles. Meanwhile, the polymerization of tetramers described in the filaments in (Barry, R.M., et al., 2014 [25]) has a conformational change which hinders the necessary site for CTP synthase activity [25]. The conformation change of the inactive tetramer makes it different from the original active tetramer. Mutants of the active tetramer interface in (Aughey, G.N., et al., 2014 [18]) and (Noree, C., et al., 2014 [24]) may not necessarily block the formation of inactive tetramer in (Barry, R.M., et al., 2014 [25]). From this point of view, to determinate the basic unit and basic structure of cytoophidia, more detailed and precise experiments should be performed in the future.

Table 3.2 Mutants and there influence to filament formation from three individual studies

Mutants	Species	Description	Filament Formation	*S. solfataricus* Counterpart	Secondary structure in *S. solfataricus*	*Drosophila* Counterpart	*Drosophila* Counterpart	Reference
V114F	*Drosophila*	Dimer interface	Decrease	116	α5	114	V	[18]
G151E	*Drosophila*	Tetramer interface	Increase	148	β6-η2	151	G	[18]
M156I	*Drosophila*	Dimer interface	Decrease	153	α6	156	M	[18]
R163H	*Drosophila*	Tetramer interface	Increase	160	α6	163	R	[18]
E160K	*Drosophila*	Dimer interface	No filament	157	α6	160	E	[18]
E161K	*S.cerevisiae*	Dimer interface	No filament	157	α6	160	E	[24]
E146A	*S.cerevisiae*	ATP Binding site	N.S.	142	β6	145	E	[24]
D70A	*S.cerevisiae*	ATP Binding site	Decrease	72	α3	70	D	[24]
R381M	*S.cerevisiae*	GTP Binding site	Increase	363	β12-α13	376	R	[24]
R381P	*S.cerevisiae*	GTP Binding site	Increase	363	β12-α13	376	R	[24]
G382A	*S.cerevisiae*	GTP Binding site	Decrease	364	β12-α13	377	G	[24]
C404G	*S.cerevisiae*	Catalytic site	N.S.	386	β13-α14	399	C	[24]
G148A	*S.cerevisiae*	Tetramer interface	Increase	144	β6-η2	147	G	[24]
S330A	*S.cerevisiae*	Phosphorylation site	Decrease	320	α12	325	A	[24]
S354A	*S.cerevisiae*	Phosphorylation site	Decrease	344	η5-β12	349	S	[24]
S424A	*S.cerevisiae*	Phosphorylation site	Decrease	406	β14	419	A	[24]
S36A	*S.cerevisiae*	Phosphorylation site	Decrease	38	β2	36	S	[24]
E277R	*E. coli*	Linker interface	No filament	279	α11	286	R	[25]
F281R	*E. coli*	Linker interface	No filament	283	α11	290	R	[25]
N285D	*E. coli*	Linker interface	No filament	287	α11	294	T	[25]
E289R	*E. coli*	Linker interface	No filament	293	β10	298	E	[25]
E155K	*E. coli*	Dimer interface	No filament	157	α6	160	E	[25]

3.3.5 Comparison of function between IMPDH- and CTP synthase-based cytoophidia

From this study, I showed that the formation of CTP synthase-based cytoophidia might be a way to downregulate the overall enzyme activity of CTP synthase. CTP synthase-based cytoophidia were induced by starvation or a quiescent-like state. Surprisingly, the overexpression of CTP synthase upregulated the overall glutamine level in cells, showing that the bringing-in of over-dosed CTP synthase did not help to consume more glutamine and produce more CTP. On the contrary, the overall CTP synthase activity was downregulated though filamentation (Figure 3.14) [18].

However, in the situation of IMPDH, inhibition of cell growth like starvation of rapamycin treatment triggers the disassembly of IMPDH [27]. As introduced previously (see 1.3), treatment of the CTP synthase inhibitor DAU promoted the formation of both CTP synthase-based cytoophidia and IMPDH-based cytoophidia. However, the GTP level was upregulated in this scenario, suggesting that, unlike CTP synthase-based cytoophidia, the formation of IMPDH-based cytoophidia upregulates the overall enzyme activity of IMPDH (Figure 3.15) [27].

The cause of different behaviours of these two kinds of cytoophidia is still unknown. The future research on this difference may focus on the different aggregation methods of subunits of these two cytoophidia. Structural studies showed that human IMPDH1 EM-scale fibres are piled up as a linear stacking of octameric IMPDH1 [61]. The active form of IMPDH is a tetramer [62]. More evidence is needed to decide whether the different stacking behaviour leads to different activity of these two cytoophidia.

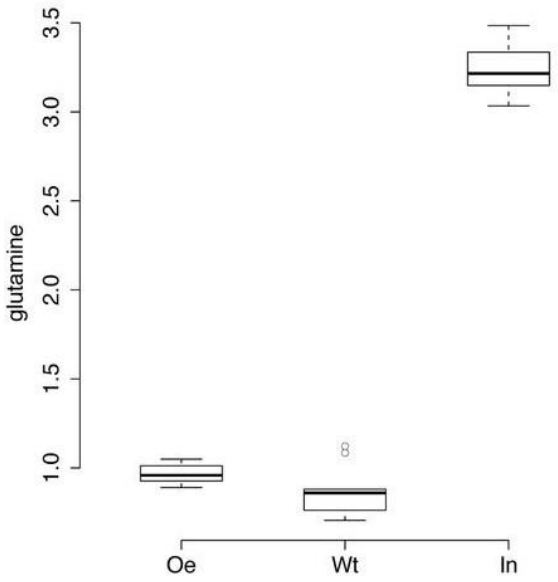


Figure 3.14 The levels of glutamine in three groups of cells

Oe: Cells with CTP synthase overexpression; Wt: Wild-type; In: Cells treated with DON Overexpression of CTP synthase inhibited CTP synthase overall enzyme efficiency. Data are shown in a boxplot (picture adapted from [18]).

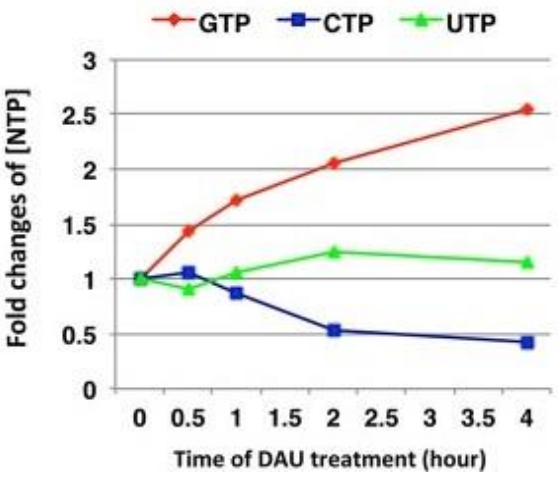


Figure 3.15 The levels of nucleotide during DAU treatment in HEK 293T cells

Treatment of CTP synthase inhibitor DAU promoted the formation of both CTP synthase-based cytoophidia and IMPDH-based cytoophidia. The upregulated GTP level suggested IMPDH-based cytoophidia as an active reactor (picture adapted from [27]).

Chapter 4 Filamentation of metabolic enzymes in *Saccharomyces cerevisiae*

4.1 Introduction

4.1.1 Protein localization in the budding yeast

It is known that the compartmentation of proteins has great significance in elevating the efficiency of biological processes in cells by arranging related proteins spatially and temporally. The comprehensive knowledge on the localization of proteins in cells is important for the understanding of protein interactions and protein function. With the knowledge of protein localization, biological processes become three-dimensional data sets with information of space and time, whereas previous information was one-dimensional. The budding yeast *Saccharomyces cerevisiae* was the first eukaryotic genome to be completely sequenced in 1996 [34]. The most up-to-date data from SGD (18/01/2017) showed that there are 6,604 ORFs in the budding yeast *S. cerevisiae* genome. The first large-scale screening of the budding yeast protein localization was completed in 1999 using the transposon-tagging strategy [63]. With this plasmid-based overexpression method, a total number of 2,744 proteins were identified according to their localization [64]. The limit of this transposon-tagging strategy mainly lies in the argument that overexpression of proteins may interrupt transport mechanisms and lead to the abnormal localization of proteins. The tagging efficiency also limits the available data to around 40% of all budding yeast ORFs. In 2003, another group made an endogenous promoter tagging by inserting GFP into the C-terminal of target proteins, successfully tagging 6,029 proteins [35]. 4,156 of these showed GFP positive signals in the mid-logarithmic phase. Pictures were taken by fluorescence microscopy and analysed. In this research, protein localization was classified into 12 categories. Another 11 categories were added, combined with marker mRFP co-localization experiments (Table 4.1).

After the publication of these results, a commercialized budding yeast endogenous GFP labelled library was established. However, there are several limits for the screening in 2003. Firstly, the resolution of fluorescence microscope screening could not tell apart cellular foci and filament. The study of cellular fine structures calls for a high-resolution detecting method. Secondly, with the poor resolution, it became unreliable to apply mRFP co-localization method to determinate protein subcellular localization. Moreover, in this screening, samples are fixed in mid-exponential phase, which limited the discovery of lots of dynamic structures which appear in other growth phases. The C-terminal fusion of GFP also causes mislocalization of some proteins.

Even though the localization data of proteins need to be carefully treated when doing research on individual proteins, this literature provided us with a good overall reference on protein localization in the exponential phase, and with excellent material for studying large-scale aggregates in yeast. The screening of filament-forming proteins in this chapter is based on this Yeast GFP Clone Collection.

Table 4.1 Subcellular localization categories

Table adapted from [35]

GFP localization	GFP and RFP co-localizaton
Cell periphery	Cytoskeleton
Bud	Actin cytoskeleton
Bud neck	Spindle pole
Cytoskeleton	Nucleolus
Microtubule	Nuclear periphery
Cytoplasm	Golgi apparatus
Nucleus*	Transport vesicle
Mitochondrion*	Early Golgi/COPI
Endoplasmic reticulum	Late Golgi/clathrin
Vacuole	Endoplasmic reticulum to Golgi
Vacuolar membrane	Endosome
Punctate	Peroxisome
Ambiguous	Lipid particle

4.1.2 Membraneless organelles in the budding yeast *Saccharomyces cerevisiae*

As a result of the spread of sophisticated microscopic systems and antibody-based detecting methods, more and more organelle-like structures have been found in eukaryotes, suggesting that cell compartmentalization is a much more complicated system than we have ever imagined. In the budding yeast *S. cerevisiae,* lots of large-scale membraneless aggregates have been found over the last decade. Components and function of these aggregates differ. The well-studied structures in the budding yeast *S. cerevisiae* include cytoplasmic processing bodies (P-bodies) and stress granules.

P-bodies were first found in 1997 and described as "small granules discrete prominent foci" [65]. Later on, functional studies showed that P-bodies are RNA protein granules which contain untranslated mRNAs complex with translation repressors. Nonsense-mediated decay, mRNA decapping, mRNA storage, translation repression and microRNA-mediated repression were described as the major function of P-bodies [66].

Stress granules are another kind of mRNA protein granules, often induced under stress conditions. They are not generally present in normal cells and usually form in response to stresses which cause translation initiation defects [66].

Even though stress granules and P-bodies share protein and RNA components, both appear under stresses. They are two different granule-like structures according to function. Stress granules are believed associated with mRNAs and translation initiation inhibition, while P-bodies are believed to play a role in mRNA degradation [67].

4.1.3 Filament-forming proteins in *Saccharomyces cerevisiae*

In 2009, a partial screen under fluorescence microscope of around 800 strains in the yeast GFP clone collection identified 33 proteins that are able to form self-assembling punctate structures under stress in the budding yeast *S. cerevisiae*[68]. This research is the first screen for protein location in the stationary phase, but only one-sixth of available genes were screened and the resolution of fluorescence microscope prevented the discovery of fine structures in cells. A further research study in 2010 screened 40% of the available collection, and identified 9 proteins that form filament in cells and 29 proteins that forms foci in the cytoplasm which were not able to form filament structures (Figure 4.1) [4]. This was the first systematic study on filament-forming proteins in the budding yeast. The filament-forming proteins identified in this research were Glt1p, Psa1p, Ura7/8p, Gcd2p, Gcd6p, Gcd7p, Gcn3p, and Sui2p, but due to incomplete screening, some important and significant filament-forming proteins may have not been discovered.

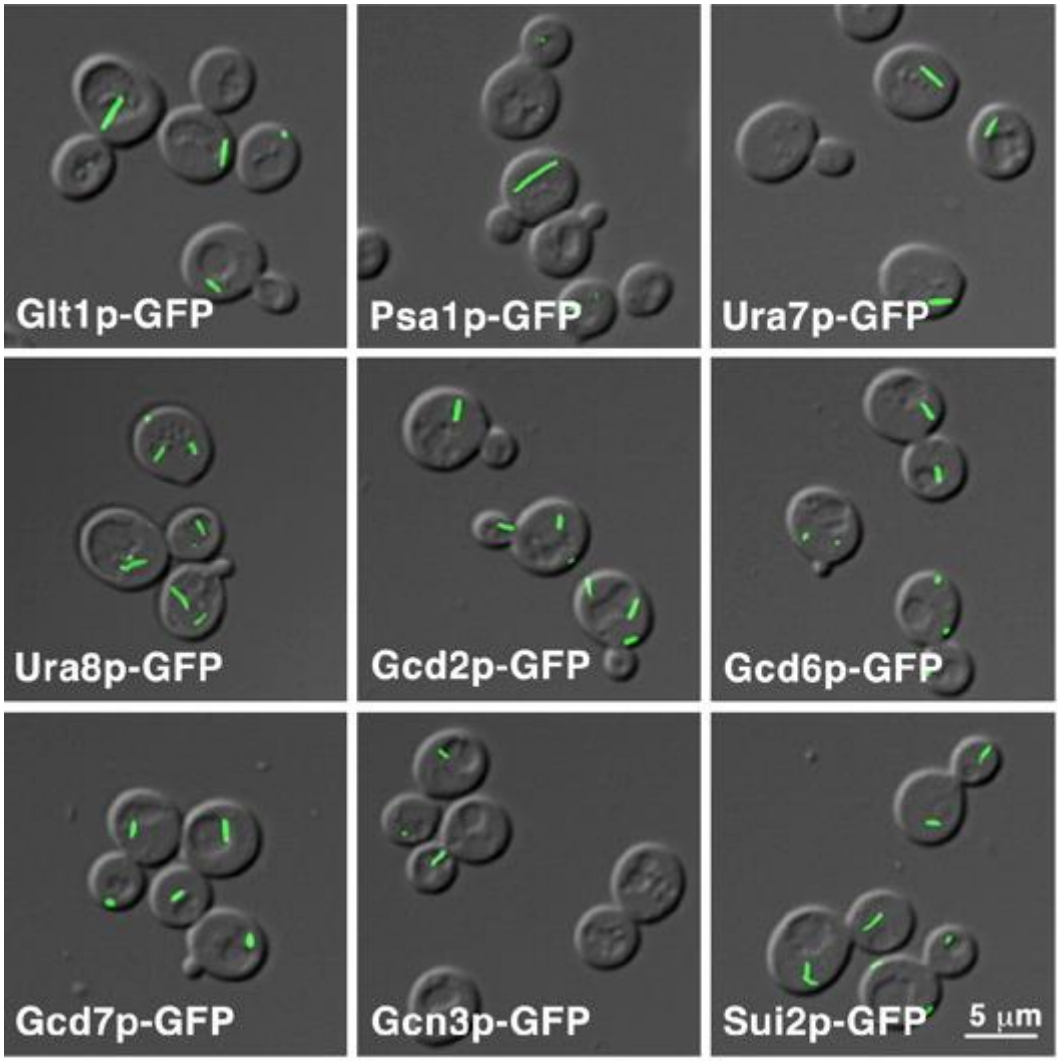


Figure 4.1 Filament-forming proteins identified by Noree et al

Glt1p, Psa1p, Ura7/8p, Gcd2p, Gcd6p, Gcd7p, Gcn3p, and Sui2p were identified as filament-forming proteins in Noree, C. et al., 2010. (Figure adapted from [4])

4.1.4 Growth phase regulation of the Yeast Saccharomyces cerevisiae

Several distinct growth phases are observed when culturing yeast cells in a glucose-based rich medium such as YPD. During the first 24 hours, cells grow rapidly, with a doubling time of around 90 minutes [69]. Yeast cells use glucose, and primarily get energy from fermentation to deal with the huge energy demand of growing so fast. After around one day of culturing, the diauxic shift occurs when the glucose is consumed up. At this point, cells readapt to a respiratory metabolism rather than fermentation to use other non-fermentable carbon source to tackle the shortage of energy in a low glucose environment. The cells keep on growing relatively slowly after the diauxic shift, which is named the post-diauxic phase. The post-diauxic phase lasts for approximately five to seven days. After the post-diauxic phase, cells enter the stationary phase as a result of carbon starvation. During this phase, cells are quiescent and in G0 phase. Stationary-phase cells are also unbudded and contain an unreplicated complement of DNA [70, 71].

Even though we define the stationary phase according to the physiologically quiescent state of yeast cells here, it is worth mentioning that much of the literature defines the start of the stationary phase as the diauxic shift, and combine what we have named the post-diauxic phase and the stationary phase in a different "stationary phase". This is not surprising, since these studies mainly focus on the comparison of rapidly growing cells in the exponential phase with the extremely slow-growing "stationary phase". In this thesis, I define the stages more precisely, since the exponential phase, post-diauxic phase and stationary cells are morphologically and physiologically different.

Morphologically speaking, the stationary phase cells are refractile, while the exponential phase cells are not refractile under a phase-contrast microscope, which is due to the thick and less porous cell walls of the stationary phase cells [72, 73]. The thickened cell walls of the

stationary phase cells also make them more resistant to environmental stresses and certain toxic drugs than exponential cells [74]. Surprisingly, the stationary phase cells are able to react to some environmental signals such as heat shock, oxidative stress, and some drugs, such as methyl methane sulfonic acid [75, 76].

From the perspective of signalling network regulation, some core signalling protein kinases are precisely controlled to ensure the nutrient and metabolic transition of the exponential and the stationary phase. The Target of Rapamycin (TOR) and protein kinase A (PKA) pathways are negative regulators for cells transiting into the stationary phase.

The inhibition of TORC1, a key TOR pathway complex by the drug rapamycin results in a quiescence-like state [77]. TORC1 is regulated by the abundance and quality of the carbon and nitrogen sources, as well as the presence of stresses. Starvation, oxidative stress and osmotic stress result in the inhibition of TORC1 [78]. Inhibition of TORC1 causes downstream gene expression changes and pushes cells into a quiescence-like state. Although inhibition of TORC1 is necessary for quiescent cells, it is not a sufficient condition. Rapamycin-inhibited cells do not appear identical to stationary phase cells in the aspect of translation inhibition, cell mass accumulating and gene expression profile [71].

The PKA pathway is active in the presence of high cellular cAMP concentration. Mutants lacking adenylate cyclase activity are unable to proliferate and remain in a state similar to a stationary phase [79], whereas the constitutive activation of PKA results in cell death at the diauxic shift when normal cells downregulate PKA pathway for cell metabolic transition[80].

The Snf1 pathway is one well-studied positive regulator for cells transiting into the stationary phase. Snf1p is activated when the cell's ATP/AMP ratio drops. When glucose levels decrease, Snf1p is activated within five minutes, thus activating downstream gene expression

for alternative carbon source utilisation. SNF1 mutants cannot survive in alternative carbon source such as ethanol [81].

These three major pathways share some common upstream regulators and downstream regulation targets, weaving into a complicated regulatory network of quiescence. Gray et al. [71] put forward a working model for the entry of quiescence. They divided it into two distinct changes. The first transition is the diauxic shift reprograming, and the second is the entry to a truly quiescent state. Genome-wide expression changes support the two distinct changes [82]. The putative TOR, PKA and Snf1 pathways mainly act at the first transition. Pathways during the second transition are not yet well studied.

4.1.5 Aims of this chapter

For this chapter, I led a screening with two colleagues (Hakimi Kassim and Yong Huang) of the whole yeast GFP clone collection (4,159 strains) for filament-forming proteins after one day of culturing. Besides the filament-forming proteins, I also searched for foci-forming proteins screened from this collection. After the screening, I made a brief study on the function, localization and interaction of all filament-forming proteins.

4.2 Results

4.2.1 Foci-forming proteins in the budding yeast

The library I used in the screening was the *S. cerevisiae* strains GFP clone collection, comprising 4,159 GFP-tagged open reading frames (ORF) [35]. The screening consisted of two parts. During the primary screening, strains were copied and transferred on solid YPD plates for storage. Strains were then transferred to 150μL liquid YPD medium in 96 well-plates for 24 hours at 32°C of culturing before fixation. Pictures were taken under fluorescent microscope. Strains containing foci-like or filament-like structures were picked, and a second round of screening under confocal microscope was carried out on these strains to verify results and collect fine pictures of filament or foci-forming proteins. During the verification, candidate strains were picked up and cultured in 150μL liquid YPD medium in 0.6mL EP tubes for 24 hours at 32°C before fixation. Pictures were taken under 63X confocal microscope. Pictures were then analysed using ImageJ software.

In total, we discovered 114 proteins which form intracellular aggregates in the budding yeast *S. cerevisiae* after 24 hours of culturing in the second-round screening. The ones we defined as the intracellular aggregate forming proteins had to meet the following standard: more than 1% of cells captured contained the intracellular GFP signal, which was restricted to a single bud-like structure or filament. Among the intracellular aggregate forming proteins, we defined those structures which were longer than 0.75μm as filament-forming proteins and those shorter than 0.75μm as foci-forming proteins. This standard was applied in (Noree, C., et al., 2014 [24]), since two peaks were observed in the length distribution curve with the cutoff value at 0.75 μm. We discovered and confirmed 21 filament-forming proteins in this study, and 93 foci-forming proteins. A detailed description of the foci-forming proteins is shown in the following Table 4.2.

Table 4.2 Foci-forming proteins in *S. cerevisiae*

Protein	Name Description	Biological Process
Abp1	Actin Binding Protein	Actin cortical patch assembly/barbed-end actin filament capping/protein localization
Ade17	ADEnine	'De novo' IMP biosynthetic process/purine nucleotide biosynthetic process
Ade4	ADEnine requiring	'De novo' IMP biosynthetic process
Aha1	Activator of Heat shock protein 90 ATPase	Cellular response to heat/protein folding
Aip1	Actin Interacting Protein	Actin filament depolymerisation/response to osmotic stress
Ald4	ALdehyde Dehydrogenase	Acetate biosynthetic process
Ald6	ALdehyde Dehydrogenase	Acetate biosynthetic process/NADPH regeneration/response to salt stress
Arb1	ATP-binding cassette protein involved in Ribosome Biogenesis	Ribosomal small subunit export from nucleus/ ribosome biogenesis
Brx1	Xenopus laevis Brix homolog	Ribosomal large subunit assembly
Cbf5	Centromere Binding Factor	rRNA processing/rRNA pseudouridine synthesis/snRNA pseudouridine synthesis
Cdc19	Cell Division Cycle	Glycolytic process/pyruvate metabolic process
Cic1	Core Interacting Component	Protein catabolic process
Coq5	COenzyme Q	Aerobic respiration/ubiquinone biosynthetic process
Cox19	Protein required for cytochrome c oxidase assembly	Metal ion transport/mitochondrial respiratory chain complex IV assembly
Erg6	ERGosterol biosynthesis	Ergosterol biosynthetic process
Fpr3	Fk 506-sensitive Proline Rotamase	Meiotic recombination checkpoint/nucleosome assembly
Fpr4	FKBP Proline Rotamase	negative regulation of histone H3-K36 methylation/nucleosome assembly
Gar1	Glycine arginine rich domains	rRNA processing/ snRNA pseudouridine synthesis
Gcd1	General Control Derepressed	Negative regulation of cellular response to amino acid starvation/
Gcd2	General Control Derepressed	Regulation of translational initiation
Gdb1	Glycogen debranching enzyme	Glycogen catabolic process
Glc7	GLyCogen	Ascospore formation/cell budding/cellular ion homeostasis/chromosome segregation

Protein	Name Description	Biological Process
Gpd1	Glycerol-3-Phosphate Dehydrogenase	Intracellular accumulation of glycerol/ NADH oxidation
Gpm1	Glycerate PhosphoMutase	Gluconeogenesis/glycolytic process
Hmo1	High MObility group (HMG) family	DNA packaging/dsDNA loop formation/
Hsc82	Cytoplasmic chaperone of the Hsp90 family	Cellular response to heat /proteasome assembly /protein folding /protein refolding
Hsp104	Heat Shock Protein	Cellular heat acclimation/chaperone cofactor-dependent protein refolding/
Hsp26	Heat Shock Protein	Cellular response to heat/ protein folding
Hsp42	Heat Shock Protein	Cytoskeleton organization
Hsp78	Heat Shock Protein	Cellular response to heat/ mitochondrial genome maintenance/ protein refolding/
Htz1	Histone Two A Z1	Chromatin remodeling/chromatin silencing at silent mating-type cassette
Ilv1	IsoLeucine-plus-Valine requiring	Isoleucine biosynthetic process
Ilv2	IsoLeucine-plus-Valine requiring	Branched-chain amino acid biosynthetic process
Img2	Mitochondrial ribosomal protein of the large subunit	Mitochondrial translation
Isd11	Cysteine desulfurase (Nfs1p) activator	Iron-sulfur cluster assembly
Kgd1	Mitochondrial α-ketoglutarate dehydrogenase complex subunit	2-oxoglutarate metabolic process/tricarboxylic acid cycle
Lpd1	Dihydrolipoamide dehydrogenas	2-oxoglutarate metabolic process /glycine catabolic process/
Mak21	MAintenance of Killer	Ribosomal large subunit assembly
Mdy2	Mating-Deficient Yeast	Cell morphogenesis involved in conjugation with cellular fusion
Mmf1	Mitochondrial protein required for transamination of isoleucine	Isoleucine biosynthetic process/mitochondrial translation
Mss116	Mitochondrial transcription elongation factor	Group I intron splicing/Group II intron splicing/RNA folding/
Net1	Nucleolar silencing Establishing factor and Telophase regulator	Nucleolus organization
Nhp2	Non-Histone Protein	Cleavage involved in rRNA processing/rRNA pseudouridine synthesis
Nip7	Nuclear ImPort	Assembly of large subunit precursor of preribosome
Noc2	NucleOlar Complex associated	Ribosomal large subunit biogenesis

Protein	Name Description	Biological Process
Noc3	NucleOlar Complex associated	DNA replication initiation
Nop10	NucleOlar Protein	Cleavage involved in rRNA processing/rRNA pseudouridine synthesis
Nop12	NucleOlar Protein	Maturation of LSU-rRNA from tricistronic rRNA transcript
Nop15	NucleOlar Protein	Actomyosin contractile ring assembly/ribosomal large subunit biogenesis
Nop2	NucleOlar Protein	Assembly of large subunit precursor of preribosome
Nop4	NucleOlar Protein	Maturation of LSU-rRNA from tricistronic rRNA transcript
Nop56	NucleOlar Protein of 56.8 kDa	rRNA modification/rRNA processing
Nop58	NucleOlar Protein of 58 kDa	Pre-rRNA processing
Nop7	NucleOlar Protein	Cell cycle DNA replication
Pby1	P-BodY associated protein	Biological process unknown/ nuclear-transcribed mRNA catabolic process
Pda1	E1 alpha subunit of the pyruvate dehydrogenase (PDH) complex	Acetyl-CoA biosynthetic process from pyruvate/pseudohyphal growth
Pex11	PEroXin	Fatty acid oxidation/peroxisome fission
Pnc1	Pyrazinamidase and NiCotinamidase	Chromatin silencing at rDNA/chromatin silencing at telomere/
Por1	Mitochondrial porin (voltage-dependent anion channel)	Apoptotic process/cell redox homeostasis/DNA transport/ion transport /
Pre10	PRoteinase yscE	Proteasomal ubiquitin-independent protein catabolic process/
Pre4	PRoteinase yscE	Proteasomal ubiquitin-independent protein catabolic process/
Pre6	PRoteinase yscE	Proteasomal ubiquitin-independent protein catabolic process/
Prp43	Pre-mRNA Processing	Maturation of 5.8S rRNA from tricistronic rRNA transcript
Prs5	PhosphoRibosylpyrophosphate Synthetase	5-phosphoribose 1-diphosphate biosynthetic process
Rfa1	Replication Factor A	DNA repair/DNA replication/DNA topological change
Rfa2	Replication Factor A	DNA repair/DNA replication/DNA topological change
Rnr2	RiboNucleotide Reductase	Deoxyribonucleotide biosynthetic process
Rnr4	RiboNucleotide Reductase	Deoxyribonucleotide biosynthetic process
Rpn11	Regulatory Particle Non-ATPase	Mitochondrial fission/peroxisome fission/proteasome storage granule assembly
Rps22A	Ribosomal Protein of the Small subunit	Cytoplasmic translation
Rps22B	Ribosomal Protein of the Small subunit	Cytoplasmic translation

Protein	Name Description	Biological Process
Rpt1	Regulatory Particle Triple-A protein	Positive regulation of protein catabolic process
Sac6	Suppressor of ACtin	Actin filament organization
Sam1	S-AdenosylMethionine requiring	Methionine metabolic process/ S-adenosylmethionine biosynthetic process
Scl1	Suppressor of Crl3 Lethality	Proteasomal ubiquitin-independent protein catabolic process
Shm2	Serine HydroxyMethyltransferase	One-carbon metabolic process
Sis1	SIt4 Suppressor	Misfolded protein transport
Smc5	Structural Maintenance of Chromosomes	Chromosome separation
Srp40	Serine Rich Protein	Nucleocytoplasmic transport
Srv2	Suppressor of RasVal19	Actin filament organization/actin filament severing/Ras protein signal transduction
Ssa1	Stress-Seventy subfamily A	Clathrin coat disassembly/cytoplasmic translation/protein folding
Ssa2	Stress-Seventy subfamily A	Protein folding/SRP-dependent co-translational protein targeting to membrane
Tdh3	Triose-phosphate DeHydrogenase	Apoptotic process/gluconeogenesis/glycolytic process
Thr1	THReonine requiring	Homoserine metabolic process/isoleucine metabolic process
Tif6	Translation Initiation Factor	Assembly of large subunit precursor of preribosome
Tim50	Translocase of the Inner Mitochondrial membrane	Protein import into mitochondrial matrix
Tps1	Trehalose-6-Phosphate Synthase	Cellular carbohydrate metabolic process/cellular response to desiccation
Utp8	U Three Protein	Maturation of SSU-rRNA from tricistronic rRNA transcript /
Vma4	V-type proton ATPase subunit E	Vacuolar acidification
Wtm1	WD repeat containing Transcriptional Modulator	Maintenance of protein location in nucleus
Yra1	Yeast RNA Annealing protein	mRNA export from nucleus/negative regulation of ATP-dependent RNA helicase activity/
Ytm1	Ribosome biogenesis protein	Chromosome organization/ribosomal large subunit biogenesis
Zim17	ZInc finger Motif protein of 17 kDa	Mitochondrion organization/protein folding/protein import into mitochondrial matrix

4.2.2 Filament-forming proteins in the budding yeast

This screening confirmed that all nine proteins identified in Noree's study [4] (i.e. Glt1p, Psa1p, Ura7p, Ura8p, Gcd2p, Gcd6p, Gcd7p, Gcn3p and Sui2p) and all four septin proteins (i.e. Cdc10p, Cdc11p, Cdc12p and Shs1p) available in the collection can form filaments (Figure 4.2). Short filaments and foci assembled by Gln1p could be detected, but those foci did not meet the standard for filaments, even after starvation treatment.

In addition, nine novel proteins were identified that formed large-scale filaments detectable under light microscope (Figure 4.3). They are Acc1p (acetyl-CoA carboxylase), Asn1p/Asn2p (asparagine synthetase), Gcd1p (eIF2B-γ), Gdb1p (glycogen debranching enzyme), Gdh2p (glutamate dehydrogenase), Pfk1p/Pfk2p (phosphofructokinase) and Tsa1p (thioredoxin peroxidase). To simplify the terminology, we refer to these metabolic enzyme-containing serpent-shaped structures as cytoophidia in the following passages. A detailed description of the foci-forming proteins is shown in the following Table 4.3.

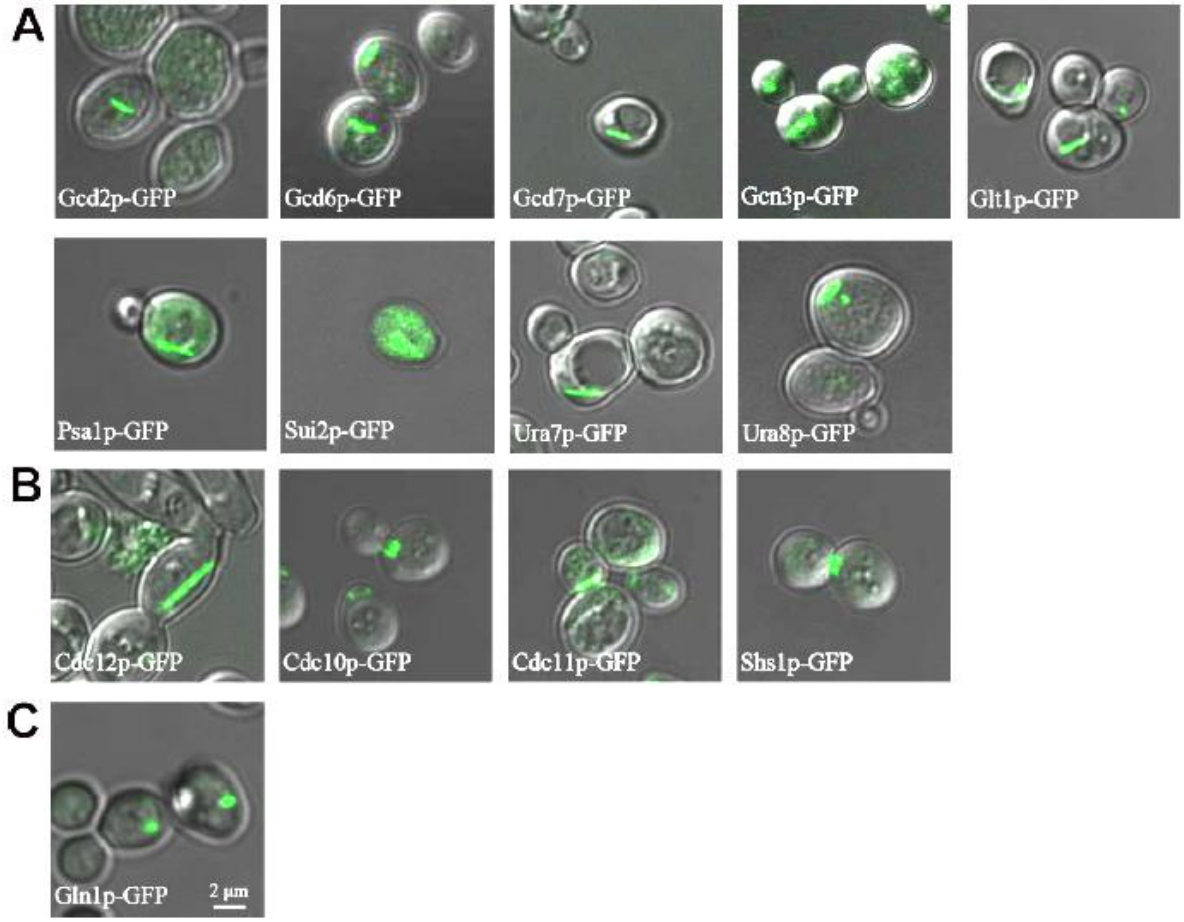


Figure 4.2 Confirmation of filament-forming proteins in *S. cerevisiae*

(A) Nine proteins (Gcd2p, Gcd6p, Gcd7p, Gcn3p, Glt1p, Psa1p, Sui2p, Ura7p, and Ura8p) were reported in a previous study [4]; **(B)** Filament-forming proteins (Cdc10p, Cdc11p, Cdc12p and Shs1p) in septin complex; **(C)** Gln1p (glutamine synthetase) can form short filaments and foci in *S. cerevisiae*, supporting a finding reported previously [83]. Scale bar, 2 μm

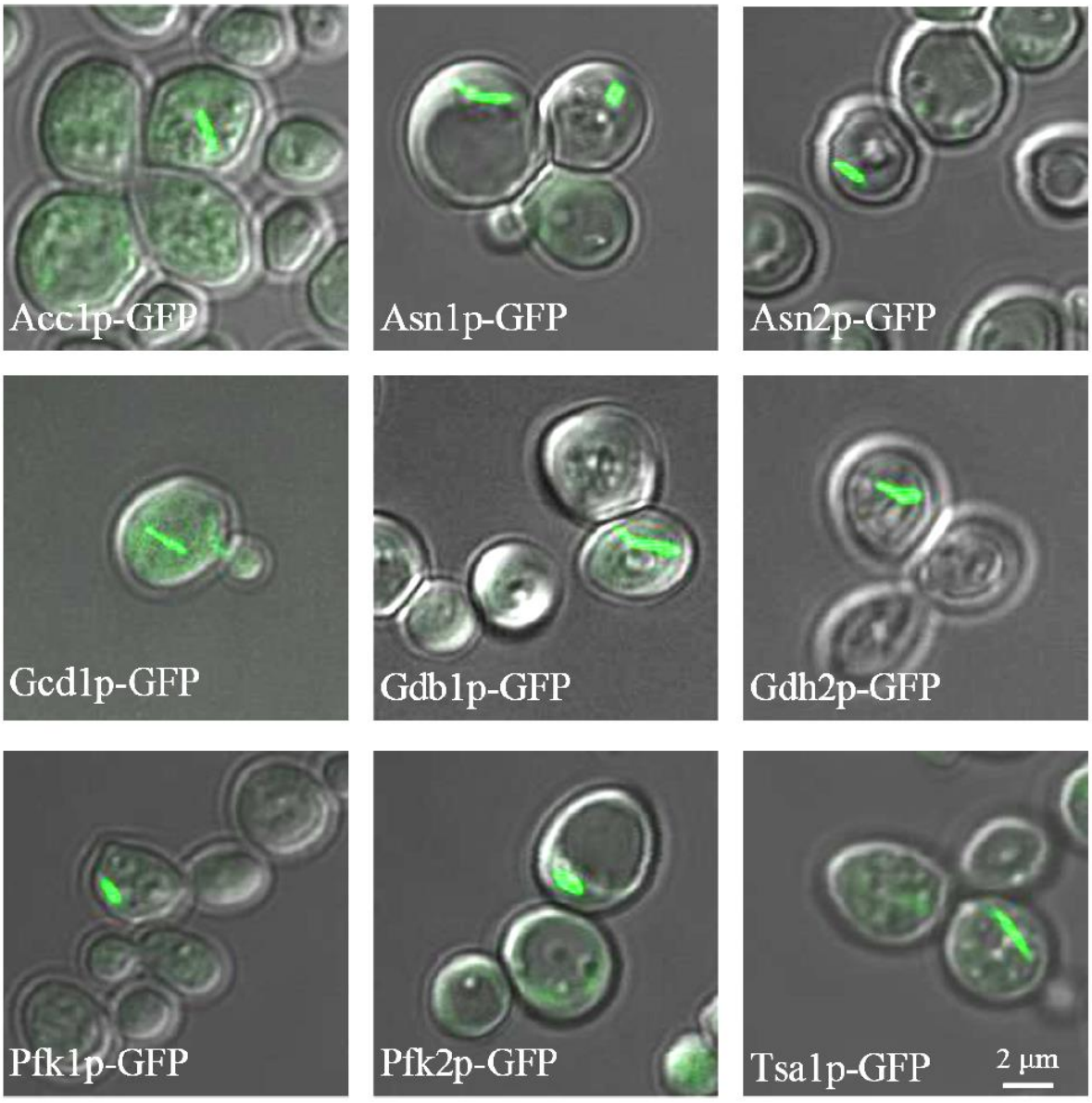


Figure 4.3 Novel filament-forming proteins identified in *S. cerevisiae*

Acc1p, acetyl-CoA carboxylase; Asn1p, asparagine synthetase; Asn2p, asparagine synthetase; Gcd1p, eIF2B-gamma; Gdb1p, glycogen debranching enzyme; Gdh2p, glutamate dehydrogenase; Pfk1p, phosphofructokinase; Pfk2p, phosphofructokinase; Tsa1p, thioredoxin peroxidase. Scale bars, 2 µm

Table 4.3 Filament-forming proteins in *S. cerevisiae*

Protein	Name description	Biological process	Published structures (References)
Acc1	**Acetyl-CoA Carboxylase**	**Long-chain fatty acid biosynthetic process**	Filaments (this study)
Asn1	**Asparagine requiring**	**Asparagine biosynthetic process**	Filaments (this study)
Asn2	**Asparagine requiring**	**Asparagine biosynthetic process**	Foci [68] Filaments(this study)
Cdc10	Cell Division Cycle	Septin ring assembly	Filaments [84, 85]
Cdc11	Cell Division Cycle	Septin ring assembly	Filaments [11, 12]
Cdc12	Cell Division Cycle	Septin ring assembly	Filaments [11, 12]
Gcd1	**General Control Derepressed**	**Regulation of translational initiation**	Filaments (this study)
Gcd2	General Control Derepressed	Regulation of translational initiation	Filaments [4]
Gcd6	General Control Derepressed	Regulation of translational initiation	Filaments [4]
Gcd7	General Control Derepressed	Regulation of translational initiation	Filaments [4]
Gcn3	General Control Nonderepressible	Regulation of translational initiation	Filaments [4]
Gdb1	**Glycogen debranching enzyme**	**Glycogen catabolic process**	Foci [4]
Gdh2	**Glutamate Dehydrogenase**	**Nitrogen compound metabolic process**	Filaments (this study)
Gln1	Glutamine metabolism	Glutamine biosynthetic process	Filaments (this study)
Glt1	Glutamate synthase	Glutamate biosynthetic process	Filaments [4, 83]; Foci [68]
Pfk1	**Phosphofructokinase**	**Glycolytic process**	Filaments (this study)
Pfk2	**Phosphofructokinase**	**Glycolytic process**	Filaments (this study)
Psa1	GDP-mannose pyrophosphorylase	GDP-mannose biosynthetic process	Filaments [4]
Shs1	Seventh homolog of septin	Septin ring assembly	Filaments [84, 85]
Sui2	Suppressor of Initiator codon	Regulation of translational initiation	Filaments [4]
Tsa1	**Thiol-Specific Antioxidant**	**Cell redox homeostasis**	Filaments (this study)
Ura7	URAcil requiring	CTP biosynthetic process	Filaments [4]
Ura8	URAcil requiring	CTP biosynthetic process	Filaments [4]

Proteins in bold are identified as novel filament-forming proteins in this study.

Acetyl-CoA carboxylase catalyses the irreversible carboxylation of acetyl-CoA to malonyl-CoA. The function of acetyl-CoA carboxylase is to provide the malonyl-CoA substrate for fatty acid biosynthesis. It has been known for a long time that acetyl-CoA carboxylase can be polymerised into EM-scale fibres in mammals [86, 87]. Polymerisation of this enzyme upregulates the enzyme activity. A recent study reported that Acc1p diffused in the cytoplasm under normal growth conditions. However, prolonged starvation induces Acc1p to form rod-like structures in the budding yeast *S. cerevisiae* [88]. Our screening found that Acc1p is capable of forming large-scale filaments under normal growth conditions.

In the budding yeast, two genes, *ASN1* and *ASN2*, encode asparagine synthetase using aspartate and glutamine as the substrates and catalyse an ATP-dependent reaction to produce asparagine [89]. In this study, I found that Asn1p and Asn2p have very similar distributions in the budding yeast, and both can form filaments in vivo. Studies in *E. coli* and beef pancreas suggested that asparagine synthetase functions as a dimeric enzyme [90, 91]. Lack of asparagine synthetase may cause cell apoptosis [92]. Due to its important role in amino acid synthesis, asparagine synthetase is a common target in the treatment of acute lymphoblastic leukaemia, as well as prostate and other kinds of cancer [93-95]. These features attracted my attention. More detailed experiments about the regulation of Asn1p/Asn2p filament assembly are described in the Chapter 5.

Noree et al. [4] have shown that five representative subunits of the eIF2 and eIF2B complexes, Gcd2p (eIF2B-δ), Gcd6p (eIF2B-ε), Gcd7p (eIF2B-β), Gcn3p (eIF2B-α), and Sui2p (eIF2-α), are present in the same filament. Here we identified an additional subunit of the eIF2/2B complex, Gcd1p (eIF2B-γ), which formed a similar filamentous structure. Although GFP-tagged Gcd1p (eIF2B-γ) was previously reported in foci in the budding yeast *S. cerevisiae* [96], the images in that study showed filament-like structures which are in line with the results of the current study.

Glycogen is a multi-branched polysaccharide of glucose residues, which serves as a form of energy storage in animals and yeast. The accumulation of glycogen responds to nutrient restriction, heat, osmotic and saline stress. A rapid mobilisation of glycogen by two enzymes, glycogen phosphorylase and the glycogen debranching enzyme, is necessary for the resumption of growth of non-proliferating yeast cells. The glycogen debranching enzyme Gdb1p has been identified by Noree et al. [4] as a foci-forming protein that is incapable of forming filaments, but our screening indicated that Gdb1p is able to assemble into filaments under normal growth conditions. Gdb1p contains two enzyme activities as α-1,4-glucanotransferase and α-1,6-glucosidase. Interestingly, filamentation of β-glucosidase was first observed in electron micrographs of oat plastids in 1965 [97]. More recently, biochemical analyses have suggested that the filament is the active form of the β-glucosidase enzyme [52].

In the budding yeast, two NADP+-dependent glutamate dehydrogenases (NADP-GDHs) encoded by *GDH1* and *GDH3* catalyse the synthesis of glutamate from ammonium and α-ketoglutarate. *GDH2* encodes NAD+-dependent glutamate dehydrogenase (NAD-GDH), which degrades glutamate, producing ammonium and α-ketoglutarate [98]. Our screening identified that Gdh2p, but not Gdh1p or Gdh3p, can form filaments in vivo in the budding yeast. A future study on the function and mechanism of Gdh2p-filament assembly, compared with its isoenzymes Gdh1p or Gdh3p, may bring us more valuable information on metabolic enzyme filament assembly.

Phosphofructokinase 1 (PFK) catalyses the phosphorylation of fructose 6-phosphate to fructose 1,6-bisphosphate by ATP, which is a principal regulatory step in glycolysis. The yeast orthologue of human phosphofructokinase-1 consists of heterooctamers $\alpha_4\beta_4$. Pfk1p (α subunit) and Pfk2p (β subunit) are homologous to each other. Under electron microscopy, cross-linked rabbit muscle Pfk1p has been observed to form dimeric, tetrameric, octameric

and filamentous structures in vitro [99]. Immunofluorescence images have shown the filamentous arrangement of Pfk1p in the budding yeast [100]. Like Pfk1p, Pfk2p can also form filaments in the budding yeast in vivo, suggesting that the filament-forming property is an evolutionarily conserved and ancient feature of PFK.

Oxidative stress results from oxygen metabolism and occurs in the cells of all aerobic organisms. Oxidative stress reflects a state in which reactive oxygen species exceed a biological system's ability to readily detoxify the reactive intermediates or to repair the resulting damage. Oxygen-utilising cells have evolved defence mechanisms to protect against the damage caused by oxidative stress, called the oxidative stress response (OSR). Thioredoxin peroxidase, Tsa1p, plays an important role in OSR. Tsa1p can self-associate to form high-molecular weight chaperone complex under oxidative stress [101]. Our screening has revealed that Tsa1p can form filaments in vivo.

4.2.3 Heterogeneities of cytoophidia in *Saccharomyces cerevisiae*

Inspired by the variation of Ura7p filaments during different stages of culturing [4], I decided to verify the compartmentation of proteins identified in previous studies in fast-growing exponential phase to test the dynamic of different cytoophidia along the growth curve of yeast.

Yeast was cultured for one day and diluted 1:30 to the OD 0.15 as a start point, and cultured for three hours to the OD value 0.35-0.4 (the OD value differed slightly between samples) before being fixed. Pictures were taken by confocal microscopy.

The results showed that most of the previous identified proteins did not form filament in the exponential phase (Table 4.4). According to the gene expression omnibus (GEO) data

GSE55508 [102], the average fold changes between the exponential phase and the diauxic shift vary widely among proteins. Even though most proteins share the property of not forming filaments before the diauxic shift, the fold changes differ a lot. Gdb1p, Gdh2p and Ura8p have a significant increase ($p<0.05$) of mRNA level after the diauxic shift, while Asn1p, Asn2p, Gcd7p, Pfk1p, Pfk2p, and Ura7p have a significant decrease ($p<0.05$) of mRNA level in the post-diauxic phase and changes in other proteins (Ccd12p, Gcd2p, Tsa1p) are not significant ($p<0.05$). This suggests that the filament-forming processes are not totally expression-level dependent and different regulation mechanisms may occur according to the individual filament-forming protein.

There are two strains shows different behaviour compared with others. Acc1p filament percentage is similar in those two phases. However, in the exponential phase, Acc1p forms additional foci structures which cannot be detected after the diauxic shift. These foci structures may be preliminary filaments which can turn into filaments in the later phases.

Moreover, Glt1p shows a higher percentage of filaments during the exponential phase than the post-diauxic phase, while Glt1p has a higher expression level in the exponential phase. This is totally different from those filament-forming proteins with a higher percentage of filaments in the post-diauxic phase. The underlying filament assembly mechanism may be different.

Table 4.4 Comparison of percentage of cells containing cytoophidia between the exponential phase and the diauxic shift

(mRNA level fold-change data from[102]. Arrow directions indicate up/downregulated mRNA level at the diauxic shift compared with the exponential phase.)

Phase	Exponential phase		Diauxic shift		Fold change of mRNA level (diauxic shift / exponential)
OD	0.35-0.4		5.0-6.0		
Time	3 hours		1 day		
Strains	Description	Percentage	Description	Percentage	
ASN1	Cytoplasmic	0.0%	Filament	15.5%	0.39↓
ASN2	Cytoplasmic	0.0%	Filament	17.5%	0.78↓
CDC12	Cytoplasmic	0.0%	Filament	28.8%	0.96↓
GCD2	Cytoplasmic	0.0%	Filament	8.1%	0.77↓
GCD7	Cytoplasmic	0.0%	Filament	18.2%	0.52↓
GDB1	Cytoplasmic	0.0%	Filament	5.7%	7.78↑
GDH2	Cytoplasmic	0.0%	Filament	3.0%	6.18↑
PFK1	Cytoplasmic	0.0%	Filament	3.0%	0.84↓
PFK2	Cytoplasmic	0.0%	Filament	4.8%	0.86↓
TSA1	Cytoplasmic	0.0%	Filament	8.2%	1.17↑
URA7	Cytoplasmic	0.0%	Filament	30.8%	0.30↓
URA8	Cytoplasmic	0.0%	Filament	12.3%	1.80↑
GLT1	Filament	8.1%	Filament	1.1%	0.60↓
ACC1	Filament Foci	8.6% 18.5%	Filament	9.1%	2.05↑

4.2.4 Nutrient deprivation induces filament formation in most cases

Previous studies showed that nutrient deprivation can induce Ura7p filament formation in the budding yeast [4] and CTP synthase filament formation in *Drosophila* S2R+ cells (Chapter 3 of this thesis). To investigate whether each filament-forming protein identified in the screening I conducted has a similar response to nutrient deprivation, yeasts in their exponential phase (three hours OD 0.35-0.4) were centrifuged and the medium was replaced by PBS and cultured for another six hours. After six hours of nutrient deprivation, OD reached 0.6. The yeast was fixed in 4% PFA for confocal imaging.

Of those strains, four (Gcd7p, Gdb1p, Pfk2p and Ura8p) remained without any filaments. In another four strains (Asn1p, Asn2p, Cdc12p and Pfk1p), filaments were detected and the percentage of filament-forming cells after PBS treatment was less than that of the diauxic shift.

Another three proteins (Gcd2p, Glt1p and Ura7p) can be induced to form filament. The percentage of filament-forming cells after PBS treatment was more than that of the diauxic shift. Among them, Ura7p had nearly four-fold cytoophidium abundance compared with the post-diauxic phase.

Tsa1p lost filaments after PBS treatment, but small foci formed in this situation. In Acc1p and Gdh2p, foci and filaments co-existed in the budding yeast (Table 4.5).

There is no obvious difference according to protein function among the three groups of proteins which PBS cannot induce filament/ PBS induced filament less than the diauxic shift/ PBS induced filament more than the diauxic shift. Interestingly, as two genome replication Ura7p and Ura8p showed totally different behaviour while Asn1p and Asn2p showed similar behaviour.

Table 4.5 Comparison of the percentage of cells containing cytoophidia in nutrient-deprived cells and after the diauxic shift

	PBS treatment		Post-diauxic phase	
OD	**0.6-0.7**		**5.0-6.0**	
Strains	**Distribution**	**Percentage**	**Distribution**	**Percentage**
PBS cannot induce filament				
GCD7	Cytoplasmic	0.0%	Filament	18.2%
GDB1	Cytoplasmic	0.0%	Filament	5.7%
PFK2	Cytoplasmic	0.0%	Filament	4.8%
URA8	Cytoplasmic	0.0%	Filament	12.3%
PBS induced filament/less than the diauxic shift				
ASN1	Filament	6.9%	Filament	15.5%
ASN2	Filament	0.8%	Filament	17.5%
CDC12	Filament	2.6%	Filament	28.8%
PFK1	Filament	0.2%	Filament	3.0%
PBS induced filament/more than the diauxic shift				
GCD2	Filament	9.0%	Filament	8.1%
GLT1	Filament	14.0%	Filament	1.1%
URA7	Filament	78.2%	Filament	30.8%
Foci prevalent under starvation				
TSA1	Foci	26.8%	Filament	8.2%
ACC1	Filament	25.8%	Filament	9.1%
	Foci	41.9%		
GDH2	Filament	1.4%	Filament	3.0%
	Foci	56.4%		

4.2.5 Prolonged culturing cannot make foci-forming proteins form filaments

Previous experiments showed that some of the filament-forming proteins formed foci-like structures instead of filaments or accompanying filaments in some situations (see sections 4.2.3, 4.2.4). This suggested that filament-forming proteins aggregate in different ways depending on cellular metabolic environment. During the culturing of filament-forming protein strains, I found that prolonged culturing increased filament length and increased percentage of filament-positive cells. To identify more filament-forming proteins, I undertook prolonged culturing for all of the foci-forming proteins (including filament-forming proteins as control) discovered in the previous experiments.

Cells were diluted to the OD value 0.05 in YPD medium as the start point for culturing. Culturing samples were collected and fixed at day eight. Pictures were taken with a 63X objective on a laser-scanning confocal microscope (Leica TCS SP5 II confocal microscope).

The results showed that, except for previously identified filament-forming proteins, none of the foci-forming proteins showed the phenotype of filament-forming according to the standard (0.75μm in length) of filament I described in section 4.2.1. This suggested that these foci structures in the foci-forming proteins might be fundamentally different from the filament structure in filament-forming proteins and they were not interchangeable.

4.2.6 Filamentation in the nucleus

It was previously found that CTP synthase can form both cytoplasmic cytoophidia (C-cytoophidia) and nuclear cytoophidia (N-cytoophidia) in mammalian cells [19]. It was also observed that CTP synthase can form C- and N-cytoophidia in the fission yeast *S. pombe* [7]. Noree [4] observed that the two CTP synthase proteins, Ura7p and Ura8p, can form filaments in the budding yeast. However, whether Ura7p and Ura8p can form structures in the nucleus has remained unexplored. To address this issue, I closely looked at Ura7p-GFP and Ura8p-GFP cells counterstained with the DNA dye Hoechst 33342.

The result suggests that both Ura7p-GFP and Ura8p-GFP can form filamentous structures in the nucleus, as well as in cytoplasm (Fig. 4.4). Combining the results regarding the subcellular distribution of CTP synthase in *S. cerevisiae*, *S. pombe* and mammalian cells, I can conclude that both C- and N-cytoophidia are highly conserved during evolution.

Encouraged by these observations, I carefully checked other filament-forming proteins in the budding yeast. Both Asn1p and Asn2p were found to form nuclear filaments as well as cytoplasmic filaments (Figure 4.4). For Asn1p and Asn2p strains, two cytoophidia are usually observed in one cell. One is usually located in cytoplasm, and seemed longer in length and thicker in diameter. The other is usually located in the nuclear area, and is relatively small. This “pair pattern” is very common and obvious in the Asn1p and Asn2p strains after the diauxic shift.

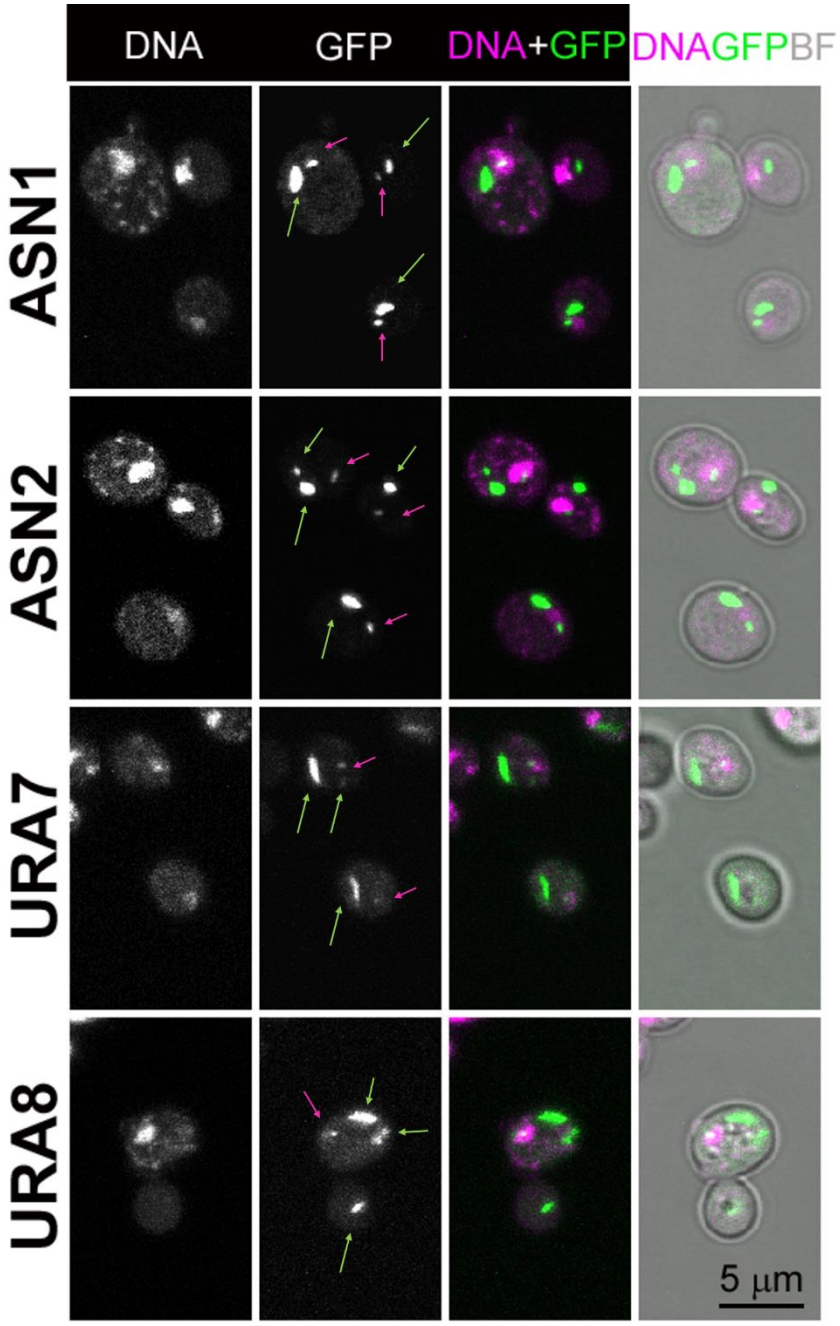


Figure 4.4 Filaments forming in the cytoplasm and nucleus

Budding yeast cells expressing GFP-tagged ORFs were observed under confocal microscope. Both isoforms of CTP synthase, Ura7p and Ura8p, can form cytoophidia in cytoplasm and in the nucleus, which is consistent with our previous findings in *S. pombe* [7] and mammalian cells [19]. Both isoforms of asparagine synthetase, Asn1p and Asn2p, can also form cytoophidia in cytoplasm and in the nucleus. Note that cytoplasmic cytoophidia are longer and thicker than nuclear cytoophidia. Scale bars, 5μm. Green arrow indicates cytoplasmic cytoophidium. Magenta arrow indicates nuclear cytoophidium.

4.2.7 Clusters of filament-forming proteins

To explore how those filament-forming proteins interplay and interact with each other as well as key proteins and pathways, a protein network analysis was performed by utilising the STRING database version 10 [36]. Protein-protein interactions are showed in the form of nodes and lines. Coloured lines between proteins indicate different types of interactions, such as neighbourhood, co-occurrence, experiments, text-mining, co-expression, databases, and homology.

From the network analysis (Figure 4.5), I find that the filament-forming proteins discovered are divided into three major groups: metabolic enzymes, translation initiators and septin proteins. Most of the metabolic filament-forming proteins are highly related to each other in the network map, indicating that those metabolic filament-forming proteins may share lots of similarity from the aspect of filament-formation process and regulation.

A detail pathway analysis has been undertaken (Table 4.7). The results illustrate the STRING gene set enrichments for those filament-forming proteins against Kyoto Encyclopedia of Genes and Genomes (KEGG) pathways with significance rank $P<0.05$. Enrichment of the eIF2/2B complex (Gcd1p, Gcd6p, Gcd2p, Gcd7p, Gcn3p and Sui2p) indicates the strong association with the RNA transport pathway.

Apart from septin proteins and eIF2/2B complex, 12 of the other 13 proteins were enriched in metabolic pathways. Especially in the alanine, aspartate and glutamine metabolism, five proteins were enriched (Asn1p, Asn2p, Gdh2p, Gln1p and Glt1p). Among these five proteins, three of them were closely related to nitrogen metabolism.

A group of glutamine/glutamate related proteins are enriched in the screening of filament-forming proteins. They are Asn1p, Asn2p, Gdh2p, Gln1p, Glt1p, Ura7p and Ura8p. The

enrichment of glutamine/glutamate related protein may indicate potential relationship between cytoophidia and glutamine/glutamate metabolism (Table 4.6).

Gene	Glutamine in reaction	Glutamate in reaction
ASN1	Substrate	Product
ASN2	Substrate	Product
GLN1	Product	Substrate
GDH2	N/A	Substrate
GLT1	Substrate	Product
URA7	Substrate	Product
URA8	Substrate	Product

Table 4.6 Table of filament-forming proteins related to glutamine/glutamate metabolism

4.2.8 Clusters of foci-forming proteins

I also did a similar network analysis for the foci-forming proteins (including the filament-forming proteins) using the STRING database version 10 [32].

The network analysis (Figure 4.6) provides an overall view of the grouping of foci-forming proteins. In the lower part of the figure, lots of nuclear or nucleolar proteins are enriched. They are mainly related to rRNA biogenesis and processing in the nucleus or nucleolus. In the higher part of the figure, lots of metabolic enzymes are enriched. Several important pathways are involved, such as the glutamine metabolic process, the alpha-amino acid metabolic process, and the isoleucine metabolic process (Table 4.8). From this point of view, a part of enzymes in amino acid synthesis or process tend to form foci or filamentous structures.

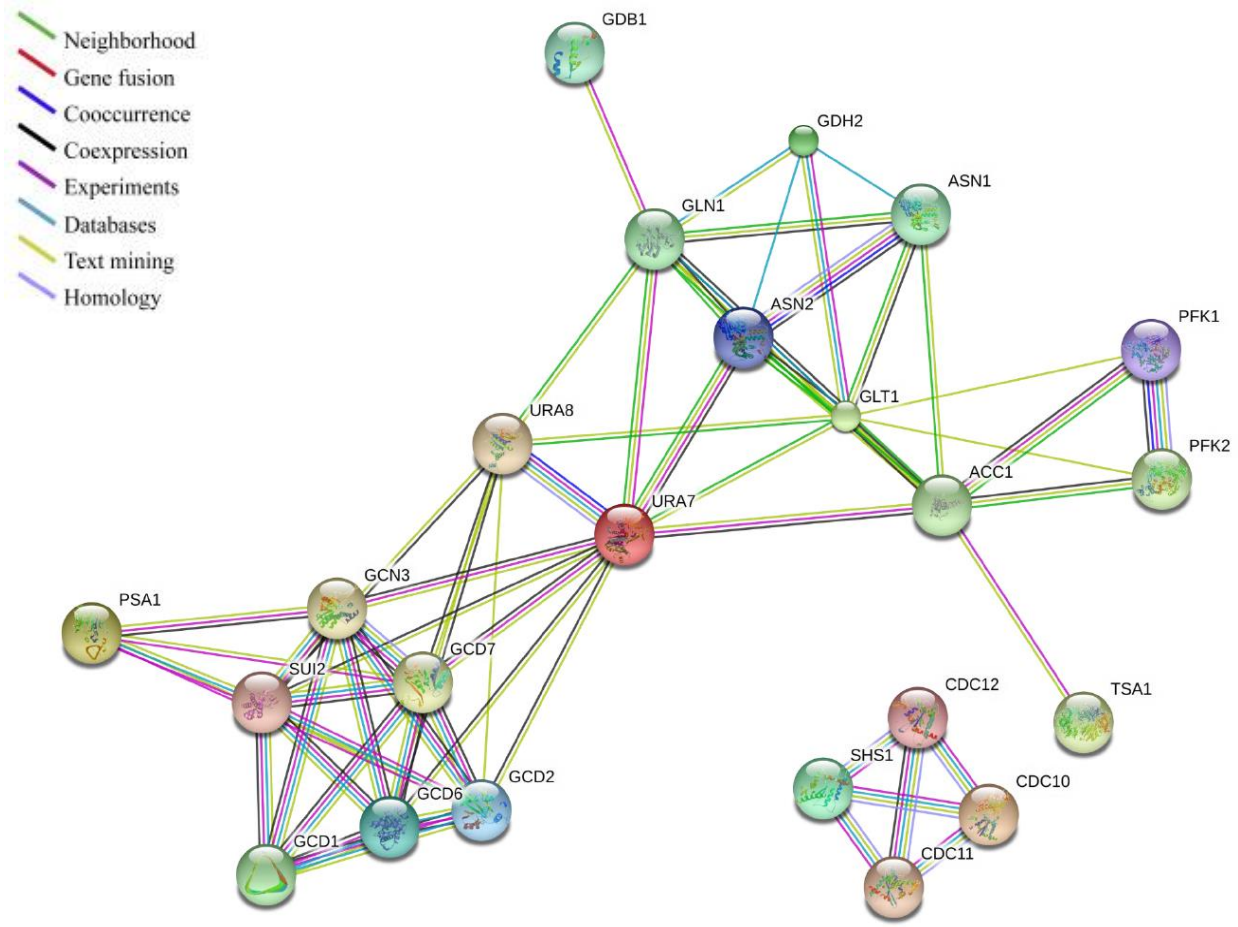


Figure 4.5 Protein-protein analysis of filament-forming proteins in the budding yeast

The protein network was obtained with STRING under medium confidence 0.400. Nodes of proteins indicate the availability of 3D protein structure information, and coloured lines between proteins indicate the various types of interaction evidence.

Table 4.7 KEGG pathways analysis of filament-forming proteins in STRING 10

KEGG pathway ID	Term	Number	Gene name	*P*-value	*P*-value_FDR
sce250	Alanine, aspartate and glutamate metabolism	5	*ASN1, GLN1, ASN2, GDH2, GLT1*	4.06E-08	4.34E-06
sce3013	RNA transport	6	*GCD2, GCD1, GCN3, GCD7, GCD6, SUI2*	2.07E-07	1.11E-05
sce1100	Metabolic pathways	12	*ASN2, ACC1, ASN1, GLN1, PSA1, GLT1, GDH2, PFK2, URA7, GDB1, PFK1, URA8*	5.19E-07	1.85E-05
sce910	Nitrogen metabolism	3	*GLN1, GDH2, GLT1*	7.05E-07	1.89E-05
sce1120	Microbial metabolism in diverse environments	6	*ASN1, ASN2, GLN1, PFK1, PFK2, GLT1*	1.23E-05	2.62E-04
sce51	Fructose and mannose metabolism	3	*PFK1, PFK2, PSA1*	6.85E-05	1.22E-03
sce1110	Biosynthesis of secondary metabolites	6	*ASN2, PFK2, ASN1, PSA1, PFK1, GLT1*	2.12E-04	3.25E-03
sce1230	Biosynthesis of amino acids	4	*GLN1, PFK1, PFK2, GLT1*	6.90E-04	9.23E-03
sce52	Galactose metabolism	2	*PFK1, PFK2*	2.50E-03	2.98E-02
sce30	Pentose phosphate pathway	2	*PFK1, PFK2*	4.05E-03	3.94E-02
sce680	Methane metabolism	2	*PFK1, PFK2*	4.05E-03	3.94E-02
sce330	Arginine and proline metabolism	2	*GLN1, GDH2*	4.95E-03	4.41E-02

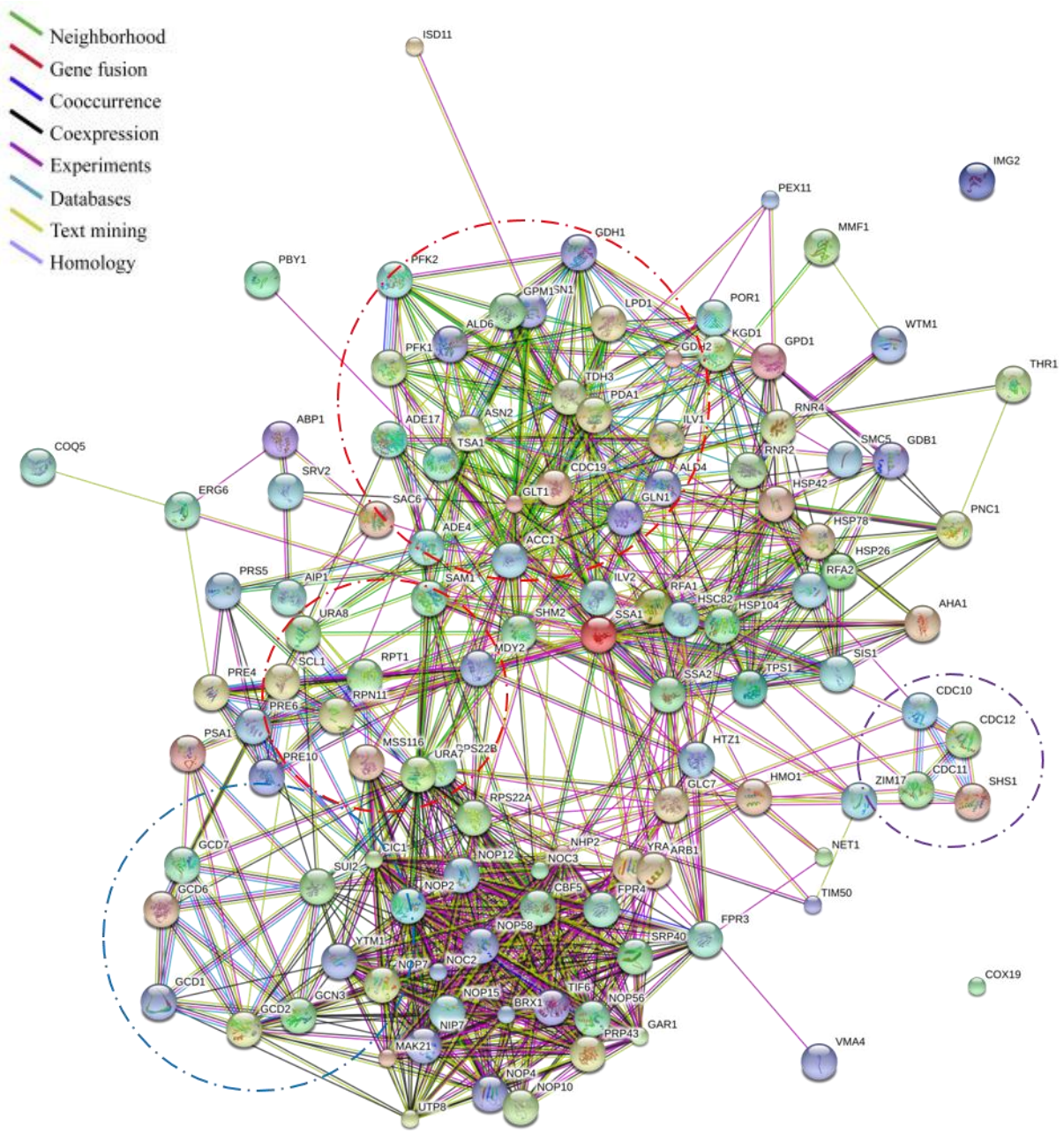


Figure 4.6 Protein-protein analysis of foci-forming (filament-forming proteins included) proteins in the budding yeast

The protein network was obtained with STRING under medium confidence 0.400. Nodes of proteins indicate the availability of 3D protein structure information, and coloured lines between proteins indicate the various types of interaction evidence. Circles show the places where are abundant with filament-forming proteins.

Table 4.8 Pathway analysis of foci-forming proteins

#pathway ID	Pathway description	Observed gene count	False discovery rate
1110	Biosynthesis of secondary metabolites	23	7.20E-09
1100	Metabolic pathways	36	1.08E-08
1120	Microbial metabolism in diverse environments	17	4.18E-08
1230	Biosynthesis of amino acids	13	2.87E-06
10	Glycolysis / Gluconeogenesis	9	6.21E-06
250	Alanine, aspartate and glutamate metabolism	7	9.09E-06
910	Nitrogen metabolism	4	1.78E-05
1200	Carbon metabolism	11	2.73E-05
3008	Ribosome biogenesis in eukaryotes	9	4.08E-05
620	Pyruvate metabolism	6	0.000174
3050	Proteasome	6	0.000226
260	Glycine, serine and threonine metabolism	5	0.00129
330	Arginine and proline metabolism	5	0.00129
3013	RNA transport	7	0.00301
280	Valine, leucine and isoleucine degradation	3	0.00633
640	Propanoate metabolism	3	0.00633
310	Lysine degradation	3	0.00723
680	Methane metabolism	4	0.00723
380	Tryptophan metabolism	3	0.0124
4141	Protein processing in endoplasmic reticulum	6	0.0124
230	Purine metabolism	6	0.0277
51	Fructose and mannose metabolism	3	0.0365

4.3 Discussion

4.3.1 Comparison of protein localization data with previous screening

In the introduction to this chapter, I mentioned several screenings that have provided us with some information on the localization of proteins in the budding yeast. Here I made a comparison of protein descriptions between my study, the putative "Yeast GFP fusion localization database", and the first study of filament-forming proteins in yeast by Noree et al. in 2010 [4].

The comparison of results (Table 4.9) from this study and the Yeast GFP database on the localization of proteins during the exponential phase showed similar results in most of those strains. Even though the low resolution of pictures from Yeast GFP database reduces the reliability of its localization data, the addition of co-localization markers provides us with more information.

Our research has perfectly verified filament-forming proteins identified in Noree's research under similar conditions and found more filament-forming proteins after a complete screening of the yeast GFP library.

4.3.2 Limitations of this screening

Filament-forming proteins aggregating in non-diauxic growth conditions would not be identified in this screening, since this large-scale screen is limited to a specific growth condition (i.e. 24 hours of culturing). In fact, we already have the overall localization of two of the most representative phases (i.e. the exponential phase cells from the Yeast GFP fusion localization database and the post-diauxic phase cells from this study). The further identification of protein localization of under other growth conditions or stresses may be helpful to solve our doubts in the filament regulation, but the present screening approach

seems too costly for detailed screening in every single condition. One possible way to elevate efficiency during multi-conditions screening is the candidate approach, with the establishment of sub-libraries grouped according to known protein function before screening.

Another limit of this study as well as all studies utilizing the GFP fusion proteins is the possible false positive results caused by the GFP tag. It was reported that GFP has a propensity to form non-covalently dimers in certain situations which may cause artificial aggregation of GFP-fused proteins [103]. This effect was more common when fusion protein is overexpressed and GFP is at a high concentration. This artificial effect can be removed by introducing an A206K mutation to the GFP protein. This mutation is important for more precise studies on filament-forming protein. During our research in the cytoophidia, we found that the GFP-tagged artificial filament in human cell line tend to be not able to dissolve once formed. However, the cytoophidia formed by A206K mutated GFP-tagged CTP synthase in human cell lines are highly dynamic and dissolvable. The ability to dissolve may be criteria to tell apart cytoophidia induced or stabilised by the GFP tag.

4.3.3 Summary

In summary, I performed a genome-wide screen of the endogenous GFP-tagged budding yeast library and identified nine novel filament-forming proteins. They are Acc1p (acetyl-CoA carboxylase), Asn1p/Asn2p (asparagine synthetase), Gcd1p (eIF2B-γ), Gdb1p (glycogen debranching enzyme), Gdh2p (glutamate dehydrogenase), Pfk1p/Pfk2p (phosphofructokinase) and Tsa1p (thioredoxin peroxidase). 93 foci-forming proteins were also identified. The filament-forming proteins can be classified into 3 major groups (metabolic enzymes, septin proteins and translation initiation factors). They are highly regulated by growth conditions which may prevent some candidates from being discovered in the previous screens. I also demonstrated that a few glutamine-utilising enzymes form

distinct cytoophidia both in the cytoplasm and in the nucleus, providing a new and detailed view of filamentation in cells. The identification of filament-forming proteins and similar kinds allows us to link metabolic pathways and cell compartmentalization.

Table 4.9 Comparison of protein localization data with previous screening

References	This study	This study	Yeast GFP fusion localization Database[35]	Noree[4]
Time point	Exponential phase	Diauxic shift	Exponential phase	Saturation
ASN1	Cytoplasm	Filament	Cytoplasm	N/A
ASN2	Cytoplasm	Filament	Cytoplasm	N/A
CDC12	Cytoplasm	Filament	Bud neck/cell periphery	N/A
GCD2	Cytoplasm	Filament	Cytoplasm	Filament
GCD7	Cytoplasm	Filament	Cytoplasm/punctate composite	Filament
GDB1	Cytoplasm	Filament	Cytoplasm	N/A
GDH2	Cytoplasm	Filament	Cytoplasm	N/A
PFK1	Cytoplasm	Filament	Cytoplasm	N/A
PFK2	Cytoplasm	Filament	Cytoplasm	N/A
TSA1	Cytoplasm	Filament	Cytoplasm/punctate composite	N/A
URA7	Cytoplasm	Filament	Cytoplasm	Filament
URA8	Cytoplasm	Filament	Cytoplasm	Filament
GLT1	Filament	Filament	Ambiguous	Filament
ACC1	Filament/Foci	Filament	Cytoplasm/punctate composite	N/A

Chapter 5 Growth and stress regulation of yeast ASNS filaments

5.1 Introduction

5.1.1 Asparagine synthetase catalytic activity and regulation

The enzyme asparagine synthetase (ASNS) is involved in amino acid biosynthesis and catalysing the conversion of L-aspartate and L-glutamine into L-asparagine and L-glutamate. ATP is used to activate aspartate in this reaction[104]. The substrate aspartate is produced from oxaloacetate by transamination, a key compound in the citric acid cycle. Aspartate is also the precursor of the other four amino acids: threonine, isoleucine, methionine and lysine. While its name reveals the basic function in asparagine synthesizing, this enzyme also has an impact on glutamine homeostasis by consuming glutamine and producing glutamate.

The study of bovine ASNS indicated that the structure of glutamine-dependent ASNS is composed of two distinct domains (Figure 5.1). The N-terminal domain belongs to the N-terminal amidohydrolase enzyme superfamily [105, 106], which mediates hydrolytic reactions. The N-terminal active site of ASNS catalyses the glutamine hydrolysis to form glutamate and ammonia. Enzymes possessing structurally homologous glutamine-hydrolysing domains include GPATase (glutamine 5'-phosphoribosyl-1-pyrophosphate aminotransferase) and GFAT (glutamine fructose-6-phosphate aminotransferase) [107-110]. The C-terminal domain is similar to ATP pyrophosphatase, an enzyme superfamily including GMPS(guanosine-5'-monophosphate synthetase), argininosuccinate synthetase, BLS(beta-lactam synthetase) and ThiI [104]. The C-terminal of ASNS catalyses the activation of aspartate by ATP [111, 112]. Studies of *E.coli* glutamine-dependent ASNS and bovine pancreas ASNS suggest that ASNS functions as a dimeric enzyme [90, 91].

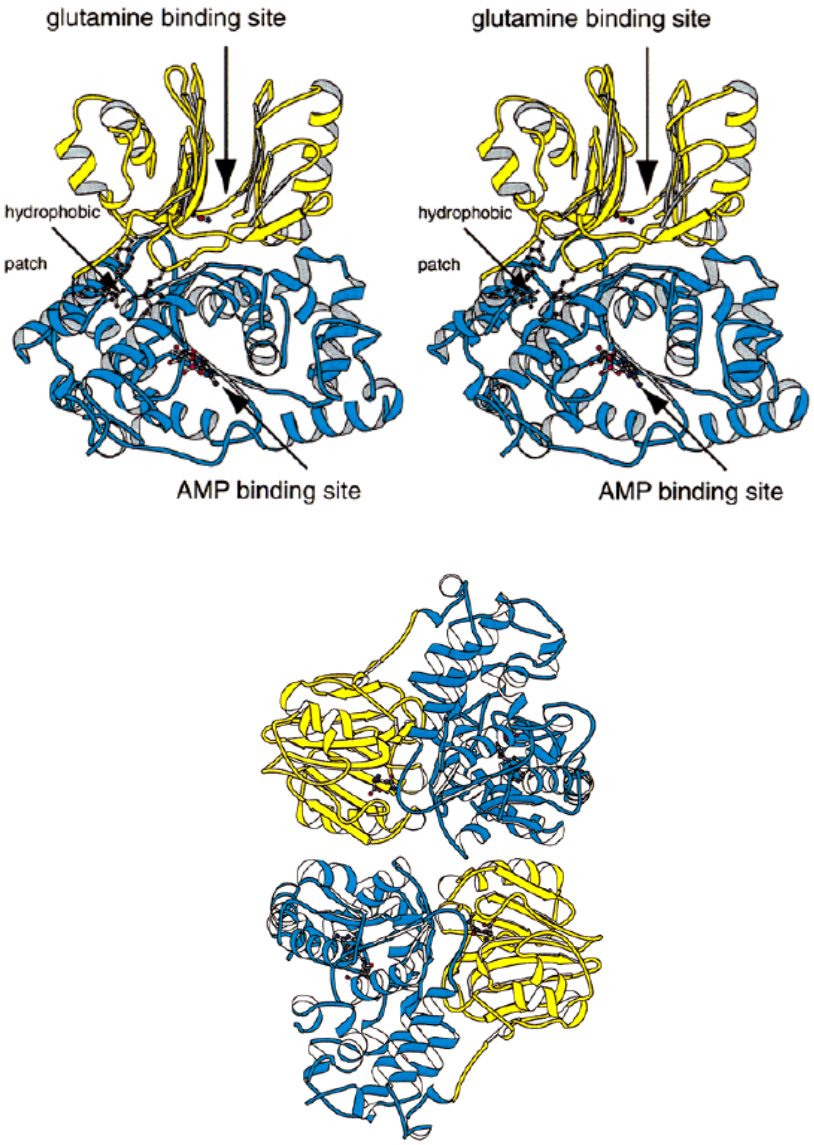


Figure 5.1 Asparagine synthetase ribbon structure of *E.coli*

Asparagine synthetase functions as a dimer. The C-terminal (blue) ATP binding domain and N-terminal (yellow) glutamine hydrolysis domain are shown (figure adapted from [91])

There are two different forms of ASNS in bacteria. One uses ammonia as a nitrogen donor, and the other uses glutamine as a nitrogen donor [104], as in CTP synthase. The glutamine dependent enzyme is analogous to ASNS in yeast and mammalian systems. In the budding yeast, there are two analogues of the glutamine-dependent ASNS gene, *ASN1* and *ASN2*, which arise from the whole genome duplication [89]. In the mammalian system, only one glutamine-dependent asparagine synthetase gene exists. Three alternatively spliced transcript variants have been described for this gene in *Homo sapiens* (provided by RefSeq, May 2010).

The expression level of *ASNS* varies in different tissues in mammals. Based on a comparison of enzyme activity in tissues, the pancreas was shown to have greater expression than any other tissues [113, 114]. Except for the pancreas, *ASNS* is also highly expressed in rats' testes (R.Hustson and M.Kilberg, unpublished results). Release of ASNS proteins into serum from murine primary tumours was also observed, which indicates the potential of serum ASNS activity as a marker for pancreatic exocrine cell lysis [115].

ASNS expression level is tightly regulated by cellular stress. Gong et al. [116] were the first to determine that ASNS mRNA level increased in cells deprived of amino acids. Hutson and Kilberg [117] also demonstrated increased ASNS mRNA level following deprivation of total amino acid or single essential amino acid. Within 30 minutes of amino acid depletion, uncharged tRNA activates the GCN2 kinase, which leads to increased NF-kB activity and ATF4 synthesis. Increased ATF4 results in increased *ASNS* gene transcription. Transcription from the ASNS gene reaches its highest rate at 1-4h following nutrient stress. Between 4-24h, the transcript level is still elevated relative to the normal condition, but the rate is reduced. During this phase, the *ASNS* gene is activated by ATF3 rather than ATF4 [118].

Endoplasmic stress, such as ER protein synthesis overload, oxidative stress, or other circumstances that perturb ER function, can also regulate *ASNS* expression. ER stress

mediates the response through double-stranded RNA activated protein kinase RNA-like endoplasmic reticulum kinase (PERK). Like GCN2, the activation of PERK leads to phosphorylation of eIF2 and the increase of ATF4 synthesis. Consequently, the *ASNS* gene is activated [119].

ASNS activity can be regulated by several drugs. DON (6-diazo-5-oxo-L-norleucine), CONV (2-amino-5-chlorolevulinic acid; 5-chloro-4-oxo-L-norvaline) and DONV (5-diazo-4-oxo-L-norvaline) inhibited ASNS extracted from mouse pancreas. DON and CONV almost completely inhibited the utilization of glutamine by ASNS at the concentration of 1mM (171ug/ml), whereas DONV inhibited enzyme only by 50 percent. The inhibition of DONV is reversible, while the former two were irreversible [120]. An adenylated sulfoximine transition-state analogue was found to inhibit human ASNS with nanomolar potency (KI*=8nM), which can suppress proliferation of MOLT-4R (cell line from human T lymphoblast; acute lymphoblastic leukaemia) at the concentration of 0.1mM (IC50) [121].

5.1.2 Asparagine synthetase is relevant to human disease

The ASNase (an enzyme which degrades asparagine) therapy is a standard treatment for childhood acute lymphoblastic leukaemia (ALL) [122]. After delivering of ASNase to the bloodstream, plasma asparagine is quickly depleted, thus causing a rapid efflux of cellular asparagine and depleting cellular asparagine. Most cells are able to express sufficient ASNS to counteract this starvation of asparagine, but leukaemia cells express ASNS at a low level, which make them vulnerable to asparagine depletion [123].

However, the exposure to ASNase can result in selection for a population of leukaemia cells that are drug resistant. Those adaptive changes in resistant cells include increases in

transcription of *ASNS* gene, glutamine synthetase activity, and active glutamine transport, all of which appear to support increased asparagine biosynthesis. The inhibition of ASNS thus became a focal point for pharmaceutical study [93]. The results from patient samples show that the mechanisms of ASNase action and the drug resistance are not yet fully understood [104].

In castration-resistant stage of prostate cancer (CRPC) specimens, the *ASNS* gene showed a gain in copy number and was overexpressed at the transcript level. The depletion of asparagine with ASNS inhibitors will be a novel strategy for targeting CRPC cells [95].

It is also reported that expression of *ASNS* in a factor affecting the survival of hepatocellular carcinoma (HCC) patients, and low *ASNS* expression in HCC was correlated with worse surgical outcomes [94]. High expression of *ASNS* has also been associated with biological aggressiveness of gliomas [124]. Knockdown of *ASNS* in human epidermoid carcinoma cell line A375 cells remarkably downregulated the expression levels of *CDK4*, *CDK6*, and *CyclinD1*, and upregulated the expression of *p21*, inducing a G0/G1 cell cycle arrest and stopping cancer cells from growing [125]. From this research, we learned that the cellular activity of ASNS is very important for rapid cell reproduction, especially in the scenario of tumour tissue developing.

Although lots of facts about ASNS function and regulation have been identified in the past several decades, some questions still remain unsolved. What is the exact role ASNS plays in the homeostasis of its substrates and products? Glutamine and glutamate levels are changed during the up or down regulation of ASNS, which may affect the whole cell metabolism. Except for regulation of expression level, is there any other method which can regulate ASNS activity and amount, especially in tumour cells? The answers may help us deal with problems in ASNS-dependent drug resistant tumours and other ASNS-related tumours.

5.1.3 Stress pathways in the budding yeast *S. cerevisiae*

Unlike yeast cultured in cosy and rich YPD medium in lab, natural growing yeasts are always faced with problems such as fluctuating nutrient levels, environments with changing osmotic pressure, unpleasant temperatures, or toxic chemicals. Yeast cells (as with all organisms) have developed a system for those environment changes within a certain range. Subtle and nonlethal changes in the environment have a profound selection pressure on single-cell fast-growing and non-motile organisms such as the budding yeast. In recent years, the cellular stresses such as carbon or nitrogen nutrient stress, heat or cold stress, osmotic stress, and oxidative stress have been widely studied, and sophisticated pathway regulatory mechanisms have been put forward to explain the reactions under these stresses. Even though these models might be incomplete and simple compared to the real sophisticated systems in living cells, they provide us with an important and fundamental insight into stress of yeast cell regulation, and other eukaryotic cell.

In yeast, three genes have been identified as essential regulators of most stress-induced regulation: *HSF1*, *MSN2* and *MSN4*.

Hsf1p is a transcription factor which can regulate a set of genes containing heat shock elements (HSE), which have special "nGAAn" repeats structures [126]. *HSF1* is positively regulated by Snf1p, a landmark protein for yeast entering the stationary phase, as well as Yak1p, a protein suppressed by the exponential phase key regulator Protein Kinase A (PKA) [127].

Msn2/4 is a complex, made up of Msn2p and Msn4p. It functions as a regulator for a set of genes containing stress responsive elements (STRE), which consist of a pentameric core "CCCCT" [128]. PKA and Snf1p are both negative regulators of Msn2/4 function. PKA phosphorylation Msn2/4 to block its nuclear transportation, while Yak1p is suppressed by

PKA phosphorylates and activates Msn2/4. Snf1p phosphorylates and downregulates Msn2p [127]. TOR acts as a negative regulator by preventing the nuclear import of Msn2p and Msn4p [129].

Heat shock

Heat is one of the most studied stresses in the past 30 years. The budding yeast *S. cerevisiae* has an optimal growing temperature of between 30°C and 35°C [130]. When the temperature reaches 37°C, yeast cells activate a transcriptional program termed as the heat shock response (HSR), which alters cell metabolism and physiology for better viability under heat. When the temperature reaches 42°C, cells maintain growth in the short term but cannot survive under a chronic exposure to higher temperature, which inactivates the yeast RNA polymerase II [131]. Most investigation on the HSR utilises the temperature shift from 30 to 37°C in laboratory conditions [127].

Heat shock changes gene expression by activating Hsf1p and Msn2/4 dependent pathways. Hsf1p controls a set of HSPs, including Hsp70, Hsp90 and their cofactors, which sense misfolding of newly synthesized polypeptides. Heat shock induces misfolding of polypeptides and triggers Hsf1p activation [127]. Meanwhile, the sensing factor of the Msn2/4 pathway in heat shock is poorly understood [132]. Another set of genes named cell wall integrity (CWI) genes, which respond to perturbations of the cell wall via activation of MAP kinase, is also activated when cells are under heat shock. This pathway is induced by heat shock due to the disturbance of cell membrane or cell wall by heat. Overexpression of CWI kinase Slt2p and *HSF1* regulator Hsp90 suppresses the temperature-sensitive Hsf1 mutant phenotype, which suggests the CWI pathway is both necessary and sufficient for the heat shock phenotype [133].

Oxidative stress

Oxidative stress is the other common stress. Reactive oxygen species (ROS) are mostly produced in the process of cellular metabolism. ROS can cause serious problems such as lipid peroxidation, protein oxidation and DNA damage when cells are unable to cope with it. Despite cellular reasons, yeast cells are also faced with oxidative stress in nature when exposed to other ROS-producing organisms, exogenous ROS-producing agents, UV, and ionizing radiation [134]. The most common laboratory oxidative stress model is hydrogen peroxide (H_2O_2), because of its easy application. However, genome-wide screens of yeast deletion collection treated with different ROS have demonstrated their core function in common and individual differences, which deserve special attention during research [135] .

One of the key regulatory transcription factors for oxidative stress is Yap1p. Cytoplasmic Yap1p is directly oxidised in the presence of oxidative stress, such as diamide, which leads to the rapid accumulation of Yap1p in the nucleus and induces target gene expression. Meanwhile, oxidative stress peroxide induces gene expression in a more complex way with similar outcomes. Skn7p is another essential regulatory component related to oxidative stress. Mutants lacking both Yap1p and Skn7p were as sensitive as either single mutants to H_2O_2 [136], suggesting that these two transcriptional regulators act on the same pathway. Skn7p is reported as a constitutive nuclear protein, and it is still not clear how Skn7p senses oxidative pressure. Data suggest that Skn7p binds to the Hsf1 recognition sequence and with Hsf1 itself to regulate some H_2O_2-dependent gene induction [137]. The transcription factors Msn2p and Msn4p, which play an important part in heat shock response, are also important in oxidative stress reactions. Msn2/4 complex senses oxidative stress through Trx1/2 thioredoxins, which are oxidized in the presence of H_2O_2. The oxidized Trx1/2 causes Msn2/4 nuclear localization, and thus the transcriptional induction of downstream stress responsive elements.

Osmotic stress

Another common stress for yeast is osmotic stress. In response to osmotic shock, yeast cells physically shrink almost immediately. Cells temporarily stop growing. Glycerol channels on the cell membrane close to prevent glycerol leakage. Osmotic sensors are activated to trigger a defence process including the production of glycerol to increase plasma osmolarity. Thus the cells swell and turgor again in a new steady state [138]. The whole process lasts around one hour under 0.5M NaCl stress, and the key regulator Hog1p reaches its phosphorylation summit around 20 minutes after stress, then drops to the base level after establishment of a new steady state [139].

The main sensors of osmotic stress are Sho1p and Sln1p on the cell membrane. Activation of receptors triggers downstream MAP kinase pathway and results in the phosphorylation and nuclear translocation of key regulator Hog1p, thus activating or suppressing downstream transcription. The feedback control leads cells into a new steady state. The osmotic pathway is not insulated from other stress pathways. The key oxidative stress regulator Skn7p acts downstream of the osmotic sensor Sln1p. Hog1p also functions with the Msn2/4 complex under osmotic stress to stimulate gene expression [140].

Cold shock

Cold influences cells structurally and functionally. It decreases the reaction and diffusion rate, especially for membrane fluidity. The physical state of the membrane is a primary signal of cold shock and is sensed by Sln1p. As mentioned above, Sln1p is also an osmotic stress sensor. In the presence of a cold shock, Sln1p, together with Ypd1p and Ssk1p, activates downstream Hog1p and initiates the cold transduction pathways. It is reported that the basic mechanisms of activation by low temperature and osmotic stress could be similar or even identical [141-143]. Cold shock also influences the PKA pathway and TOR pathway through

Yvh1p. *YVH1* is the only phosphatase gene found to be induced by cold shock. Yvh1p inhibits Tpk1-3p (PKA negative regulators) and frees Msn2/4p from the inhibition of the PKA pathway, triggering Msn2/4p-related stress gene translation. Similarly, a cold shock inhibits Tap42p activity, a TOR target, which is also a key negative regulator of Msn2/4p [141].

Even though heat shock, cold shock, osmotic and oxidative stresses differ a lot as environment stresses at first glance, they share a lot of common regulators in terms of signalling pathways. The most important and common factor is the Msn2/4 complex, which is the key stress-responsive transcriptional activator. All of the stresses described above activate Msn2/4 complex nuclear transportation and its downstream STRE-dependent transcription. The HOG pathway and Hsf1p also play a role in more than one kind of stresses. The key pathways for overall nutrient and cell morphology regulation, such as the PKA pathway, PKC pathway, TOR pathway and Snf1 pathway, also respond to the environmental changes.

5.1.4 Aims of this chapter

In the last chapter, I showed that asparagine synthetase is a metabolic enzyme forming filamentous structures after one day culturing in nutrient-rich medium. Asparagine synthetase shares some common attributes with CTP synthase, such as the use of glutamine as a substrate, the forming of oligomers faced with their substrates, and nuclear localization. In this chapter, I studied the influence of the growth stage and stresses on the assembly of filament or foci structures of asparagine synthetase and CTP synthase in the budding yeast *S. cerevisiae*. The comparison of Asn1p, Asn2p and Ura7p filament regulation in different growth stages and stresses casts light on the discovery of novel potential filament regulators and regulation pathways.

5.2 Results

5.2.1 Filament formation of Asn1p, Asn2p and Ura7p keeps changing along the budding yeast growth curve

In the previous parts, I introduced the differences of cell metabolism, regulation pathway and cell morphology in the various stages of cell growth. To further investigate the formation and regulation of ASNS filaments and CTP synthase filaments in the budding yeast, three stocks of yeast cells (i.e. ASN1/YPR145W/GFP(+)12-A5, ASN2/YGR124W/GFP(+)12-F4, URA7/YBL039C/GFP(+)12-D1) from the Yeast-GFP Clone Collection (Thermo Fisher) [35] were thawed and revived in YPD medium for three days before the experiment. Cells were then diluted to the OD value 0.05 in YPD medium as the start point of culturing. Samples were collected and fixed at the culturing time points of eight hours, one day, three days, four days, six days, and eight days, at 32°C (Figure 5.2 B). Pictures were taken under 63X objective on a laser-scanning confocal microscope (Leica TCS SP5 II confocal microscope). Four pictures were taken for each sample, and three independent experiments were undertaken to confirm the results.

No filament was detected in samples at the time point of eight hours, which represents the mid-exponential phase, when cells are rapidly dividing and growing. Filaments emerged at the diauxic shift and the percentage of filament-positive cells increased with further culture. In the post-diauxic phase, the percentage of filament-positive cells was around 20-30% in the strains of Asn1/2p and 50-60% in the strain of Ura7p. After Day Five, cells gradually stopped growing and entered the stationary phase. All three samples showed a higher filament percentage even than post-diauxic phase, in Asn1/2p around 50-60% and in Ura7p around 70-80% (Fig 5.2.A).

The length of filaments was estimated by the length of 50 randomly chosen filaments in each sample. Average length of CTP synthase-based filaments increased greatly between Day One and Day Three, and then kept around 2μm, around half of the yeast diameter, regardless the increase of filament-positive cell number. However, there was no significant change in the average length of ASNS-based filaments after the first observation around 1μm on Day One. The length of ASNS-based filaments tends to have a fixed length once after fully matured after Day One. The difference of length increasing behaviour of ASNS-based filaments and CTP synthase-based filaments showed they are two different cytoophidia according to their dynamic and assembly (Fig 5.2.C).

The average number of filaments in filament-positive cells also revealed the difference in ASNS- and CTP synthase-based filaments. Asn1/2p filament-positive cells had a relatively stable average number of 1.75 filamentous structures in each filament-positive cell, while in the situation of Ura7p this number rose significantly after Day Three. From this point of view, the total increase in CTP synthase-based filament number is a combination effect of increase in filament-positive cell percentage and filament amount per cell, while ASNS-based filaments were mainly affected by the increased proportion of filament-positive cells (Fig 5.2.D).

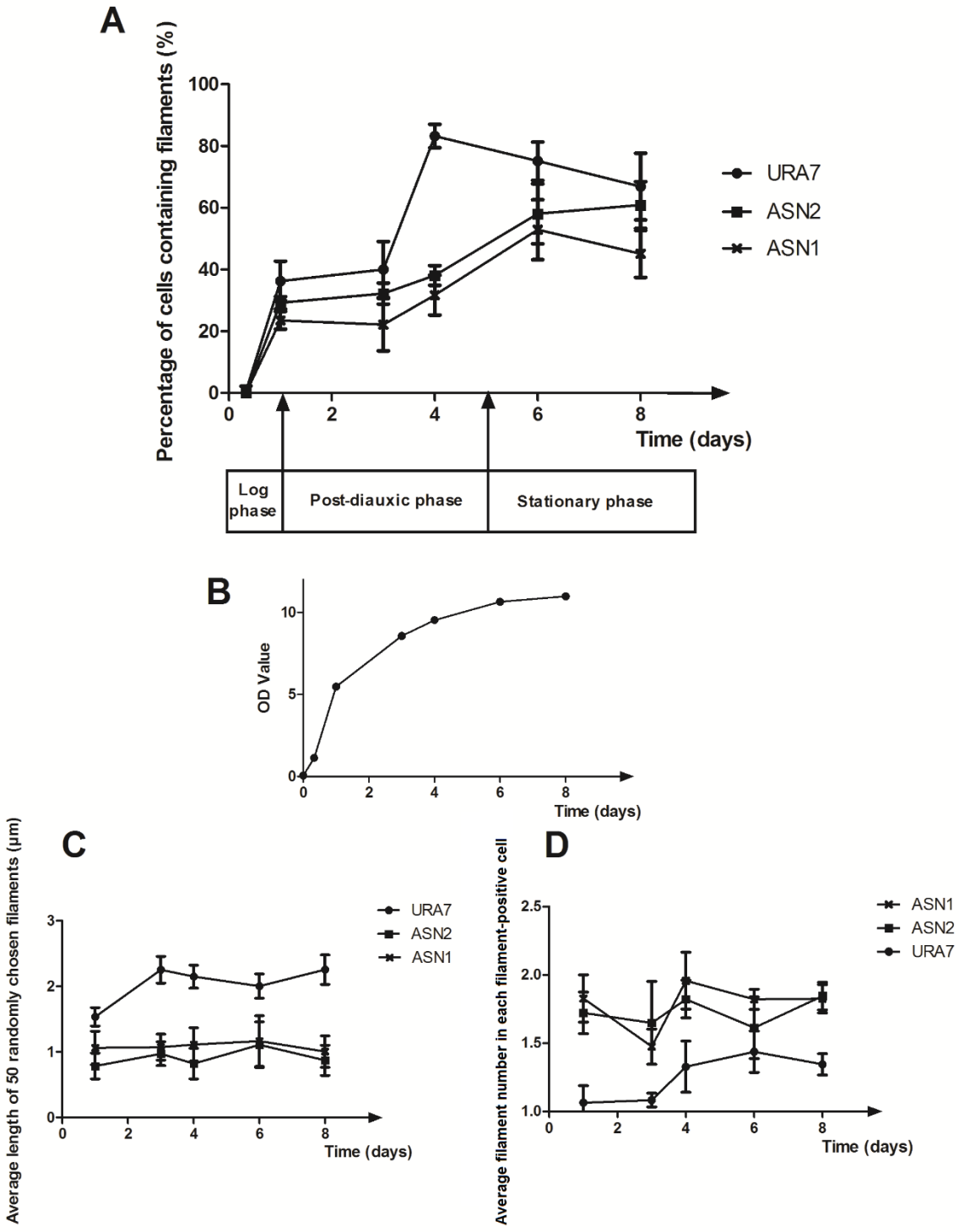


Figure 5.2 Continuing culturing of Asn1p, Asn2p and Ura7p GFP-tagged yeast.

Changes along culturing time related to **(A)** Percentage of filament-positive cells; **(B)** OD value; **(C)** Average length of filaments; **(D)** Average filament number per filament-positive cell

5.2.2 Glucose deprivation induces filament formation

In previous studies, CTP synthase was found to form filaments due to the deprivation of carbon source [4]. In their results, the studies compared five filament-forming enzymes (Gcd2p-GFP, Glt1p-GFP, Psa1p-GFP, Sui2p-GFP and Ura7p-GFP), and only Ura7p responded to carbon deprivation. To reveal whether this carbon deprivation regulation is a CTP synthase exclusive process or a more universal process, I conducted the glucose deprivation experiment in Asn1p-GFP, Asn2p-GFP and the control group Ura7p-GFP.

Exponential phase cells (12 hours of culturing) were centrifuged and added into the previous medium, YP medium (1% yeast extract, 2% peptone), distilled water and a 2% glucose solution. For those three conditions, YP medium lacks carbon source, 2% glucose solution lacks nitrogen source and growth factors, and distilled water lacks carbon source, nitrogen source and growth factors. After one hour of 32°C culturing, cells were fixed and pictures were taken by confocal microscopy. Results indicate that ASNS-based filaments show similar behaviour to CTP synthase-based filaments under carbon source starvation. Distilled water treatment induced filament formation in all three strains and YP medium induced filaments in Asn1p and Ura7p strains. The addition of glucose showed a severe inhibition effect on those starvation-induced filaments in all three strains (Figure 5.3 A, B). Unlike in the situation of Ura7p where filament percentage reached 70% after starvation, Asn1p and Asn2p were less sensitive to starvation and filament-positive cell were merely around 10%, far less than the percentage of Asn1p and Asn2p filaments when the strains reach the stationary phase. The reason underlying the difference of starvation treatment sensitivity between these two cytoophidia still remain unknown. At the diauxic shift, when cells begin to utilize other carbon sources rather than glucose, the addition of glucose pulls cells back to glucose metabolism. Results showed that the addition of glucose severely reduced filaments in all three strains (Figure 5.3 C).

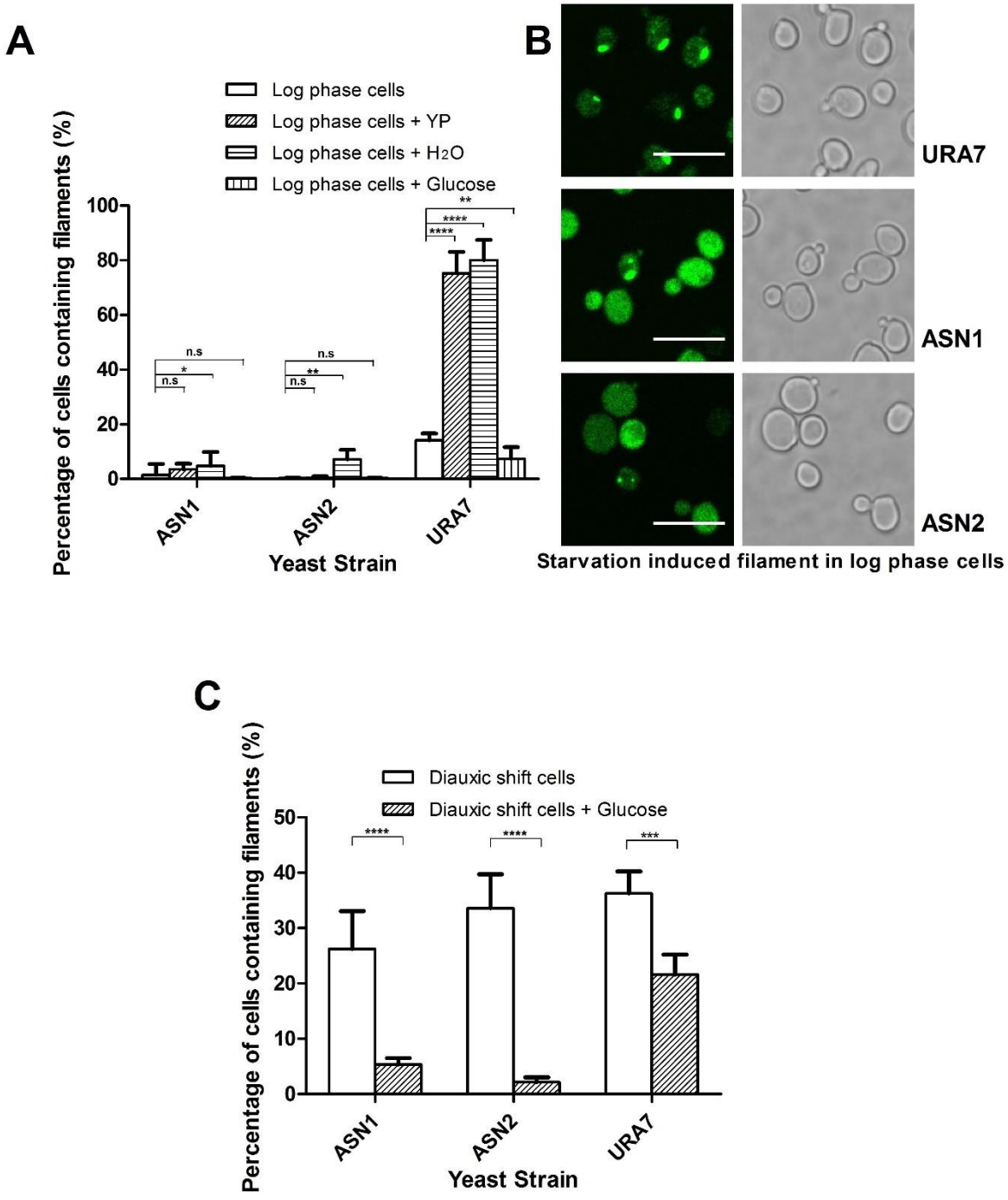


Figure 5.3 Filament formation regulated by carbon nutrient starvation

(A-B) Deprivation of glucose in medium induces Asn1p, Asn2p and Ura7p filaments in the exponential phase; **(C)** The addition of glucose at the diauxic shift causes Asn1p, Asn2p and Ura7p filaments to disassemble. Error bars show 95% confidence interval. Scale bars equal to 10µm

5.2.3 Heat shock induces filament formation

Heat shock was applied to the three budding yeast strains. Cells were cultured from the start point of OD 0.05 for eight hours, one day and three days, which correspond to the exponential phase, the diauxic shift and the post-diauxic phase. Cells were then treated with 37°C heat shock for one hour, 42°C heat shock for five minutes, and 32°C for one hour as control. After treatments, cells were fixed and pictures were taken by confocal microscopy.

In the exponential phase cells (eight hours culturing), Asn1p and Asn2p filaments were not induced by heat shock, while Ura7p filaments were induced. The percentage of filament-positive cells was around 20%. At the diauxic shift (one day of culturing), among all three stains, filaments were induced by long heat shock (37° for one hour) and rapid severe heat shock (42°C for five minutes). In the post-diauxic phase (three days of culturing), Asn1p and Asn2p filaments showed heat shock induction, while in the situation of Ura7p filament induction was not significant (Figure 5.4).

The results show that the behaviours of ASNS-based filaments and CTP synthase-based filaments in the budding yeast under heat shock are similar but not identical. CTP synthase-based filaments are more sensitive to heat shock in the exponential phase than ASNS-based filaments. The result that rapid severe heat shock (42°C for five minutes) induced ASNS-based filaments and CTP synthase-based filaments also reveals that the filament regulation of heat shock in this situation is very likely to be a quick response, such as physical or direct protein regulation, rather than time-consuming transcriptional control.

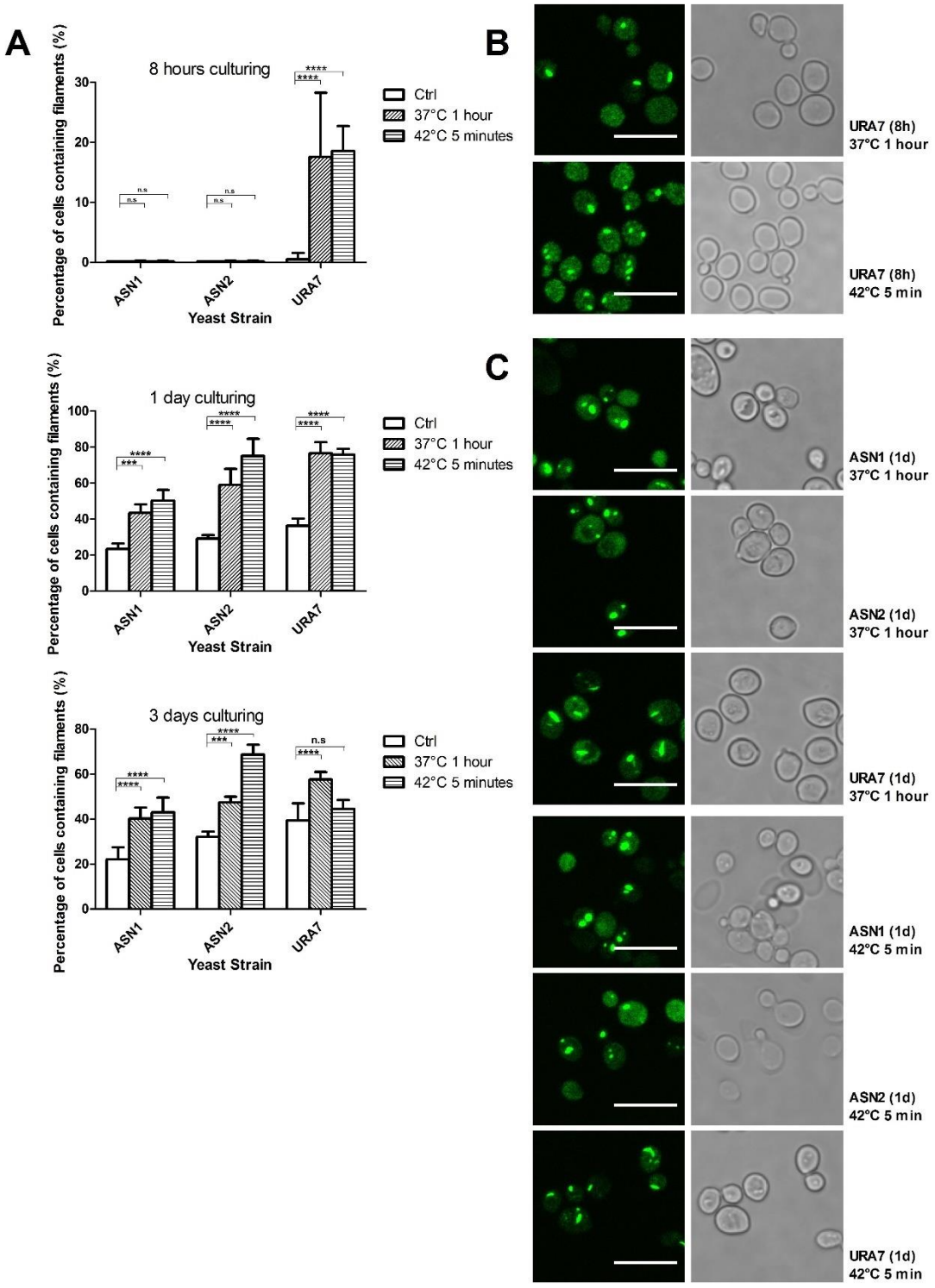


Figure 5.4 Filament formation regulated by heat shock

(A) Heat shock induces Asn1p, Asn2p and Ura7p filaments differently according to growing stage; **(B)** In the exponential phase, only Ura7p filaments are induced by heat shock; **(C)** After the diauxic shift, heat shock induces Asn1p, Asn2p and Ura7p filaments. Error bars show 95% confidence interval. Scale bars equal to 10µm.

5.2.4 Cold shock induces filament formation

To investigate the effect of cold shock on filament formation, cells were cultured from the start point of OD 0.05 for eight hours, one day, and three days, which correspond to the exponential phase, the diauxic shift and the post-diauxic phase. Cells were treated with 0°C cold shock for one hour and 32°C for one hour as control. After treatments, cells were fixed and pictures were taken by confocal microscopy.

Results are shown in Figure 5.5.In the exponential phase cells (eight hours of culturing), Asn1p and Asn2p filaments were not induced by cold shock, while Ura7p filaments were induced. The percentage of filament-positive cells was around 50%. It is important to mention that the cold-induced filaments of Ura7p are different in shape and distribution compared to the heat-induced and starvation-induced ones. Cold induced structures are more like foci in shape, and usually located near the cell wall.

At the diauxic shift (one day of culturing) in all three stains, filaments were induced by cold shock. Ura7p forms normal filamentous structures in this situation rather than foci-like structure.

In the post-diauxic phase (three days of culturing), Asn1p and Asn2p filaments were induced by cold shock, while in the situation of Ura7p filaments induction was not significant, which is similar to what has been observed in the previous heat-shock experiment. Ura7p filaments seem less sensitive to temperature stress in the post-diauxic phase.

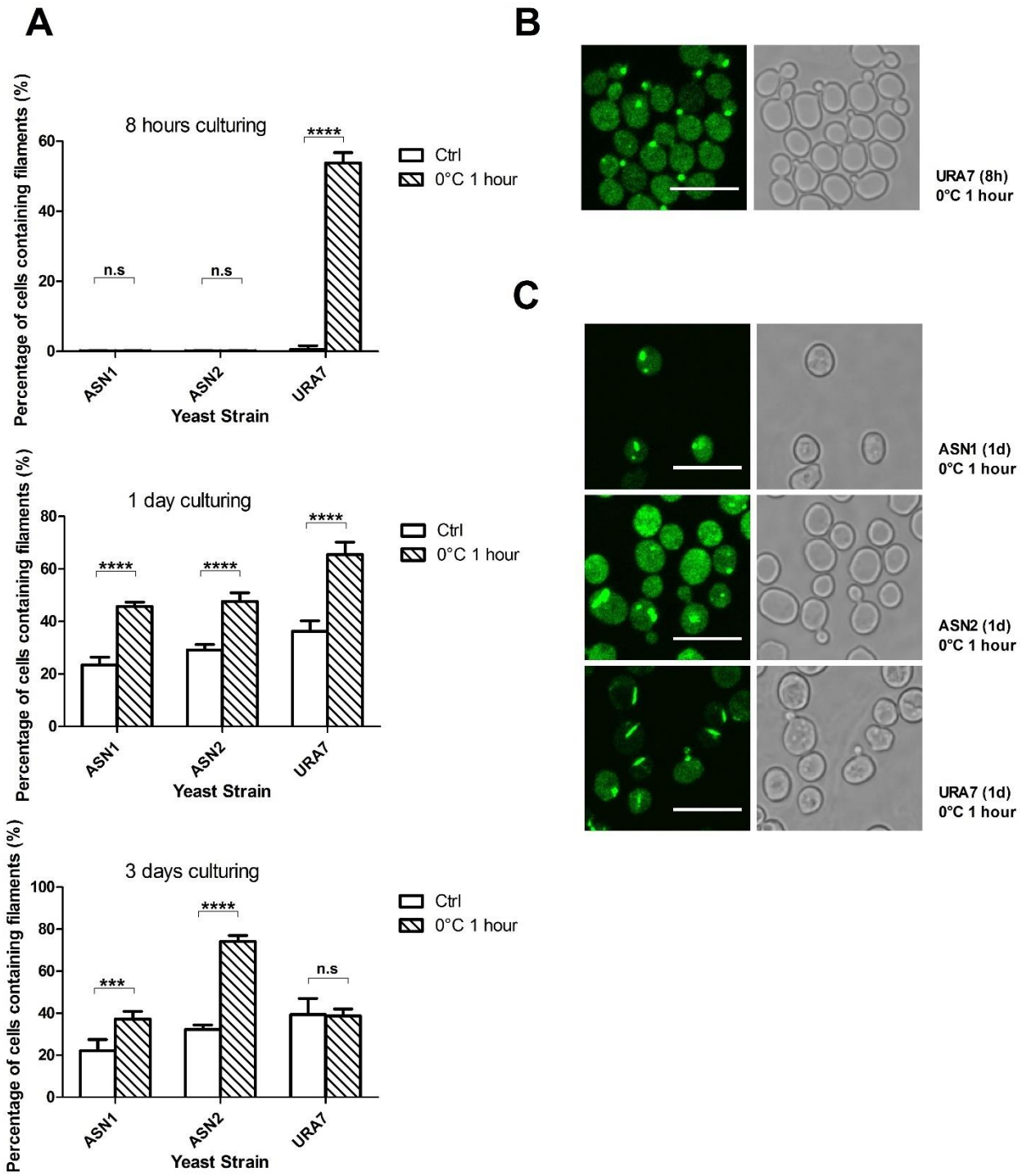


Figure 5.5 Filament formation regulated by cold shock

(A) Cold shock induces Asn1p, Asn2p and Ura7p filaments differently according to growing stages; **(B)** In the exponential phase, only Ura7p filaments were induced by cold shock; **(C)** After the diauxic shift, cold shock induces Asn1p, Asn2p and Ura7p filaments. Error bars show 95% confidence interval. Scale bars equal to 10μm.

5.2.5 Osmotic stress induces filament formation

Environmental osmotic stress leads to the morphological and metabolic changes of the budding yeast. To investigate the effect of osmotic stress on filament formation, yeast cells were cultured from the start point of OD 0.05 for eight hours, one day and three days, which correspond to the exponential phase, the diauxic shift and the post-diauxic phase. Cells were treated with the NaCl at the final concentration of 0.5M and 1M for one hour at 32°C. After treatment, cells were fixed and pictures were taken by confocal microscopy.

Results are shown in Figure 5.6. In the exponential phase cells (eight hours of culturing), Asn1p and Asn2p filaments were not induced by low concentration NaCl (0.5M), and few cells (about 5%) were induced to form filaments by high concentration NaCl (1M). Meanwhile, Ura7p formed short filaments at a relatively high percentage (70%).

At the diauxic shift (one day of culturing), Asn1p and Asn2p were induced to form filaments at a higher percentage than control. The filaments morphology is similar to normal ASNS-based filaments. Meanwhile, Ura7p filaments were also induced to a very high percentage. Most filaments had a similar morphology to the control, which are long and straight filaments, but osmotic stress also induced lots of foci-like structures in cells. Its morphology is unique to Ura7p under osmotic stress and possibly a filament precursor or filament disassembly products. Some cells even had more than ten structures.

In the post-diauxic phase (three days of culturing), Asn1p and Asn2p filaments showed stronger osmotic stress response, while in the situation of Ura7p filaments induction was even weaker than on Day One, which is similar to what has been observed in the previous heat-shock and cold-shock experiments. This shows that Ura7p filaments are less sensitive to osmotic stress after a long-time culturing.

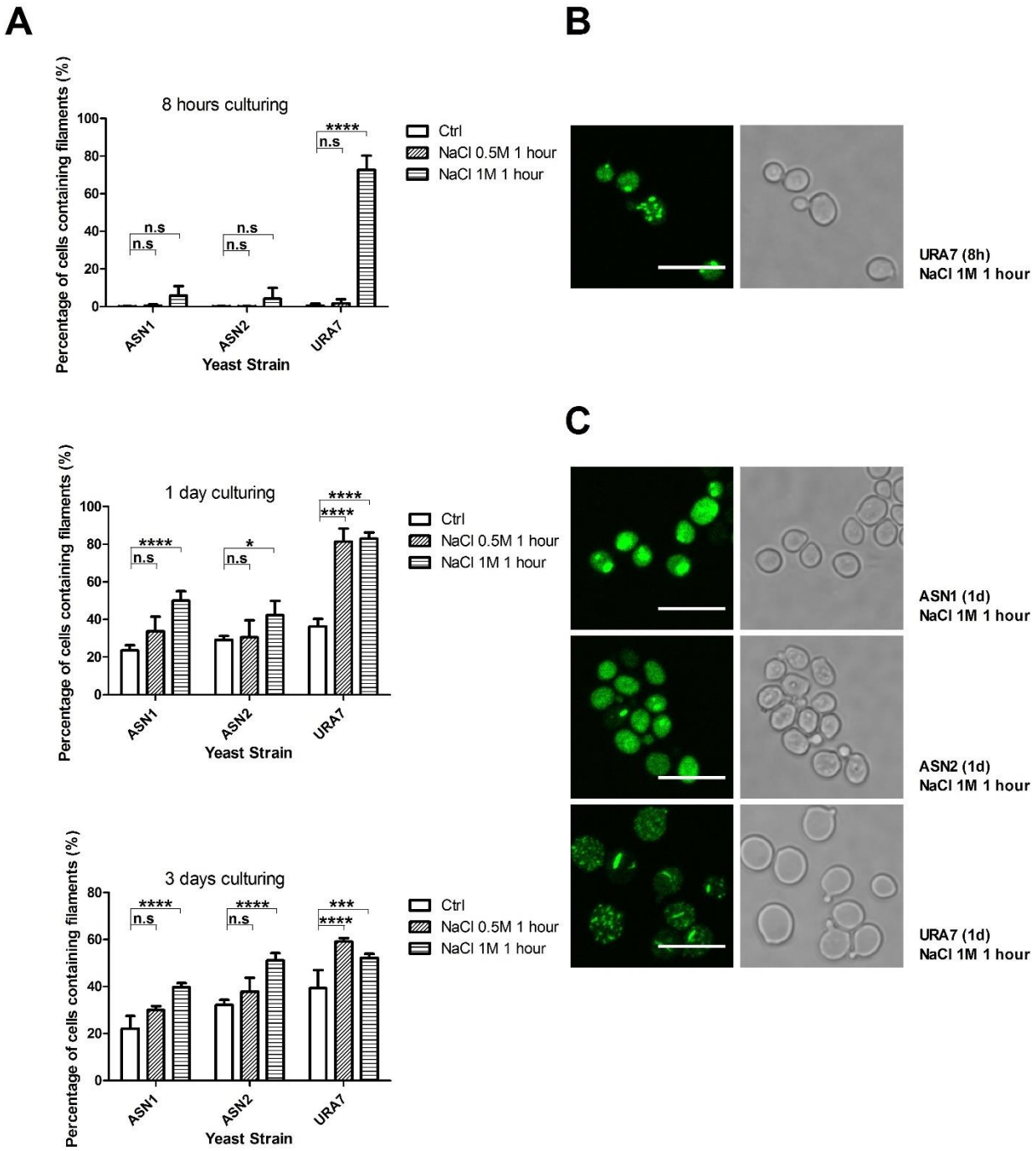


Figure 5.6 Filament formation regulated by osmotic stress

(A) Osmotic stress induces Asn1p, Asn2p and Ura7p filaments differently according to growing stages and stress intensity; **(B)** In the exponential phase, Ura7p filaments are significantly induced by osmotic stress; **(C)** After the diauxic shift, osmotic stress induces Asn1p, Asn2p and Ura7p filaments. Error bars show 95% Confidence interval. Scale bars equal to 10µm.

5.2.6 Oxidant hydrogen peroxide affects filament formation of ASN1 and ASN2

In cells, different oxidants at different concentration may trigger different oxidative stress pathways and change cell metabolism in different ways. Here I choose the most commonly used oxidant, peroxide, to explore the influence of oxidative stress to the formation of ASNS and CTP synthase-based filaments.

Yeast cells were cultured from the start point of OD 0.05 for eight hours, one day and three days, which correspond to the exponential phase, the diauxic shift and the post-diauxic phase. Cells were treated with H_2O_2 at the final concentration of 0.2mM and 2mM for one hour at 32°C. After treatments, cells were fixed and pictures were taken by confocal microscopy.

Results are shown in Figure 5.7. In the exponential phase cells (eight hours of culturing), Asn1p, Asn2p and Ura7p were all induced to assemble into filament or foci structures by high concentration H_2O_2 (2mM). Few structures were induced by low concentration H_2O_2 (0.2mM). In terms of shape, the oxidant induced Asn1p/Asn2p structures were more likely to be foci; while the oxidant induced Ura7p structures were filament-like.

At the diauxic shift (one day of culturing), Asn1p and Asn2p filaments were reduced by the addition of both low and high concentration H_2O_2, while Ura7p filaments were induced. Most filaments had the similar morphology compared to the control: long and straight filaments.

In the post-diauxic phase (three days of culturing), all strains showed a similar trend of filament induction or reduction, as well as filament shape shown after one day of culturing.

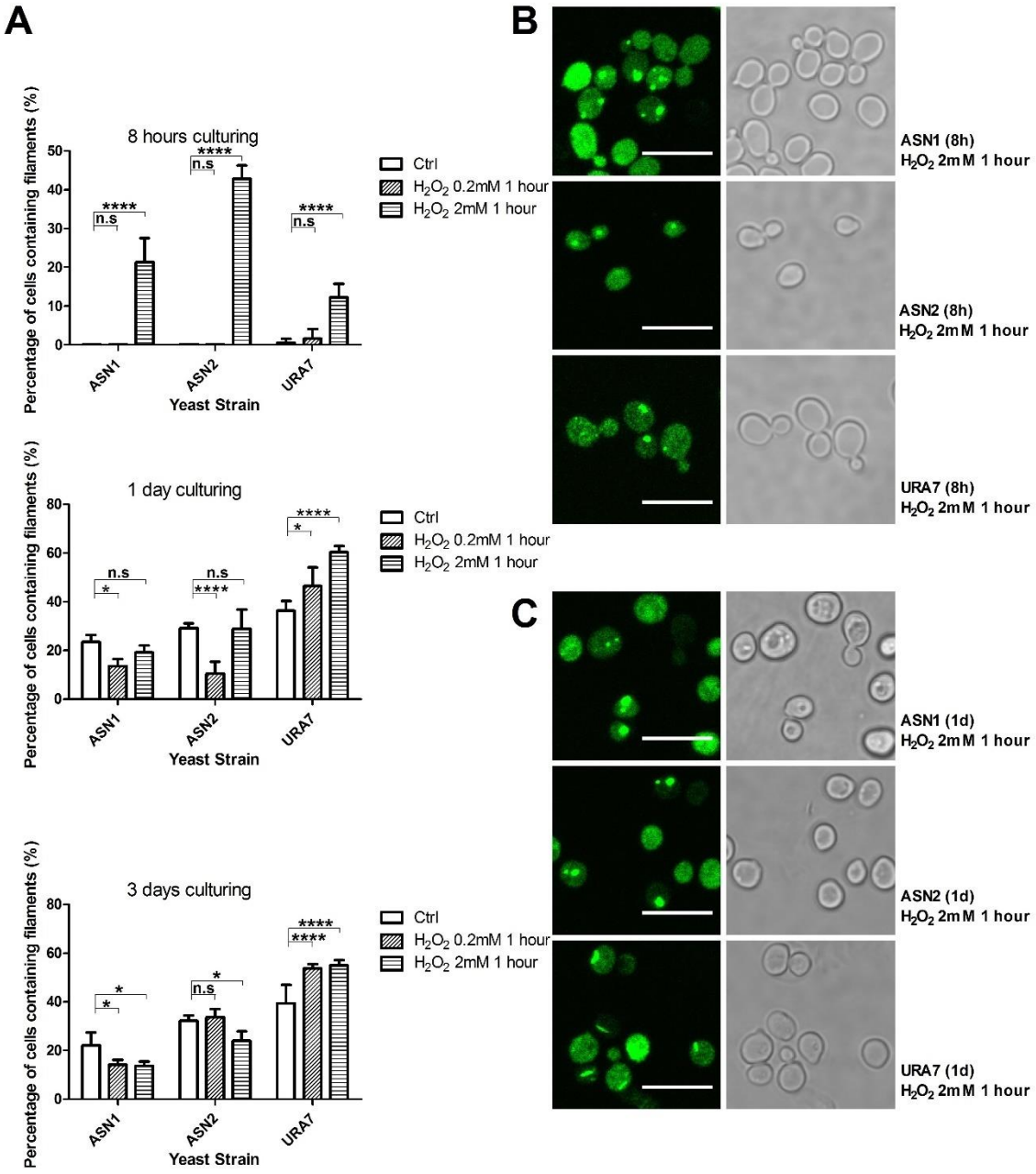


Figure 5.7 Filament formation regulated by peroxide oxidative stress

(A) H_2O_2 stress induces Asn1p, Asn2p assembly in the exponential phase and reduces Asn1p, Asn2p assembly after the diauxic shift, while Ura7p filaments were constantly induced in these three conditions; **(B)** In the exponential phase, oxidative stress induced Asn1p/Asn2p assembling structures is different in shape compared with regular Asn1p/Asn2p filaments, while Ura7p filaments are similar; **(C)** After the diauxic shift, oxidative stress reduces Asn1p, Asn2p filaments while it induces Ura7p filaments. Error bars show 95% Confidence interval. Scale bars equal to 10μm.

5.2.7 Summary of the stress-dependent Asn1p, Asn2p and Ura7p filaments

In summary of previous part of experiment, ASNS-based cytoophidia and CTP synthase-based cytoophidia started to emerge at the diauxic shift and the percentage of filament-positive cells kept on increase alone the growth curve. Glucose deprivation in exponential phase induced filament formation of both ASNS-based cytoophidia and CTP synthase-based cytoophidia. Meanwhile, ASNS-based cytoophidia and CTP synthase-based cytoophidia responded to various cellular stresses. Asn1p, Asn2p and Ura7p filaments were induced in response to most stresses, except the oxidant hydrogen peroxide which inhibited filament formation of Asn1p, Asn2p filaments after the diauxic shift. Ura7p filaments responded to most stresses in the exponential phase, while Asn1p, Asn2p filaments only responded to high oxidant stress in this phase. Here I summarize all the stress reactions to address the common points and differences between them (Table 5.1).

Strain		Asn1p			Asn2p			Ura7p		
Time point		8 hours	1 day	3 days	8 hours	1 day	3 days	8 hours	1 day	3 days
Heat shock37°C	Percentage change (%)	0	20.0↑	18.1↑	0	29.8↑	15.3↑	17.1↑	40.4↑	18.3↑
	Significance	ns	***	****	ns	****	***	****	****	****
Heat shock42°C	Percentage change (%)	0	26.8↑	20.9↑	0	46.0↑	36.4↑	18.0↑	39.5↑	5.2
	Significance	ns	****	****	ns	****	****	****	****	ns
Cold shock 0°C	Percentage change (%)	0	22.2↑	15.1↑	0	18.5↑	41.9↑	58.3↑	29.1↑	-0.8
	Significance	ns	****	***	ns	****	****	****	****	ns
NaCl 0.5M	Percentage change (%)	0.5	10.2	7.9	0	1.4	5.63	1.2	45.1↑	19.8↑
	Significance	ns	ns	ns	ns	ns	ns	ns	****	****
NaCl 1M	Percentage change (%)	5.8	26.6↑	17.7↑	4.1	13.1↑	18.9↑	72.2↑	46.7↑	12.8↑
	Significance	ns	****	****	ns	*	****	****	****	***
H_2O_2 0.2mM	Percentage change (%)	0	-10↓	-7.9↓	0	-18.6↓	1.4	1.1	10.2↑	14.4↑
	Significance	ns	*	*	ns	****	ns	ns	*	****
H_2O_2 2mM	Percentage change (%)	21.2↑	-4.3	-8.5↓	42.8↑	-0.2	-8.2↓	11.7↑	24.1↑	15.7↑
	Significance	****	ns	*	****	ns	*	****	****	****

Table 5.1 Summary of the stress responses of Asn1p, Asn2p and Ura7p filaments

↑: increase of filament-positive cells; ↓: decrease of filament-positive cells compared to the control; ns: no significance. (*P<0.05, **P<0.01, ***P<0.001, ****P<0.0001)

According to what I have observed in the oxidative stress experiment, one model is made to explain this result (Figure 5.8 A). In the exponential phase, H_2O_2 induces the formation of Asn1p/Asn2p structures. Indeed, morphologically speaking, these structures seem to be different from the ones I observed in other experiments, such as Asn1p/Asn2p filaments after the diauxic phase or under stresses such as heat, cold or osmotic. To distinguish them from the regular Asn1p/Asn2p filaments, I name them "Asn1p/Asn2p aggregates" in the following passages. However, after the diauxic shift (Day 1), when the regular Asn1p/Asn2p filament have already formed, the addition of oxidant H_2O_2 causes the formation of "Asn1p/Asn2p aggregates", leading to the disassembly of the regular Asn1p/Asn2p filament.

Further support for this hypothesis is the difference in the amount and distribution between "Asn1p/Asn2p aggregates" and regular Asn1p/Asn2p filaments. Usually, regular Asn1p/Asn2p filament-positive cells contain two Asn1p/Asn2p filaments, which are different in size and location: one is stick-like in the cytoplasm, and another is foci-like in the nucleus. However, in the "Asn1p/Asn2p aggregates" positive cells, one cell contains more structures than usual, and these structures are all of the similar size. The stick-like long filament is rarely be observed.

In Ura7p, I did not find a similar phenomenon. Oxidative stress only induced CTP synthase-based cytoophidia. The difference in H_2O_2 induced/reduced Asn1p/Asn2p and Ura7p filaments demonstrated a difference in regulation of ASNS- and CTP synthase-based filaments under oxidative stress in the budding yeast.

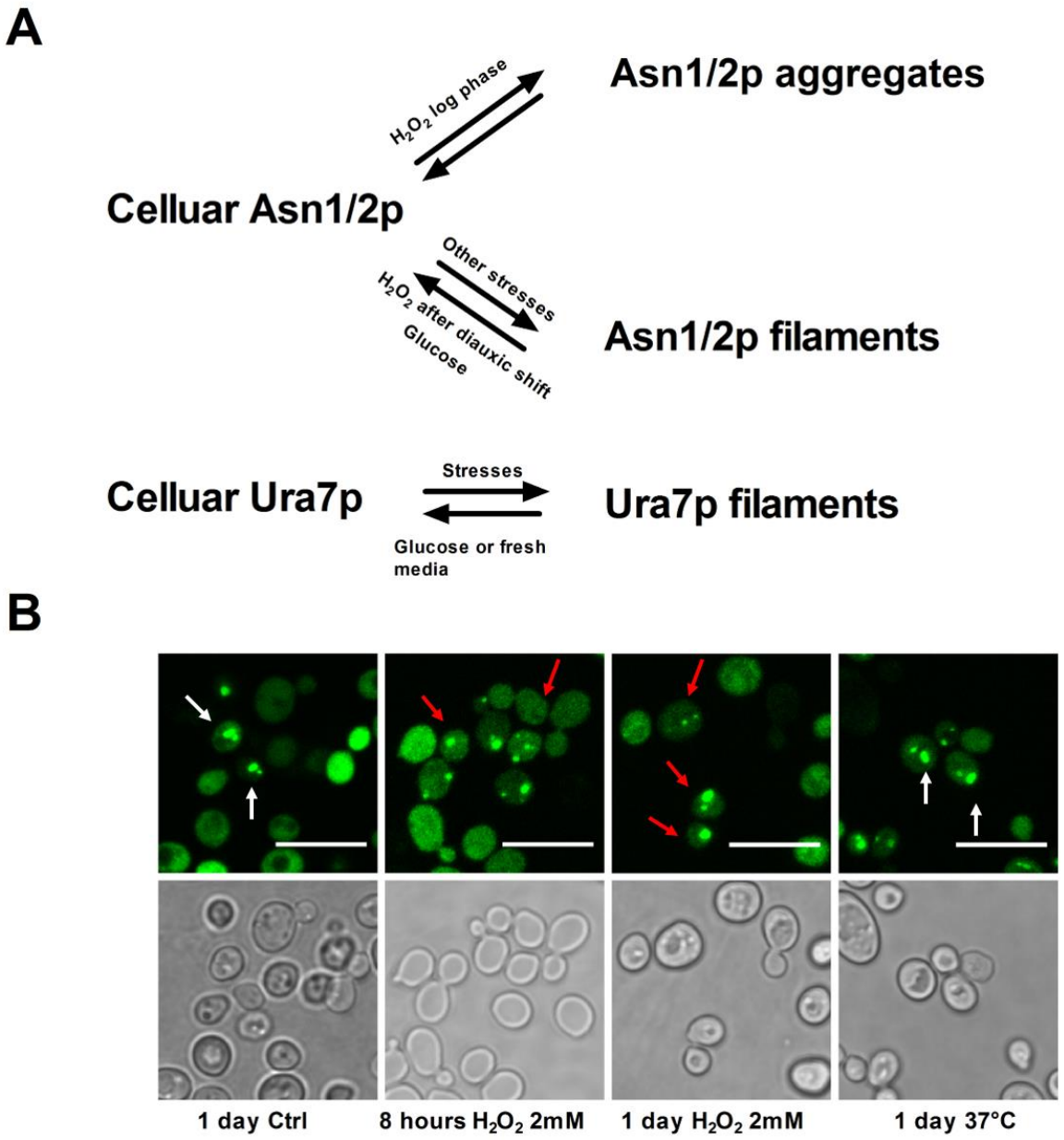


Figure 5.8 Possible model for Asn1p/Asn2p and Ura7p filaments formation under stress

(A) Possible model for differences between Asn1p/Asn2p and Ura7p filaments formation under stress. Oxidative stress dissembled Asn1p/Asn2p filaments formation and induced ASNS aggregates, while oxidative stress induced Ura7p filaments formation.
(B) Different morphology of Asn1p assembling structures. White arrow indicates Asn1p filaments, which usually exist as a pair of cytoophidia (a long cytoplasmic cytoophidium and a short nuclear cytoophidium). Red arrow indicates Asn1p/Asn2p aggregates, which are shorter in length; there is no obvious "paired" cytoophidia phenotype.

5.3 Discussion

5.3.1 Is the budding yeast filament formation under stress regulated by transcriptional control?

The major possible regulatory mechanism of CTP synthase filament formation in mammalian cells and insect cells are at the level of transcription and translation. Overexpression of CTP synthase induces CTP synthase-based filaments and knock-down of CTP synthase eliminates CTP synthase filaments in *Drosophila* cells [17]. It is not surprising that filaments tend to be longer in length or higher in frequency when the components are plentiful. Here I want to ask the question whether the induction of filament formation by stress is due to transcriptional increase of the filament-forming gene (i.e. *URA7, ASN1 and ASN2*).

I employed the transcript level data from two studies [82, 144] that include the stress-induced genomic expression level change of more than 4,700 major genes in the budding yeast. It is worth mentioning that no concrete conclusion can be drawn from this comparison, because of slight differences in treatment time, treatment dosage or system errors, but at least it provides us with some ideas concerning the relationship between expression level and filament formation.

All three genes (i.e. *URA7*, *ASN1 and ASN2*) are downregulated, following prolonged culture in YPD. Especially after the diauxic shift, the expression of these three genes is extremely low due to entering the stationary phase (Figure 5.9 A). For *URA7*, the transcript level on Day One is about 14% of that in the early exponential phase (four hours), and on Day Three it is merely 5%. However, filaments start to emerge while the expression level is downregulated, and they are present until Day Eight and perhaps even longer, suggesting that an upregulated gene expression is not necessary for filament formation. Formation of filaments in return helps to stabilize the cell enzyme pool while the transcript level is low.

From this point of view, the formation of filaments under stress is a possible survival strategy for enzyme storage. In this way, yeast avoids unnecessary energy waste and is always prepared to re-enter high-speed growth.

From transcript level change data under stress in the exponential phase (Figure 5.9 B-D), I find that for all three genes, the trend of gene downregulation appears in about the first 30 minutes after stress treatment. For osmotic pressure, which can be fixed when the new steady state is established by the osmotic pressure pathway, the transcript level nearly returns to normal after one hour (Figure 5.9 C). For 37°C heat shock, a partial restoration of the transcript level is observed, while for oxidative stress, this downregulation seems irreversible.

Unlike *URA7* which is downregulated by 60% by H_2O_2 stress, in the exponential phase cells ASN1/ASN2 transcript level only slightly decreased by 5% in response to H_2O_2 stress. However, all three filaments were strongly induced in the exponential phase by H_2O_2 stress, again weakening the transcription regulation theory and indicating that filament formation under stress is probably not linked to increased transcription of filament-forming proteins.

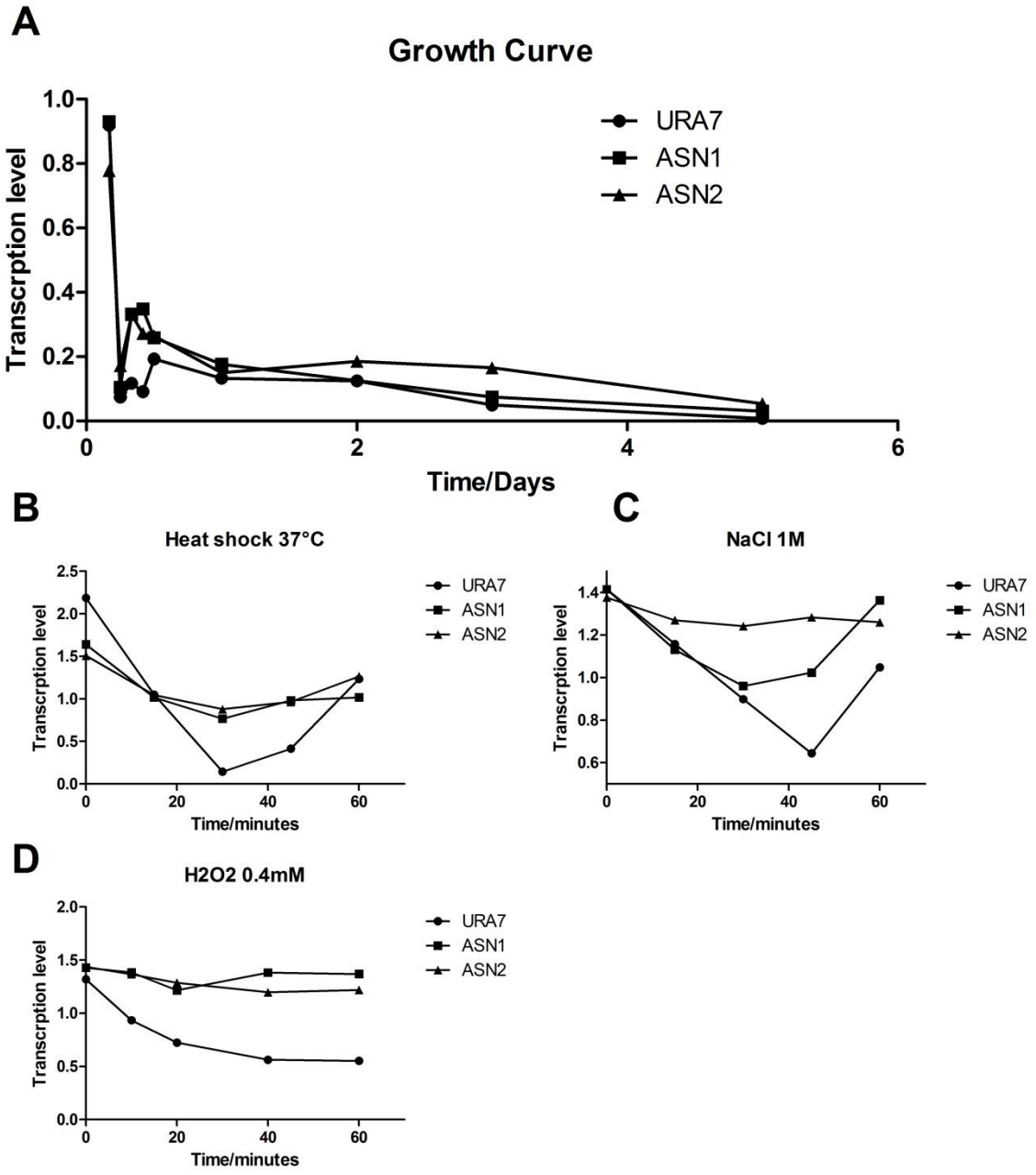


Figure 5.9 Transcript level data of Asn1/2p and Ura7p along growth curve and under stresses

(A) Transcript level change during stationary phase entry (data adapted from [82]); **(B)** Transcript level change after 37°C heat shock during exponential phase (expression data from [82]); **(C)** Transcript level change under 1M NaCl osmotic stress during exponential phase (expression data from[144]); **(D)** Transcript level change in 0.4mM H_2O_2 oxidative stress during the exponential phase (expression data from[144])

5.3.2 Comparison of Ura7p filaments stress reaction between the budding yeast *Saccharomyces cerevisiae* and the fission yeast *Schizosaccharomyces pombe*

The fission yeast *S. pombe* and the budding yeast *S. cerevisiae* are two of the most studied and related model organisms. They share many common characteristics, such as a unicellular, fungal-type cell wall, closed mitosis, and ascus-type sporangium. However, their differences are huge in every detail of their lifespans, from the scale of the cell such as morphology, mitosis and chromosome number differences to the scale of genetic and metabolic pathways. *S. cerevisiae* has 16 chromosomes with 5,770 genes, while *S. pombe* has only 3 chromosomes and 5,118 genes. A major difference in the cell cycle and entry of the stationary phase is that *S. cerevisiae* cells go into G0 quiescence phase from G1 cells, while *S. pombe* cells go into G0 quiescence phase from G2 cells. *S. cerevisiae* has a longer G1 phase and a shorter G2 phase. In contrast, *S. pombe* has a longer G2 phase and a shorter G1 phase. Meanwhile, many proteins in *S. pombe* are closer to their mammalian counterparts than they are to their *S. cerevisiae* counterparts[145]. Combined with the rRNA sequences phylogenetic trees, many molecular biologists believe that *S. pombe* is more closely related to higher eukaryotes than *S. cerevisiae*.

Here, I compare the response of CTP synthase-based filaments to stresses on *S. pombe* and *S. cerevisiae* (Table 5.2). The results turned out to be extremely interesting: *S. pombe* CTP synthase-based filaments and *S. cerevisiae* CTP synthase-based filaments behaved exactly opposite when faced with the same stresses.

Prolonged culturing	***S. pombe***	***S. cerevisiae***
Exponential phase	95%	1%
Post-diauxic phase Day3	0%	40%
Percentage difference	-95%	39%
Fold change	-100%↓	79X↑

	S. pombe	***S. cerevisiae***
Heat shock	37°C 60min	37°C 60min
Start percentage	95%	1%
End percentage	27%	18%
Percentage difference	-68%	17%
Fold change	0.28X↓	34.2X↑
Cold shock	0°C 60min	0°C 60min
Start percentage	95%	1%
End percentage	0%	54%
Percentage difference	-95%	53%
Fold change	0↓	106.6X↑
Oxidative stress	1mM H_2O_2 2h	2mM H_2O_2 1h
Start percentage	95%	1%
End percentage	80%	12%
Percentage difference	-15%	12%
Fold change	0.84X↓	23.4X↑
Osmotic stress	0.6M KCl 2h	1M NaCl 1h
Start percentage	95%	1%
End percentage	80%	73%
Percentage difference	-15%	72%
Fold change	0.84X↓	144.4X↑
Starvation	H_2O 2h	H_2O 1h
Start percentage	95%	1%
End percentage	15%	80%
Percentage difference	-80%	80%
Fold change	0.16X↓	159.4X↑

Table 5.2 Summary of the stress responses of CTP synthase-based filaments in *S. cerevisiae* and *S. pombe*

S. pombe data are from Jing Zhang (unpublished). "Percentage difference" stands for the percentage change of filament-positive cells from the start of treatment (or culturing) to the end. "Fold change" stands for the increase fold or decrease percentage of the percentage of filament-positive cells.

Firstly, in *S. cerevisiae,* CTP synthase-based filaments emerge after the diauxic shift and accumulate in the stationary phase. While in *S. pombe* CTP synthase-based filaments only exist during the fast-growing exponential phase and disassemble at the entry of the stationary phase.

Secondly, in *S. cerevisiae,* CTP synthase-based filaments are induced by stresses such as heat shock, cold shock, oxidative stress, osmotic stress and carbon source deprivation. While in *S. pombe,* CTP synthase-based filaments are all disassembled under the above conditions.

This fundamental difference in filament formation regulation between *S. pombe* and *S. cerevisiae* points to a way of discovering possible regulation factors for filament formation by comparing the differences in growing stage and stress regulation pathways between *S. pombe* and *S. cerevisiae*, as we know the cell cycle and stationary phase of these two yeasts are different between their respective G_0 features. This may link the formation of filaments to cell cycle regulation. Detailed research should be performed to verify this potential relationship.

From the point of view of transcriptional control, the CTP synthase gene in *S. pombe* is downregulated in the transition from exponential phase to the stationary phase, and also downregulated when faced with different stresses [146]. This is similar to the transcript level change of *S. cerevisiae* under the same conditions. Filaments begin to assemble in *S. cerevisiae* and disassemble in *S. pombe* when the CTP synthase gene is downregulated, showing that filament assembly or disassembly in stress conditions is not directly related to CTP synthase gene expression level change.

Moreover, as we know, cellular starvation induces cytoophidium assembly in mammalian and insects' cells. Even though the rRNA sequences phylogenetic trees and other molecular biologists suggest that *S. pombe* is more closely related to higher eukaryotes than *S.*

cerevisiae. In the perspective of filament dynamic in quiescence phase, *S. pombe* is not comparable to mammalian cells.

5.3.3 Conclusion

Stress regulation has been widely studied in yeast. CTP synthase-based filaments have been previously shown to be induced by starvation. However, there is no previous study on ASNS-based filament regulation under stresses. In this chapter, I have demonstrated filament regulation of ASNS-based filaments and CTP synthase-based filaments in a normal growth condition as well as under various stresses.

ASNS-based cytoophidia and CTP synthase-based cytoophidia started to emerge at the diauxic shift and the percentage of filament-positive cells kept on increase alone the growth curve. Glucose deprivation in exponential phase induced filament formation of both ASNS-based cytoophidia and CTP synthase-based cytoophidia. Meanwhile, ASNS-based cytoophidia and CTP synthase-based cytoophidia responded to various cellular stresses. Asn1p, Asn2p and Ura7p filaments were induced in response to most stresses, except the oxidant hydrogen peroxide inhibited filament formation of Asn1p, Asn2p filaments after the diauxic shift. Ura7p filaments responded to most stresses in the exponential phase, while Asn1p, Asn2p filaments only responded to high oxidant hydrogen peroxide stress in the exponential phase.

These results provide new insight on the regulation of cytoophidium assembly. The comparisons of the ASNS and CTP synthase filament regulation process and cytoophidium regulation in *S. pombe* and *S. cerevisiae* under the same stress may provide us with a further understanding of the similarity and diversity of filament regulation.

Chapter 6 Overall Discussion

6.1 Chronological and systematic summary of current research on cytoophidia

The study of cytoophidia started in the summer of 2010, with discoveries of unique compartmentation of CTP synthase in three different kinds of organisms: fly, bacteria, and the budding yeast. The first three studies about cytoophidia mainly focused on the function, regulation, and localization. This filamentous structure has been demonstrated to have a unique cytoskeleton function in bacteria, a starvation-induced assembly feature in the budding yeast, and a special localization and interaction with other organelles in flies [1, 3, 4]. Following this pioneering research in relatively lower model organisms, cytoophidia were discovered in mammalian cells in 2011 [5, 6]. However, as always happens at the start of newly discovered concepts, most of those studies were still limited to description rather than mechanisms. In 2014, three studies in different organisms coincidentally pointed out that the cytoophidium is a functionally inactive structure, which opened a new era for the study of mechanisms in cytoophidium function and assembly. Both the EM-scale filaments study and mutant studies provided us with profound insights into the function of cytoophidia [18, 24, 25]. Chapter 3 of this thesis is one of the three studies, and interpreted the inactive function of cytoophidia from the aspect of filamentous structure. Meanwhile, several studies related to the gene network regulation of cytoophidium formation were undertaken between 2014 and 2016. These articles performed detailed and precise studies on the regulation of filament assembly by Ack kinase, proto-oncogene Cbl and oncogene Myc [22, 23, 147]. The function and regulation of cytoophidia, which can also be described as the effect of cytoophidia o metabolic networks and the reverse effect of metabolic networks on cytoophidia, are still hot topics about cytoophidia today. The enzyme CTP synthase and another filament-forming enzyme, IMPDH, were well studied in these years, providing us with much information on

the diversity of filamentation, the interaction of different filaments, and the active function of IMPDH filaments in mammalian cells [20, 27]. Another hot topic on cytoophidia is their localization and dynamics. In 2014, nuclear filamentation of CTP synthase was first reported in mammalian cells and in *S. pombe* [7, 19]. Chapter 4 of this thesis provided us with an overview of filament-forming metabolic enzymes from a genetic screen. More metabolic enzymes were found to form filaments, which contributes more information to the study of diversity and complexity and filamentation. Based on Chapter 4, Chapter 5 provided us with a deeper view on the stress regulation process of ASN synthetase. A brief chronological summary of cytoophidia studies from 2010 till now is presented in Table 6.1.

I briefly divide the topics related to cytoophidia into several groups (Figure 6.1). The first group of studies deals with the basic features of cytoophidia (i.e. the components, localization, structure and assembly of cytoophidia, the difference of cytoophidia among species and tissues). The second group of studies is about the interaction of cytoophidia and the cell metabolic network (i.e. the regulation and cellular function of cytoophidia). The third group of studies focuses on the interaction of intercellular signalling or environmental stress and cytoophidia. This group is highly dependent on the previous supportive studies from the first and second groups. However, the third group of studies provides us with more information, such as regarding the potential clinical implications or biological meanings of cytoophidia.

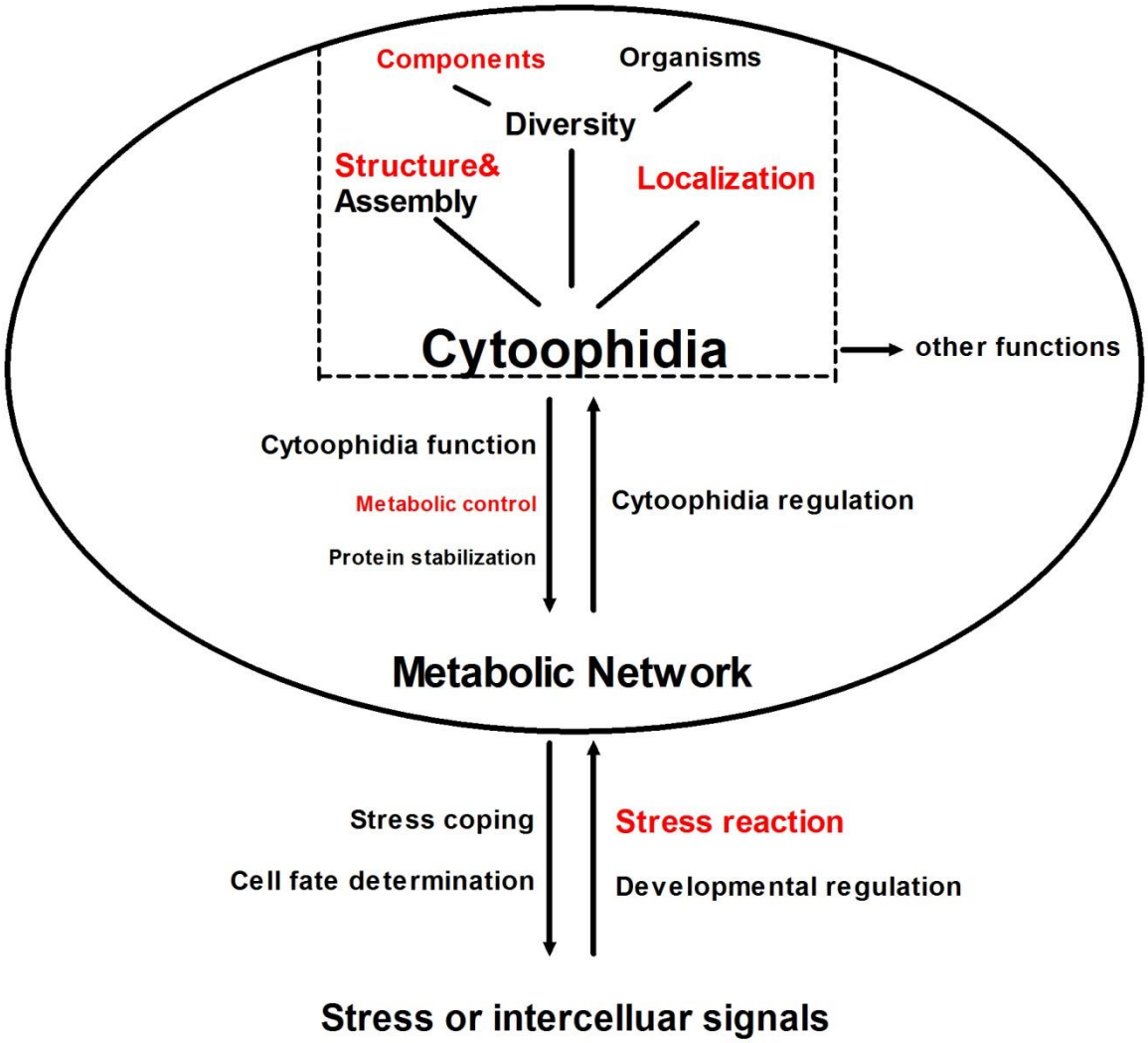


Figure 6.1 A systematic view of subjects related to cytoophidia

Red indicates topics included in this thesis

Table 6.1 Chronological summary of key research related to cytoophidia

Red indicates studies in this thesis. **Orange** indicates other study contributed by the author of this thesis but not included

Year	References	Title	Event	Subarea	Organism
2010	[1]	Intracellular compartmentation of CTP synthase in *Drosophila*	CTPS-containing cytoophidia were first identified in *Drosophila*	Localization/ Structure	*Drosophila*
2010	[3]	The metabolic enzyme CTP synthase forms cytoskeletal filaments	First identified an intracellular CTPS structure in bacteria.	Function	Bacteria
2010	[4]	Identification of novel filament-forming proteins in *Saccharomyces cerevisiae* and *Drosophila melanogaster*.	CTPS-containing cytoophidia were first identified in *S. cerevisiae*/Filament formation is regulated by mutations and regulatory ligands	Components/ Regulation	*S. cerevisiae* *Drosophila*
2011	[6]	Induction of Cytoplasmic Rods and Rings Structures by Inhibition of the CTP and GTP Synthetic Pathway in Mammalian Cells	IMPDH-containing rods and rings were identified in human cells	Components/ Regulation	Mammalian cells
2011	[5]	Glutamine analogs promote cytoophidium assembly in human and *Drosophila* cells	CTPS-containing cytoophidia were first identified in human cells	Regulation	Mammalian cells/*Drosophila*
2013	[17]	Only One Isoform of *Drosophila melanogaster* CTP Synthase Forms the Cytoophidium	The N terminus of CTPS is necessary for filamentation	Structure	*Drosophila*
2014	[148]	Molecular cell biology and immunobiology of mammalian rod/ring structures	These structures appear to decrease intracellular GTP and/or CTP pools.	Regulation/ Function	Mammalian cells
2014	[19]	**CTP synthase forms cytoophidia in the cytoplasm and nucleus**	Discovery of cytoophidia in the nucleus	Localization/ Dynamic	Mammalian cells
2014	[7]	Asymmetric inheritance of cytoophidia in *Schizosaccharomyces pombe*	Identification of nuclear cytoophidia and cytoplasmic cytoophidia in *S. pombe*; asymmetric inheritance of cytoophidia in *S. pombe*	Localization/ Dynamic	*S. pombe*

2014	[18]	**Nucleotide synthesis is regulated by cytoophidium formation during neurodevelopment and adaptive metabolism**	Filamentation downregulates CTPS enzyme activity	Regulation/ Function/ Structure	*Drosophila*
2014	[25]	Large-scale filament formation inhibits the activity of CTP synthetase	Filamentation downregulates CTPS enzyme activity. EM-scale CTPS fibres are identified.	Structure/ Function	Bacteria
2014	[24]	Common regulatory control of CTP synthase enzyme activity and filament formation	Filamentation downregulates CTPS enzyme activity.	Regulation/Function/Structure	*S. cerevisiae*
2014	[147]	Ack kinase regulates CTP synthase filaments during *Drosophila* oogenesis	Filamentation upregulates CTPS enzyme activity/DAck regulates CTPS filament	Components/ Regulation/ Function	*Drosophila*
2015	[20]	Assembly of IMPDH2-based, CTPS-based, and mixed rod/ring structures is dependent on cell type and conditions of induction	CTPS and IMPDH form independent filamentous structures	Components/ Regulation	Mammalian cells
2015	[149]	CTP Synthase Is Required for Optic Lobe Homeostasis in *Drosophila*	The role CTPS plays in brain development	Function	*Drosophila*
2015	[27]	Cytoophidium assembly reflects up-regulation of IMPDH activity	Filamentation of IMPDH upregulates its activity	Regulation/ Function	Mammalian cells
2016	[23]	Ubiquitination and filamentous structure of cytidine triphosphate synthase	The proto-oncogene Cbl regulates cytoophidium formation in *Drosophila*	Regulation	*Drosophila*
2016	[22]	The Interplay between Myc and CTP Synthase in *Drosophila*	The oncogene Myc regulates cytoophidium formation in *Drosophila*	Regulation	*Drosophila*
2016	[150]	**Filamentation of Metabolic Enzymes in *Saccharomyces cerevisiae***	Identification of 23 filament-forming proteins in a screening of 4,159 proteins in *S. cerevisiae*	Components/ Dynamics/ Regulation	*S. cerevisiae*

6.2 Oligomeric state and cytoophidium function

In Chapter 3, I presented the relationship of cytoophidium formation with the oligomerization state of CTP synthase. Meanwhile, one paper published around the same time indicated that purified CTP synthase formed EM-scale fibre in the presence of ATP and UTP [25]. Combining all of those facts, a basic model of cytoophidia can be summarized as follows. Metabolic enzymes first form certain oligomeric state which can be active or inactive regarding enzyme activity. Due to the highly symmetric morphology of oligomers, they stack on top of each other and form a longer polymer state, i.e. an EM-scale fibre. Similar or different fibres then bind to each other, probably with the help of some molecules, and form a cellular-scale filament, i.e. cytoophidium. The activity of cytoophidia is highly dependent on the basic oligomeric unit on the EM-scale fibres and also on the morphological changes during the formation of EM-scale fibres.

With the screening results in Chapter 4, I reviewed the oligomeric state, oligomer activity and filament activity of known filament-forming metabolic enzymes (Table 6.2).

From this table, I am delighted to see most of the filament-forming proteins form EM-scale fibres in vitro and possibly then aggregate into larger cytoophidia, as in our model. However, with a similar tetramer oligomeric structure, CTP synthase and IMPDH-based cytoophidia show totally opposite enzyme activity regulation after filamentation. This difference may originate from the different assembly units of oligomers into fibres, or from the different conformation changes after assembly.

A further study on the in vitro assembly of filament-forming metabolic enzymes may provide us with several assembly patterns for filament-forming proteins, and may help to explain the diversity of function and regulation of filament-forming proteins. However, as we know, the only in vitro assembly study on filament-forming metabolic enzyme till now is (Barry, R.M.,

et al., 2014 [25]). They designed a system to simultaneously monitor the assembly and activity of purified *E. coli* CTP synthase based on a fluorometer. CTP synthase polymerization was measured by right-angle light scattering and CTP synthase activity was measured by specific absorbance of CTP products. This method provided us a protocol to measure the dynamic of EM-scaled filament in vitro. They also provided cryo-EM structure of CTP synthase EM-scaled filament, which suggested how molecules were assembled on CTP synthase EM-scaled filament. The methodology of this article could be introduced for the study of other filament-forming proteins or filament-forming protein in other organisms in order to explain the diversity of function and regulation of filament-forming proteins.

Table 6.2 Oligomeric state of filament-forming metabolic enzymes

Oligomeric state and oligomer activity show the data in the budding yeast, unless otherwise indicated. Filament activity and EM fibre identification show results from existing research, without the limitation of organisms.

Protein	Oligomeric State	Filament activity	Oligomer activity	EM fibre
Acc1p	Trimer	Enhanced[51]	Trimer/active	[51]
Asn1p/Asn2p	Dimer	Unknown	Dimer/active	Unknown
Gdb1p	Monomer in mammalian dimer/ Tetramer in *S. solfataricus*	Enhanced(beta-glucosidase)[52]	Unknown	[52]
Gdh2p	Tetramer[151]	Unknown	Tetramer/active	[56]
Gln1p	Decamer[54]	Unknown	Unknown	[54]
Glt1p	Trimer[152]	Unknown	Unknown	Unknown
Pfk1p/Pfk2p	Pfk1p tetramer and Pfk2p tetramer form heterooctamer[153]	Unknown	Tetramer/active	-
Psa1p	Hexamer in *Leishmania Mexicana* [154]	Unknown	Hexamer/active	Unknown
Tsa1p	Dimer[155]	Unknown	Unknown	Unknown
CTPS (Ura7p/Ura8p)	Tetramer	Reduced[18, 24, 25]	Tetramer/active	[25]
IMPDH(mammalian)	Tetramer (mammalian)	Enhanced[27]	Tetramer/active	[26]

6.3 Further study and challenges concerning the components of cytoophidia

The components of cytoophidia have already been introduced in the introduction. However, our knowledge of cytoophidium components is still quite limited. Chapter 4 of this thesis provided us with an overall view of all filament-forming proteins in the budding yeast after one day of culturing. The discovery of filament-forming proteins Asn1p and Asn2p and their similarity to Ura7p directly led to the detailed study on Asn1p and Asn2p stress regulation in Chapter 5.

The study of cytoophidium components is very attractive for future study. According to recent research, there are several ways to examine cytoophidium components. The first approach is to identify the location of proteins which physically interact with CTP synthase or other identified filament-forming proteins. Proteins in the CTP synthase-based cytoophidia are likely to interact physically with CTP synthase. However, this approach depends on very precise interaction experiments or databases. Meanwhile, protein-protein physical interaction is neither sufficient nor necessary for co-localization on cytoophidia. This method can be an important reference for component identification.

The second approach is genome-wide screening of florescence-tagged proteins to search for filament-forming proteins. This approach is employed in Chapter 4 of this thesis. Further co-localization studies on these filament-forming proteins can be done to verify detailed protein compartmentation. However, as we know the cytoophidia are highly dynamic under various circumstances. The screen result is merely a single sample under a certain condition. However, screens with multiple conditions seem not to be an economical approach with present technologies.

Another approach is the purification of large cytoophidia in overexpressed CTP synthase mammalian cell lines. By mild lysis of cells, large cytoophidia can be released into buffer.

After proper purification process, mass spectrometry can be undertaken to identify components of cytoophidia. In one of my trial, mammalian cell line 293T which were transfected with stable GFP-tagged CTPS was lysed with mild lysis buffer and cytoophidia were observed to release into buffer under fluorescence microscope. However, after collection and purification procedures, samples did not meet the standard for mass spectrometry. Unlike two approaches above, this approach can include almost all proteins on cytoophidia. Better lysis, collection and purification procedures are the keys for the success of this approach in the future.

The study of components will identify more molecules on the cytoophidia. The discovery of other metabolic enzymes may help us to understand the diversity and similarity of filament-forming protein. The discovery of other proteins on the cytoophidia may provide us with a clearer view on the detailed mechanisms of filament formation and regulation.

6.4 Is cytoophidium an enzyme stabilizer against protein degradation? A hypothetical model and future direction for analysing cytoophidium function

The assembly and disassembly of filaments is a highly energy consuming process. Without proper benefits, this process is very easy to be kicked out during the evolution. In Chapter 3, I talked about cytoophidia may act as an inactive storage pool for CTP synthase. The formation of filaments possibly protects enzymes from the binding and ubiquitination of E3 ligase. From this hypothesis, I build up a model for the stabilization and selection effect of cytoophidia. After the translation of mRNA into polypeptide, proteins are folded. Misfolded proteins may cause serious problems if they are not probably treated in cytoplasm. The ubiquitination system can degrade those misfolded proteins, but lots of misfolded proteins can form amyloid-like aggregation structures, which are commonly transported and degraded

in the lysosome [156]. Even though cytoophidia and amyloid structures may share similar micro-fibres as a basic structure, their destinations are distinct. Assembly into cytoophidia means preservation and survival, and assembly into amyloids means destruction (Figure 6.2).

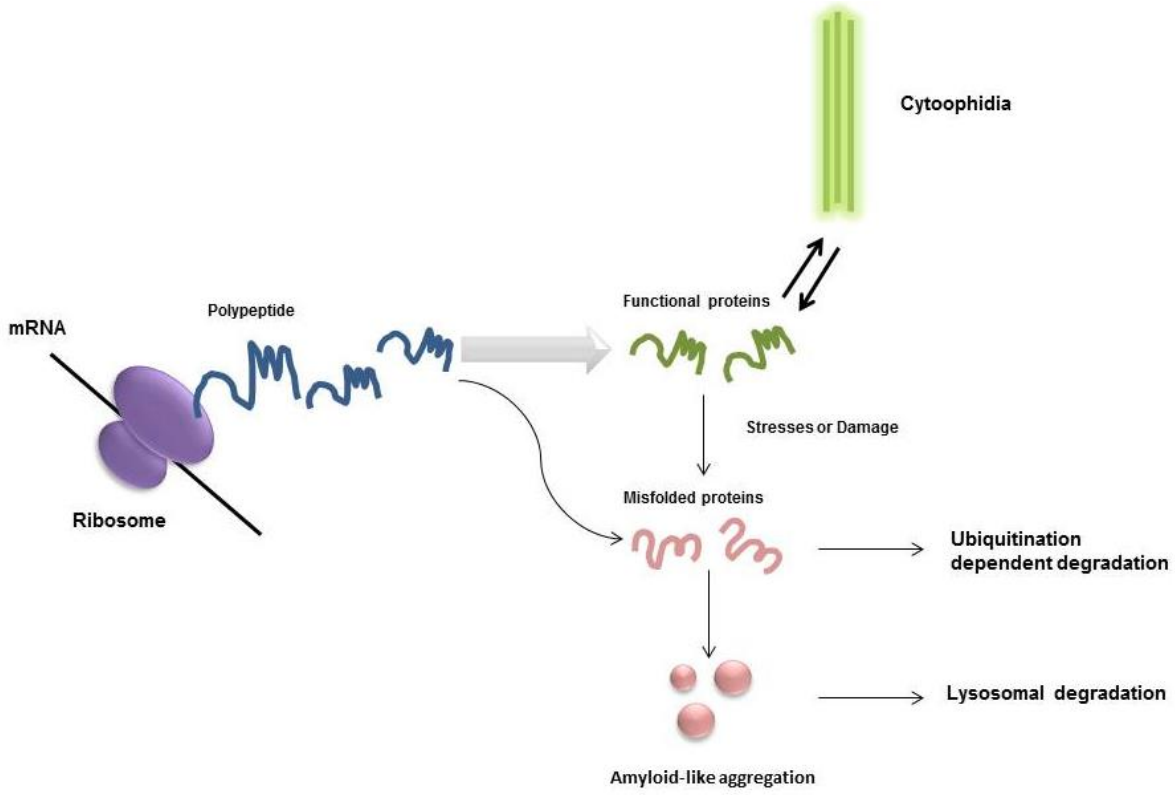


Figure 6.2 A hypothetical model for cytoophidium function as an enzyme stabilizer

After the translation of mRNA into polypeptide, misfolded proteins can form amyloid-like aggregation structures, which are commonly transported and degraded in the lysosome. The formation of filaments possibly protects functional enzymes from the binding and ubiquitination of E3 ligase.

In a previous study on the relationship of ubiquitination and cytoophidia, Pai lab suggested that ubiquitination is required for cytoophidium formation in *Drosophila* [23]. Blockage of E3 ligase pathways caused the disappearance of filaments. In our model, the blockage of E3 ligase ubiquitination causes the accumulation of misfolded proteins. The huge number of misfolded proteins may amplify their competitive binding with functional proteins, thus reducing the filament formation potency of functional proteins, and leading to the reduction of cytoophidia. The results from Pai lab fit this model well. However, this model is merely a hypothesis without the presence of concrete experimental data on the stabilization function of cytoophidia. This may be a possible future direction for cytoophidium functional study.

Meanwhile, stress conditions usually induce the damage or misfolding of proteins. From this model, we can predict that the denaturing or misfolding of proteins may decrease the number of functional proteins and cause the disassembly of cytoophidia. However, this is contradicted by the results I showed in Chapter 5, which indicated that the mechanism of filament regulation under stress is much more complex than we expected. Other regulation methods may play a more important role than the mechanism mentioned here.

As a conserved structure in cells, cytoophidia may have some fundamental and important function we have never thought about. Future study on the assembly mechanisms, stress reactions, ubiquitination regulation and other unknow function of cytoophidia will deepen our understanding of the whole view of cell biology and metabolism.

6.5 The study on filament-forming proteins: the implications for diseases

The formation of short EM-scale fibres is very common among metabolic enzymes. This is believed to be a consequence of the highly symmetrical structures of most metabolic enzymes, which is essential for allosteric regulation [47]. From the screening results in Chapter 4, glutamine synthetase can form cytoophidia in the budding yeast. Glutamine synthetase was previously documented forming filamentous structures in the mammalian eye, which are named lengsin. In fact, lots of filament-forming metabolic enzymes and stress proteins act as structural proteins in the eye lens structure of animal, which were named as crystallins. Crystallins include stress proteins such as small heat shock proteins and metabolic enzymes such as argininosuccinate lyase, lactate dehydrogenase, and aldehyde dehydrogenase [157]. These enzymes are very important for maintaining eye structure. Malfunction of some of those enzymes have been shown to cause cataracts in human as well as mouse model [158]. Future studies on the micro-structure of cytoophidia and crystallins will provide us with overviews of the filament-forming process of metabolic enzymes, as well as of structural enzymes, which may provide us with a better understanding of eye physiology and pathology.

Meanwhile, many misfolded proteins are prone to stick together and form fibrous structures, finally becoming amyloid aggregates. The formation of amyloid aggregates is believed to be the cause of Alzheimer's disease and many other diseases. Even though many studies have focused on the pathology of Alzheimer's, little is known about the process of filament assembly. The assembly of cytoophidia and the assembly of pathological proteins may share a common regulative system. The study on cytoophidium assembly regulation will unveil the physiological filamentation process in cell metabolism, which can be a very important reference for amyloid aggregation: the pathological filamentation process.

Many metabolic enzymes are promising targets for human cancer therapy due to the hyperproliferative property of cancer cells. However, one of the limitations for most chemotherapy is the lack of specificity, leading to a toxic effect on normal tissues. In Chapter 3, I have mentioned that the study on cytoophidium function may reveal an additional regulation method for metabolic enzymes, i.e. the formation of inactive or active filaments. Research on the relationship between filament formation and cell proliferation may cast light on the discovery of new targets for cancer treatment by the interference of filament-formation based enzyme regulation.

From another perspective, the property of filament formation is very promising to identify a certain group of cells sharing similar metabolic patterns. An increasing number of cell tags based on the information of filament-formation can be introduced, along with the discovery of various filament-forming proteins and the deepening of the study of relationship between filament formation and the metabolic network. I mentioned before that CTP synthase-based cytoophidia are found to be regulated by the proto-oncogene Myc and Cbl. These studies support the idea that certain cancer models may change the filament-forming pattern of CTP synthase through its impact on the whole metabolic network. If the correlation between filament formation and cell aberrant growth is proven to be reliable enough, filament formation can be chosen as a proper indicator for cancer cell identification.

6.6 Concluding remarks

In this thesis, I have described a screening of filament-forming proteins in the budding yeast, the following study on candidate proteins Asn1p/Asn2p in the presence of stresses, and the functional study of inactive cytoophidia in *Drosophila*. This thesis not only provides an overall picture of filament-forming proteins with nine new filament-forming proteins discovered, but also provides a detailed view on cytoophidium function and its interaction with stress. The study on cytoophidia is still in its infant stage, and every detailed discovery will have a profound impact on further studies. This work also highlights the inactivation of CTP synthase filaments, and also the filaments' sensitivity towards metabolic regulation. Despite the present discoveries, it is still very hard to predict the way in which cytoophidia might surprise us in future. With more cutting-edge technologies and more expertise from related disciplines, the study of this fundamental biological phenomenon may provide us with a new insight into cell biology, priceless information for other biological studies, and discoveries relating to disease diagnoses and treatments.

References

1. Liu, J.L., Intracellular compartmentation of CTP synthase in *Drosophila*. J Genet Genomics, 2010. 37(5): p. 281-96.
2. Liu, J.L., The enigmatic cytoophidium: compartmentation of CTP synthase via filament formation. Bioessays, 2011. 33(3): p. 159-64.
3. Ingerson-Mahar, M., et al., The metabolic enzyme CTP synthase forms cytoskeletal filaments. Nat Cell Biol, 2010. 12(8): p. 739-46.
4. Noree, C., et al., Identification of novel filament-forming proteins in *Saccharomyces cerevisiae* and *Drosophila melanogaster*. J Cell Biol, 2010. 190(4): p. 541-51.
5. Chen, K., et al., Glutamine analogs promote cytoophidium assembly in human and *Drosophila* cells. J Genet Genomics, 2011. 38(9): p. 391-402.
6. Carcamo, W.C., et al., Induction of cytoplasmic rods and rings structures by inhibition of the CTP and GTP synthetic pathway in mammalian cells. PLoS One, 2011. 6(12): p. e29690.
7. Zhang, J., L. Hulme, and J.L. Liu, Asymmetric inheritance of cytoophidia in *Schizosaccharomyces pombe*. Biol Open, 2014. 3(11): p. 1092-7.
8. van Kuilenburg, A.B., et al., Isoforms of human CTP synthetase. Adv Exp Med Biol, 2000. 486: p. 257-61.
9. von der Saal, W., P.M. Anderson, and J.J. Villafranca, Mechanistic investigations of *Escherichia coli* cytidine-5'-triphosphate synthetase. Detection of an intermediate by positional isotope exchange experiments. J Biol Chem, 1985. 260(28): p. 14993-7.
10. MacDonnell, J.E., F.A. Lunn, and S.L. Bearne, Inhibition of *E. coli* CTP synthase by the "positive" allosteric effector GTP. Biochim Biophys Acta, 2004. 1699(1-2): p. 213-20.
11. Endrizzi, J.A., et al., Mechanisms of product feedback regulation and drug resistance in cytidine triphosphate synthetases from the structure of a CTP-inhibited complex. Biochemistry, 2005. 44(41): p. 13491-9.
12. Lunn, F.A., J.E. MacDonnell, and S.L. Bearne, Structural requirements for the activation of *Escherichia coli* CTP synthase by the allosteric effector GTP are stringent, but requirements for inhibition are lax. J Biol Chem, 2008. 283(4): p. 2010-20.

13. Kassel, K.M., et al., Regulation of human cytidine triphosphate synthetase 2 by phosphorylation. J Biol Chem, 2010. 285(44): p. 33727-36.
14. Pinkus, L.M., Glutamine binding sites. Methods Enzymol, 1977. 46: p. 414-27.
15. Robertson, J.G., L.J. Sparvero, and J.J. Villafranca, Inactivation and covalent modification of CTP synthetase by thiourea dioxide. Protein Sci, 1992. 1(10): p. 1298-307.
16. Roy, A.C., F.A. Lunn, and S.L. Bearne, Inhibition of CTP synthase from *Escherichia coli* by xanthines and uric acids. Bioorg Med Chem Lett, 2010. 20(1): p. 141-4.
17. Azzam, G. and J.L. Liu, Only one isoform of *Drosophila melanogaster* CTP synthase forms the cytoophidium. PLoS Genet, 2013. 9(2): p. e1003256.
18. Aughey, G.N., et al., Nucleotide synthesis is regulated by cytoophidium formation during neurodevelopment and adaptive metabolism. Biol Open, 2014. 3(11): p. 1045-56.
19. Gou, K.M., et al., CTP synthase forms cytoophidia in the cytoplasm and nucleus. Exp Cell Res, 2014. 323(1): p. 242-53.
20. Keppeke, G.D., et al., Assembly of IMPDH2-based, CTPS-based, and mixed rod/ring structures is dependent on cell type and conditions of induction. J Genet Genomics, 2015. 42(6): p. 287-99.
21. Liu, J.L., The Cytoophidium and Its Kind: Filamentation and Compartmentation of Metabolic Enzymes. Annu Rev Cell Dev Biol, 2016. 32: p. 349-372.
22. Aughey, G.N., S.J. Grice, and J.L. Liu, The Interplay between Myc and CTP Synthase in *Drosophila*. PLoS Genet, 2016. 12(2): p. e1005867.
23. Pai, L.M., et al., Ubiquitination and filamentous structure of cytidine triphosphate synthase. Fly (Austin), 2016. 10(3): p. 108-14.
24. Noree, C., et al., Common regulatory control of CTP synthase enzyme activity and filament formation. Mol Biol Cell, 2014. 25(15): p. 2282-90.
25. Barry, R.M., et al., Large-scale filament formation inhibits the activity of CTP synthetase. Elife, 2014. 3: p. e03638.
26. Ji, Y., et al., Regulation of the interaction of inosine monophosphate dehydrogenase with mycophenolic Acid by GTP. J Biol Chem, 2006. 281(1): p. 206-12.
27. Chang, C.C., et al., Cytoophidium assembly reflects upregulation of IMPDH activity. J Cell Sci, 2015. 128(19): p. 3550-5.
28. Kizaki, H., et al., Increased cytidine 5'-triphosphate synthetase activity in rat and human tumors. Cancer Res, 1980. 40(11): p. 3921-7.

29. Schimmel, K.J., H. Gelderblom, and H.J. Guchelaar, Cyclopentenyl cytosine (CPEC): an overview of its in vitro and in vivo activity. Curr Cancer Drug Targets, 2007. 7(5): p. 504-9.
30. Martin, E., et al., CTP synthase 1 deficiency in humans reveals its central role in lymphocyte proliferation. Nature, 2014. 510(7504): p. 288-92.
31. Keppeke, G.D., et al., Longitudinal study of a human drug-induced model of autoantibody to cytoplasmic rods/rings following HCV therapy with ribavirin and interferon-alpha. PLoS One, 2012. 7(9): p. e45392.
32. Adams, M.D., et al., The genome sequence of *Drosophila melanogaster*. Science, 2000. 287(5461): p. 2185-95.
33. Reiter, L.T., et al., A systematic analysis of human disease-associated gene sequences in *Drosophila melanogaster*. Genome Res, 2001. 11(6): p. 1114-25.
34. Goffeau, A., et al., Life with 6000 genes. Science, 1996. 274(5287): p. 546, 563-7.
35. Huh, W.K., et al., Global analysis of protein localization in budding yeast. Nature, 2003. 425(6959): p. 686-91.
36. Szklarczyk, D., et al., STRING v10: protein-protein interaction networks, integrated over the tree of life. Nucleic Acids Res, 2015. 43(Database issue): p. D447-52.
37. Anderson, P.M., CTP synthetase from *Escherichia coli*: an improved purification procedure and characterization of hysteretic and enzyme concentration effects on kinetic properties. Biochemistry, 1983. 22(13): p. 3285-92.
38. Levitzki, A. and D.E. Koshland, Jr., Ligand-induced dimer-to-tetramer transformation in cytosine triphosphate synthetase. Biochemistry, 1972. 11(2): p. 247-53.
39. Pappas, A., et al., Nucleotide-dependent tetramerization of CTP synthetase from *Saccharomyces cerevisiae*. J Biol Chem, 1998. 273(26): p. 15954-60.
40. Robertson, J.G., Determination of subunit dissociation constants in native and inactivated CTP synthetase by sedimentation equilibrium. Biochemistry, 1995. 34(22): p. 7533-41.
41. Endrizzi, J.A., et al., Crystal structure of *Escherichia coli* cytidine triphosphate synthetase, a nucleotide-regulated glutamine amidotransferase/ATP-dependent amidoligase fusion protein and homologue of anticancer and antiparasitic drug targets. Biochemistry, 2004. 43(21): p. 6447-63.
42. Lauritsen, I., et al., Structure of the dimeric form of CTP synthase from *Sulfolobus solfataricus*. Acta Crystallogr Sect F Struct Biol Cryst Commun, 2011. 67(Pt 2): p. 201-8.

43. Goodsell, D.S. and A.J. Olson, Structural symmetry and protein function. Annu Rev Biophys Biomol Struct, 2000. 29: p. 105-53.
44. Hopkinson, D.A., Y.H. Edwards, and H. Harris, The distributions of subunit numbers and subunit sizes of enzymes: a study of the products of 100 human gene loci. Ann Hum Genet, 1976. 39(4): p. 383-411.
45. Traut, T.W., Enzymes of nucleotide metabolism: the significance of subunit size and polymer size for biological function and regulatory properties. CRC Crit Rev Biochem, 1988. 23(2): p. 121-69.
46. Goodsell, D.S., Inside a living cell. Trends Biochem Sci, 1991. 16(6): p. 203-6.
47. Traut, T.W., Dissociation of enzyme oligomers: a mechanism for allosteric regulation. Crit Rev Biochem Mol Biol, 1994. 29(2): p. 125-63.
48. Ali, M.H. and B. Imperiali, Protein oligomerization: how and why. Bioorg Med Chem, 2005. 13(17): p. 5013-20.
49. Nooren, I.M. and J.M. Thornton, Structural characterisation and functional significance of transient protein-protein interactions. J Mol Biol, 2003. 325(5): p. 991-1018.
50. Diacovich, L., et al., Crystal structure of the beta-subunit of acyl-CoA carboxylase: structure-based engineering of substrate specificity. Biochemistry, 2004. 43(44): p. 14027-36.
51. Kim, C.W., et al., Induced polymerization of mammalian acetyl-CoA carboxylase by MIG12 provides a tertiary level of regulation of fatty acid synthesis. Proc Natl Acad Sci U S A, 2010. 107(21): p. 9626-31.
52. Kim, S.Y., et al., Novel type of enzyme multimerization enhances substrate affinity of oat beta-glucosidase. J Struct Biol, 2005. 150(1): p. 1-10.
53. Miller, R.E., E. Shelton, and E.R. Stadtman, Zinc-induced paracrystalline aggregation of glutamine synthetase. Arch Biochem Biophys, 1974. 163(1): p. 155-71.
54. He, Y.X., et al., Crystal structure of *Saccharomyces cerevisiae* glutamine synthetase Gln1 suggests a nanotube-like supramolecular assembly. Proteins, 2009. 76(1): p. 249-54.
55. Harding, R.L., et al., Lengsin expression and function during zebrafish lens formation. Exp Eye Res, 2008. 86(5): p. 807-18.
56. Josephs, R. and G. Borisy, Self-assembly of glutamic dehydrogenase into ordered superstructures: multichain tubes formed by association of single molecules. J Mol Biol, 1972. 65(1): p. 127-55.

57. O'Connell, J.D., et al., Dynamic reorganization of metabolic enzymes into intracellular bodies. Annu Rev Cell Dev Biol, 2012. 28: p. 89-111.
58. Aronow, B. and B. Ullman, In situ regulation of mammalian CTP synthetase by allosteric inhibition. J Biol Chem, 1987. 262(11): p. 5106-12.
59. Long, C.W. and A.B. Pardee, Cytidine triphosphate synthetase of *Escherichia coli* B. I. Purification and kinetics. J Biol Chem, 1967. 242(20): p. 4715-21.
60. Ostrander, D.B., et al., Effect of CTP synthetase regulation by CTP on phospholipid synthesis in *Saccharomyces cerevisiae*. J Biol Chem, 1998. 273(30): p. 18992-9001.
61. Labesse, G., et al., MgATP regulates allostery and fiber formation in IMPDHs. Structure, 2013. 21(6): p. 975-85.
62. Zhang, R., et al., Characteristics and crystal structure of bacterial inosine-5'-monophosphate dehydrogenase. Biochemistry, 1999. 38(15): p. 4691-700.
63. Ross-Macdonald, P., et al., Large-scale analysis of the yeast genome by transposon tagging and gene disruption. Nature, 1999. 402(6760): p. 413-8.
64. Kumar, A., et al., Subcellular localization of the yeast proteome. Genes Dev, 2002. 16(6): p. 707-19.
65. Bashkirov, V.I., et al., A mouse cytoplasmic exoribonuclease (mXRN1p) with preference for G4 tetraplex substrates. J Cell Biol, 1997. 136(4): p. 761-73.
66. Buchan, J.R., D. Muhlrad, and R. Parker, P bodies promote stress granule assembly in Saccharomyces cerevisiae. J Cell Biol, 2008. 183(3): p. 441-55.
67. Kedersha, N., et al., Stress granules and processing bodies are dynamically linked sites of mRNP remodeling. J Cell Biol, 2005. 169(6): p. 871-84.
68. Narayanaswamy, R., et al., Widespread reorganization of metabolic enzymes into reversible assemblies upon nutrient starvation. Proc Natl Acad Sci U S A, 2009. 106(25): p. 10147-52.
69. Sherman, F., Getting started with yeast. Methods Enzymol, 2002. 350: p. 3-41.
70. Werner-Washburne, M., et al., Stationary phase in the yeast *Saccharomyces cerevisiae*. Microbiol Rev, 1993. 57(2): p. 383-401.
71. Gray, J.V., et al., "Sleeping beauty": quiescence in *Saccharomyces cerevisiae*. Microbiol Mol Biol Rev, 2004. 68(2): p. 187-206.
72. de Nobel, J.G., et al., The glucanase-soluble mannoproteins limit cell wall porosity in *Saccharomyces cerevisiae*. Yeast, 1990. 6(6): p. 491-9.

73. De Nobel, J.G., et al., An assay of relative cell wall porosity in *Saccharomyces cerevisiae*, *Kluyveromyces lactis* and *Schizosaccharomyces pombe*. Yeast, 1990. 6(6): p. 483-90.
74. De Nobel, H., et al., Cell wall perturbation in yeast results in dual phosphorylation of the Slt2/Mpk1 MAP kinase and in an Slt2-mediated increase in FKS2-lacZ expression, glucanase resistance and thermotolerance. Microbiology, 2000. 146 (Pt 9): p. 2121-32.
75. Cyrne, L., et al., Regulation of antioxidant enzymes gene expression in the yeast *Saccharomyces cerevisiae* during stationary phase. Free Radic Biol Med, 2003. 34(3): p. 385-93.
76. Jelinsky, S.A., et al., Regulatory networks revealed by transcriptional profiling of damaged *Saccharomyces cerevisiae* cells: Rpn4 links base excision repair with proteasomes. Molecular and Cellular Biology, 2000. 20(21): p. 8157-67.
77. Barbet, N.C., et al., TOR controls translation initiation and early G1 progression in yeast. Mol Biol Cell, 1996. 7(1): p. 25-42.
78. Urban, J., et al., Sch9 is a major target of TORC1 in *Saccharomyces cerevisiae*. Mol Cell, 2007. 26(5): p. 663-74.
79. Boutelet, F., A. Petitjean, and F. Hilger, Yeast cdc35 mutants are defective in adenylate cyclase and are allelic with cyr1 mutants while CAS1, a new gene, is involved in the regulation of adenylate cyclase. EMBO J, 1985. 4(10): p. 2635-41.
80. Werner-Washburne, M., et al., Yeast Hsp70 RNA levels vary in response to the physiological status of the cell. J Bacteriol, 1989. 171(5): p. 2680-8.
81. Hardie, D.G., D. Carling, and M. Carlson, The AMP-activated/SNF1 protein kinase subfamily: metabolic sensors of the eukaryotic cell? Annu Rev Biochem, 1998. 67: p. 821-55.
82. Gasch, A.P., et al., Genomic expression programs in the response of yeast cells to environmental changes. Mol Biol Cell, 2000. 11(12): p. 4241-57.
83. Petrovska, I., et al., Filament formation by metabolic enzymes is a specific adaptation to an advanced state of cellular starvation. Elife, 2014.
84. McMurray, M.A., et al., Septin filament formation is essential in budding yeast. Dev Cell, 2011. 20(4): p. 540-9.
85. Versele, M. and J. Thorner, Septin collar formation in budding yeast requires GTP binding and direct phosphorylation by the PAK, Cla4. J Cell Biol, 2004. 164(5): p. 701-15.

86. Kleinschmidt, A.K., J. Moss, and D.M. Lane, Acetyl coenzyme A carboxylase: filamentous nature of the animal enzymes. Science, 1969. 166(3910): p. 1276-8.
87. Meredith, M.J. and M.D. Lane, Acetyl-CoA carboxylase. Evidence for polymeric filament to protomer transition in the intact avian liver cell. J Biol Chem, 1978. 253(10): p. 3381-3.
88. Suresh, H.G., et al., Prolonged starvation drives reversible sequestration of lipid biosynthetic enzymes and organelle reorganization in *Saccharomyces cerevisiae*. Mol Biol Cell, 2015. 26(9): p. 1601-15.
89. Dang, V.D., et al., Cloning of the ASN1 and ASN2 genes encoding asparagine synthetases in *Saccharomyces cerevisiae*: differential regulation by the CCAAT-box-binding factor. Mol Microbiol, 1996. 22(4): p. 681-92.
90. Gantt, J.S. and S.M. Arfin, Elevated levels of asparagine synthetase activity in physiologically and genetically derepressed Chinese hamster ovary cells are due to increased rates of enzyme synthesis. J Biol Chem, 1981. 256(14): p. 7311-5.
91. Larsen, T.M., et al., Three-dimensional structure of *Escherichia coli* asparagine synthetase B: A short journey from substrate to product. Biochemistry, 2000. 39(24): p. 7330.
92. Zhang, J., et al., Asparagine plays a critical role in regulating cellular adaptation to glutamine depletion. Mol Cell, 2014. 56(2): p. 205-18.
93. Aslanian, A.M., B.S. Fletcher, and M.S. Kilberg, Asparagine synthetase expression alone is sufficient to induce l-asparaginase resistance in MOLT-4 human leukaemia cells. Biochem J, 2001. 357(Pt 1): p. 321-8.
94. Panosyan, E.H., et al., Asparagine depletion potentiates the cytotoxic effect of chemotherapy against brain tumors. Mol Cancer Res, 2014. 12(5): p. 694-702.
95. Sircar, K., et al., Integrative molecular profiling reveals asparagine synthetase is a target in castration-resistant prostate cancer. Am J Pathol, 2012. 180(3): p. 895-903.
96. Campbell, S.G., N.P. Hoyle, and M.P. Ashe, Dynamic cycling of eIF2 through a large eIF2B-containing cytoplasmic body: implications for translation control. J Cell Biol, 2005. 170(6): p. 925-34.
97. Gunning, B.E., The Fine Structure of Chloroplast Stroma Following Aldehyde Osmium-Tetroxide Fixation. J Cell Biol, 1965. 24: p. 79-93.
98. DeLuna, A., et al., NADP-glutamate dehydrogenase isoenzymes of *Saccharomyces cerevisiae*. Purification, kinetic properties, and physiological roles. J Biol Chem, 2001. 276(47): p. 43775-83.

99. Telford, J.N., P.M. Lad, and G.G. Hammes, Electron microscope study of native and crosslinked rabbit muscle phosphofructokinase. Proc Natl Acad Sci U S A, 1975. 72(8): p. 3054-6.
100. Schwock, J., et al., Interaction of 6-phosphofructokinase with cytosolic proteins of *Saccharomyces cerevisiae*. Yeast, 2004. 21(6): p. 483-94.
101. MacDiarmid, C.W., et al., Peroxiredoxin chaperone activity is critical for protein homeostasis in zinc-deficient yeast. J Biol Chem, 2013. 288(43): p. 31313-27.
102. Wanichthanarak, K., N. Wongtosrad, and D. Petranovic, Genome-wide expression analyses of the stationary phase model of ageing in yeast. Mech Ageing Dev, 2015. 149: p. 65-74.
103. Costantini, L.M., et al., Assessing the tendency of fluorescent proteins to oligomerize under physiologic conditions. Traffic, 2012. 13(5): p. 643-9.
104. Richards, N.G. and M.S. Kilberg, Asparagine synthetase chemotherapy. Annu Rev Biochem, 2006. 75: p. 629-54.
105. Oinonen, C. and J. Rouvinen, Structural comparison of Ntn-hydrolases. Protein Sci, 2000. 9(12): p. 2329-37.
106. Brannigan, J.A., et al., A Protein Catalytic Framework with an N-Terminal Nucleophile Is Capable of Self-Activation (Vol 378, Pg 416, 1995). Nature, 1995. 378(6557): p. 644-644.
107. Zalkin, H. and J.L. Smith, Enzymes utilizing glutamine as an amide donor. Advances in Enzymology, Vol 72, 1998. 72: p. 87-+.
108. Krahn, J.M., et al., Coupled formation of an amidotransferase interdomain ammonia channel and a phosphoribosyltransferase active site. Biochemistry, 1997. 36(37): p. 11061-11068.
109. Massiere, F. and M.A. Badet-Denisot, The mechanism of glutamine-dependent amidotransferases. Cellular and Molecular Life Sciences, 1998. 54(3): p. 205-222.
110. Teplyakov, A., et al., Channeling of ammonia in glucosamine-6-phosphate synthase. J Mol Biol, 2001. 313(5): p. 1093-102.
111. Luehr, C.A. and S.M. Schuster, Purification and characterization of beef pancreatic asparagine synthetase. Arch Biochem Biophys, 1985. 237(2): p. 335-46.
112. Boehlein, S.K., et al., Kinetic mechanism of *Escherichia coli* asparagine synthetase B. Biochemistry, 1998. 37(38): p. 13230-8.

113. Milman, H.A. and D.A. Cooney, The distribution of L-asparagine synthetase in the principal organs of several mammalian and avian species. Biochem J, 1974. 142(1): p. 27-35.
114. Milman, H.A., D.A. Cooney, and D.M. Young, Role of pancreatic L-asparagine synthetase in homeostasis of L-asparagine. Am J Physiol, 1979. 236(6): p. E746-53.
115. Cooney, D.A., et al., L-Asparagine synthetase in serum as a marker for neoplasia. Cancer Res, 1976. 36(9 pt.1): p. 3238-45.
116. Gong, S.S., L. Guerrini, and C. Basilico, Regulation of Asparagine Synthetase Gene-Expression by Amino-Acid Starvation. Molecular and Cellular Biology, 1991. 11(12): p. 6059-6066.
117. Hutson, R.G. and M.S. Kilberg, Cloning of rat asparagine synthetase and specificity of the amino acid-dependent control of its mRNA content. Biochem J, 1994. 304 (Pt 3): p. 745-50.
118. Chen, H., et al., Amino acid deprivation induces the transcription rate of the human asparagine synthetase gene through a timed program of expression and promoter binding of nutrient-responsive basic region/leucine zipper transcription factors as well as localized histone acetylation. J Biol Chem, 2004. 279(49): p. 50829-39.
119. Harding, H.P., et al., Regulated translation initiation controls stress-induced gene expression in mammalian cells. Mol Cell, 2000. 6(5): p. 1099-108.
120. Jayaram, H.N., et al., Don, conv and donv--I. Inhibition of L-asparagine synthetase in vitro. Biochem Pharmacol, 1976. 25(14): p. 1571-82.
121. Ikeuchi, H., et al., A sulfoximine-based inhibitor of human asparagine synthetase kills L-asparaginase-resistant leukemia cells. Bioorg Med Chem, 2012. 20(19): p. 5915-27.
122. Hersh, E.M., Immunosuppression by L-asparaginase and related enzymes. Transplantation, 1971. 12(5): p. 368-76.
123. Richards, N.G. and S.M. Schuster, Mechanistic issues in asparagine synthetase catalysis. Adv Enzymol Relat Areas Mol Biol, 1998. 72: p. 145-98.
124. Zhang, B., et al., Asparagine synthetase is an independent predictor of surgical survival and a potential therapeutic target in hepatocellular carcinoma. Br J Cancer, 2013. 109(1): p. 14-23.
125. Li, H., et al., Knockdown of asparagine synthetase by RNAi suppresses cell growth in human melanoma cells and epidermoid carcinoma cells. Biotechnol Appl Biochem, 2015.

126. Sorger, P.K. and H.R. Pelham, Purification and characterization of a heat-shock element binding protein from yeast. EMBO J, 1987. 6(10): p. 3035-41.
127. Morano, K.A., C.M. Grant, and W.S. Moye-Rowley, The response to heat shock and oxidative stress in *Saccharomyces cerevisiae*. Genetics, 2012. 190(4): p. 1157-95.
128. Wieser, R., et al., Heat shock factor-independent heat control of transcription of the CTT1 gene encoding the cytosolic catalase T of *Saccharomyces cerevisiae*. J Biol Chem, 1991. 266(19): p. 12406-11.
129. Beck, T. and M.N. Hall, The TOR signalling pathway controls nuclear localization of nutrient-regulated transcription factors. Nature, 1999. 402(6762): p. 689-92.
130. Stefanini, I., et al., Role of social wasps in *Saccharomyces cerevisiae* ecology and evolution. Proc Natl Acad Sci U S A, 2012. 109(33): p. 13398-403.
131. Yamamoto, N., et al., Regulation of thermotolerance by stress-induced transcription factors in *Saccharomyces cerevisiae*. Eukaryot Cell, 2008. 7(5): p. 783-90.
132. Thevelein, J.M., et al., Nutrient-induced signal transduction through the protein kinase A pathway and its role in the control of metabolism, stress resistance, and growth in yeast. Enzyme Microb Technol, 2000. 26(9-10): p. 819-825.
133. Truman, A.W., et al., In the yeast heat shock response, Hsf1-directed induction of Hsp90 facilitates the activation of the Slt2 (Mpk1) mitogen-activated protein kinase required for cell integrity. Eukaryot Cell, 2007. 6(4): p. 744-52.
134. Halliwell, B., Oxidative stress and neurodegeneration: where are we now? J Neurochem, 2006. 97(6): p. 1634-58.
135. Thorpe, G.W., et al., Cells have distinct mechanisms to maintain protection against different reactive oxygen species: oxidative-stress-response genes. Proc Natl Acad Sci U S A, 2004. 101(17): p. 6564-9.
136. Morgan, B.A., et al., The Skn7 response regulator controls gene expression in the oxidative stress response of the budding yeast *Saccharomyces cerevisiae*. EMBO J, 1997. 16(5): p. 1035-44.
137. Machado, A.K., B.A. Morgan, and G.F. Merrill, Thioredoxin reductase-dependent inhibition of MCB cell cycle box activity in *Saccharomyces cerevisiae*. J Biol Chem, 1997. 272(27): p. 17045-54.
138. Mager, W.H. and M. Siderius, Novel insights into the osmotic stress response of yeast. FEMS Yeast Res, 2002. 2(3): p. 251-7.
139. Klipp, E., et al., Integrative model of the response of yeast to osmotic shock. Nat Biotechnol, 2005. 23(8): p. 975-82.

140. Hohmann, S., Osmotic stress signaling and osmoadaptation in yeasts. Microbiol Mol Biol Rev, 2002. 66(2): p. 300-72.
141. Aguilera, J., F. Randez-Gil, and J.A. Prieto, Cold response in *Saccharomyces cerevisiae*: new functions for old mechanisms. FEMS Microbiol Rev, 2007. 31(3): p. 327-41.
142. Hayashi, M. and T. Maeda, Activation of the HOG pathway upon cold stress in *Saccharomyces cerevisiae*. J Biochem, 2006. 139(4): p. 797-803.
143. Panadero, J., et al., A downshift in temperature activates the high osmolarity glycerol (HOG) pathway, which determines freeze tolerance in *Saccharomyces cerevisiae*. J Biol Chem, 2006. 281(8): p. 4638-45.
144. Causton, H.C., et al., Remodeling of yeast genome expression in response to environmental changes. Mol Biol Cell, 2001. 12(2): p. 323-37.
145. Sipiczki, M., Phylogenesis of fission yeasts. Contradictions surrounding the origin of a century old genus. Antonie Van Leeuwenhoek, 1995. 68(2): p. 119-49.
146. Chen, D., et al., Global transcriptional responses of fission yeast to environmental stress. Mol Biol Cell, 2003. 14(1): p. 214-29.
147. Strochlic, T.I., et al., Ack kinase regulates CTP synthase filaments during *Drosophila* oogenesis. EMBO Rep, 2014. 15(11): p. 1184-91.
148. Carcamo, W.C., et al., Molecular cell biology and immunobiology of mammalian rod/ring structures. Int Rev Cell Mol Biol, 2014. 308: p. 35-74.
149. Tastan, O.Y. and J.L. Liu, CTP Synthase Is Required for Optic Lobe Homeostasis in *Drosophila*. J Genet Genomics, 2015. 42(5): p. 261-74.
150. Shen, Q.J., et al., Filamentation of Metabolic Enzymes in *Saccharomyces cerevisiae*. J Genet Genomics, 2016. 43(6): p. 393-404.
151. Breitkreutz, A., et al., A global protein kinase and phosphatase interaction network in yeast. Science, 2010. 328(5981): p. 1043-6.
152. Cogoni, C., et al., *Saccharomyces cerevisiae* has a single glutamate synthase gene coding for a plant-like high-molecular-weight polypeptide. J Bacteriol, 1995. 177(3): p. 792-8.
153. Kriegel, T., J. Behlke, and G. Kopperschlager, Hydrodynamic studies on the quaternary structure of reacting yeast phosphofructokinase. Biomed Biochim Acta, 1987. 46(5): p. 349-55.
154. Davis, A.J., et al., Properties of GDP-mannose pyrophosphorylase, a critical enzyme and drug target in Leishmania mexicana. J Biol Chem, 2004. 279(13): p. 12462-8.

155. Biteau, B., J. Labarre, and M.B. Toledano, ATP-dependent reduction of cysteine-sulphinic acid by *S. cerevisiae* sulphiredoxin. Nature, 2003. 425(6961): p. 980-4.
156. Majumdar, A., et al., Activation of microglia acidifies lysosomes and leads to degradation of Alzheimer amyloid fibrils. Mol Biol Cell, 2007. 18(4): p. 1490-6.
157. Wistow, G., Lens crystallins: gene recruitment and evolutionary dynamism. Trends Biochem Sci, 1993. 18(8): p. 301-6.
158. Song, S., et al., Functions of the intermediate filament cytoskeleton in the eye lens. J Clin Invest, 2009. 119(7): p. 1837-48.

List of publication

1. ***CTP synthase forms cytoophidia in the cytoplasm and nucleus.*** (As 3rd author)

Gou KM, Chang CC, Shen QJ, Sung LY, Liu JL

Exp Cell Res, 2014. **323**(1): p. 242-53.

2. ***Nucleotide synthesis is regulated by cytoophidium formation during neurodevelopment and adaptive metabolism.*** (As co-first author)

Aughey GN, Grice SJ, Shen QJ, Xu Y, Chang CC, Azzam G, Wang PY, Freeman-Mills L, Pai LM, Sung LY, Yan J, Liu JL.

Biol Open, 2014. **3**(11): p. 1045-56.

3. ***Filamentation of Metabolic Enzymes in Saccharomyces cerevisiae.*** (As co-first author)

Shen QJ, Kassim H, Huang Y, Li H, Zhang J, Li G, Wang PY, Yan J, Ye F, Liu JL.

J Genet Genomics, 2016. **43**(6): p. 393-404.